

Muscle load sharing

An energy-based approach



Marit Praagman



Muscle load sharing

An energy-based approach

Marit Praagman

The work presented in this thesis is part of the research program of the Institute of Fundamental and Clinical Human Movement Sciences and was carried out at the Faculty of Human Movement Sciences, Vrije Universiteit, Amsterdam.

Colophon

ISBN:

978 90 8659 202 9

Cover design and lay-out:

Rachel van Esschoten (Diving Duck, www.divingduck.nl)

Printed by:

PrintPartners Ipskamp B.V. Enschede

Photography:

Istockphoto (www.istockphoto.com)

© Copyright 2008, Marit Praagman

All rights reserved. No parts of this thesis may be reproduced or transmitted in any form or by any means, electronic or mechanical, including photocopying, recording or any information storage or retrieval system, without written permission from the author.

VRIJE UNIVERSITEIT

Muscle load sharing

An energy-based approach

ACADEMISCH PROEFSCHRIFT

ter verkrijging van de graad Doctor aan
de Vrije Universiteit Amsterdam,
op gezag van de rector magnificus
prof.dr. L.M. Bouter,
in het openbaar te verdedigen
ten overstaan van de promotiecommissie
van de faculteit der Bewegingswetenschappen
op woensdag 23 april 2008 om 15.45 uur
in de aula van de universiteit,
De Boelelaan 1105

door

Marit Praagman

geboren te Geldrop

promotor: prof.dr. F.C.T. van der Helm
copromotor: dr. H.E.J. Veeger

Contents

Chapter 1	General Introduction	6
Chapter 2	Muscle oxygen consumption, determined by NIRS, in relation to external force and EMG	22
Chapter 3	The relationship between two different mechanical cost functions and muscle oxygen consumption	40
Chapter 4	The effect of elbow angle and external moment on load sharing of elbow muscles	58
Chapter 5	The effect of PCSA and moment arm distributions on the load sharing of arm muscles	84
Chapter 6	Epilogue	112
References		130
Summary		144
Samenvatting		152
Finally...		
	Dankwoord	164
	List of publications	168





Chapter 1

General Introduction

Introduction

The human movement system is a complex and ingenious system, capable of performing many different tasks in very different ways. Despite inter-individual differences, general movement patterns are seen during normal activities. It is assumed that these general patterns are defined by a general control principle that governs the large number of degrees of freedom within the motor system. Many studies have been performed investigating the possible constraints (Hardt, 1978; Crowninshield and Brand, 1981; Dul et al., 1984a, 1984b; Kaufman et al., 1991b; Happee, 1994; Van der Helm, 1994a; Buchanan and Shreeve, 1996; Alexander, 1997; Rasmussen et al., 2001; Stokes and Gardner-Morse, 2001), as well as the coordination of these patterns (Klein Breteler et al., 2002; d'Avella et al., 2006). To date it is still unknown what the exact principle of control is.

Biomechanical models can be very useful in understanding the control of the musculoskeletal system. A biomechanical model is a reduced reproduction of the musculoskeletal system in which bones, joints and muscles are represented (Figure 1.1).

Next to the application in more fundamental studies on the working and control of the musculoskeletal system (Van Soest et al., 2005; Kistemaker et al., 2007), biomechanical models can be used for applied research. They can be used to estimate the load (by calculating forces and moments) on joints, muscles or ligaments during certain activities as for instance wheelchair propulsion (Veeger et al., 2002b; Van Drongelen et al., 2005a, 2006). This is very useful as these internal forces/loads cannot, or only with great difficulty, be measured in vivo. A second powerful application of models is the 'what if' option: models can be used to predict the (mechanical) effect of surgical interventions and treatment (computer aided surgery planning), such as for instance tendon replacements (Delp et al., 1996; Magermans et al., 2004; Veeger et al., 2004). By replacing a tendon in the model to another attachment site, it can be easily evaluated how this affects for instance the movement pattern or the force that can be produced. To answer 'what if' questions large-scale muscle models, accurately representing part of the musculoskeletal system, including sufficient degrees of freedom, are necessary. Several of such models have been introduced of both lower (Delp and Loan, 1995; Koopman et al., 1995; Pandy et al., 1998; Klein Horsman et al., 2006) and upper extremity (Hogfors et al., 1987, 1991; Karlsson et al., 1992; Van der Helm, 1994a, 1997b)

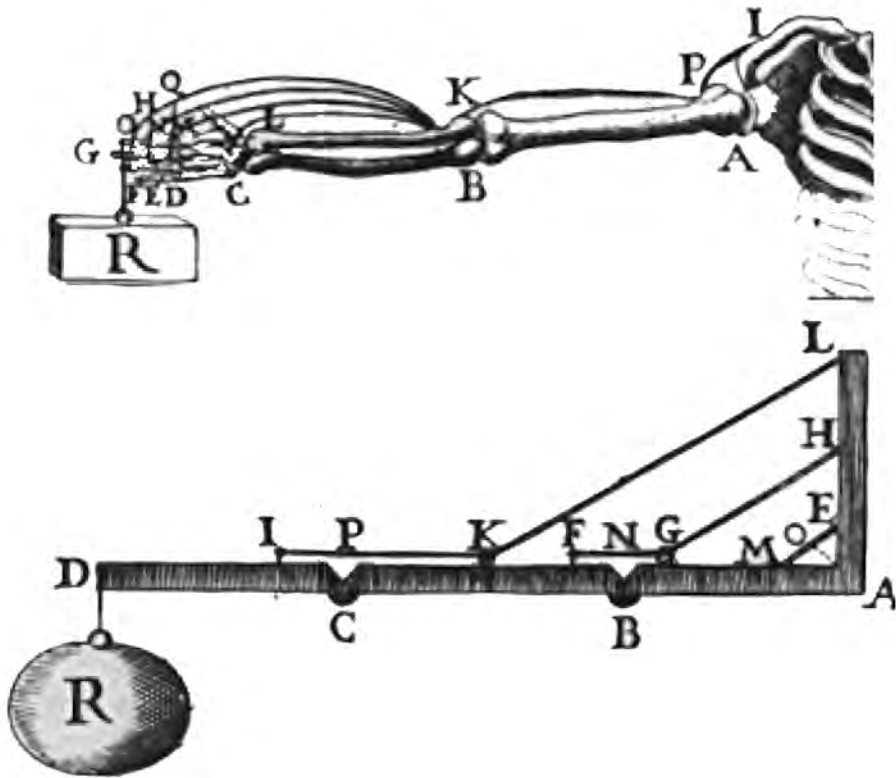


Figure 1.1 A schematic representation of a biomechanical model of the arm (detail from drawing by Borelli, 1679)

Although in modelling studies often more simplified one or two joint models have been used (Dul et al., 1984b; Challis and Kerwin, 1993; Raikova, 1996; Van den Bogert et al., 1999; Kistemaker et al., 2007), proper validation can only be done with large scale models, including all functions (degrees of freedom) of muscles.

Decreasing the actual number of degrees of freedom can lead to force-sharing solutions that cannot be extrapolated to the original system (Jinha et al., 2006b). Glitsch and Baumann (1997) concluded that even almost planar movements, such as walking and running, are associated with significant three-dimensional intersegmental moments, leading to an underestimation of internal loads up to 60% when a two-dimensional approach is used.

To date biomechanical models have been constructed, based on extensive geometrical data sets of the musculoskeletal system, including

muscle parameters such as the physiological cross sectional area, length and in some models even optimum length. To describe the muscle dynamics generally a Hill-type muscle is used which is a descriptive model, containing the non-linear force-length and force-velocity relationships. Although these models are generally assumed to be good models for the description of the force production behaviour of a muscle, they can not directly be linked to the metabolic behaviour of a muscle, or to the effect of metabolic parameters on the distribution of forces between muscles, if more than one muscle can be used for a given task (see Figure 1.1). These models therefore cannot be used to evaluate the relationship between mechanical constraints and metabolic constraints. This however would be very interesting to do. Veeger et al. (1992a, 1992b) showed that during manual wheelchair propulsion the propulsion force is not applied in the mechanically most effective way. It was hypothesised that the ineffective force propulsion is caused by a minimisation of energy expenditure of the muscles (Veeger et al., 1992a). To evaluate this hypothesis, a musculoskeletal model with both mechanical and physiological parameters would therefore be very useful. The morphology of musculoskeletal models, such as data on muscle attachment sites, muscle size and moment arms, are generally based on cadaver measurements. Although there have been several studies on muscle architecture and moment arms, (Amis et al., 1979; An et al., 1984; Veeger et al., 1991a; Murray et al., 1995; Pierrynowski, 1995; Ettema et al., 1998; Klein Breteler et al., 1999; Murray et al., 2000; Klein Horsman et al., 2007) the total amount of data suitable for modelling are limited and a large variance in the reported data is found. Most studies focus on one or two parameters only and on a limited number of muscles. In addition, the number of cadavers measured is in general limited. In general a model is based on a dataset from a single cadaver that is sometimes hardly representative for the total population. This means that the model is assumed to be a generic model, but the morphology of the model always differs somehow from the morphology of a specific subject.

The load sharing problem

Biomechanical models can be used as forward dynamic models as well as inverse dynamic models. In a forward dynamic model, muscle activation forms the input for the model and the external forces and motions are the model output. Next to the computational complexities of forward

dynamic analysis, this method is highly dependent on the link between an activation pattern and the muscle force generated by this activation pattern. Several muscle activation patterns can lead to the same movement, by different load sharing patterns. The actual activation pattern is unknown and has to be estimated somehow, which is usually done by optimisation.

Inverse dynamic models, where external forces and motions are used as input, can be used to estimate net joint moments and forces produced by muscles and ligaments. The model can calculate the net joint moments with simple Newtonian mechanics but it is unknown how these net joint moments are distributed over the individual muscle forces. In general, there are more muscles crossing a joint than is theoretically necessary in order to perform all possible movements. Take for instance a simple task in which an internal flexion moment around the elbow is required. Several muscles are crossing the elbow joint from which at least three muscles (the m. biceps brachii, the m. brachioradialis and the m. brachialis) are capable of generating the required flexion moment (Figure 1.1). It is unknown how the net moment is distributed over these three muscles. This is called the indeterminacy problem or load sharing problem. A common way to solve this problem is to use optimisation techniques. Based on the fact that general movement patterns can be observed (Bernstein, 1967), it is assumed that the central nervous system controls the musculoskeletal system in an optimal manner, optimising a certain cost or objective. In order to do this a mathematical criterion (cost function) is formulated, which has to be optimised. Finding the right criterion, that predicts the real situation, is however not an easy task. The physiological criteria are still unknown and to date only assumptions have been made. These assumptions are generally based upon experimental findings or upon a physiological belief that it will result in an adequate prediction.

Cost functions

Many different cost functions have been proposed (see Tsirakos et al., 1997 for an overview). Most optimisation criteria are chosen rather arbitrary, which is probably also partly caused by the fact that the utility of the cost function depends on the computability as well. Especially for submaximal activities it is often assumed that movements are performed while minimising energy consumption (Hardt, 1978; Van der Helm, 1991; Alexander, 1997). Most cost functions are mechanical cost functions,

based on muscle force, and therefore cannot directly calculate energy consumption. A criterion with muscle force only, does not account for any physiological capabilities or functional properties (Tsirakos et al., 1997). Since a cost function, that does not take the physiological capabilities of the muscles into account, might provide physiologically or mechanically unrealistic results, muscle force (F) is often weighted by physiological cross sectional area (PCSA) or maximal force (F_{\max}).

These functions have been used as linear as well as non-linear functions. Linear cost functions are not satisfactory since they do not predict synergistic muscle activation; they predict activity of only one muscle for each degree of freedom: the muscle with the minimum cost (the cheapest muscle). This preferred muscle is activated before the others and the other (second-best) muscles are only activated (one by one) when the first muscle reaches its maximum (sequential recruitment). This does not correspond to experimental results. Non-linear cost functions provide more physiologically realistic results. They lead to predictions in which synergistic muscles are activated and the preferred muscle only produces a larger force than the other muscles. The power of the non-linear criterion does not affect the load sharing extensively, but merely influences the magnitude of the muscle forces (Crowninshield and Brand, 1981; Challis and Kerwin, 1993; Tsirakos et al., 1997).

The effect of a cost function on the distribution of muscle forces around a joint will depend on the distribution of muscle forces around adjacent joints, based on the special function of bi-articular muscles. Furthermore, the number of degrees of freedom used for a single joint is also of great influence. Buchanan and Shreeve (1996) showed that the muscle coordination predictions are strongly dependent on the number of degrees of freedom balanced and that this even has a much larger influence on the predicted force distribution than the cost function used. Jinha et al. (2006a) also have shown that muscle activity predictions, using a one or two degrees of freedom modelling approach, do not lead to valid predictions when more multiple degrees of freedom were present in the system. As a consequence, the effect of cost functions should ideally be studied with the help of models that include all degrees of freedom instead of using simple one- or two joint models. In addition, optimisation predictions also depend on the morphological parameters used (Brand et al., 1986; Herzog, 1992; Buchanan and Shreeve, 1996; Raikova and Prilutsky, 2001).

In most cost functions used in the literature, muscle size is not taken into account, although this can be a factor of great influence, especially

when assuming that energy consumption is minimised. Muscle dimension is partly included in cost functions using the PCSA, but muscle length is usually not included. When two muscles with identical PCSA but different fibre length are maximally stimulated they will produce the same force. The energy cost of the muscle with the shortest fibres will, however, be less than the energy cost of the muscle with the larger fibres. The latter muscle has more sarcomeres in series and the metabolic cost is the summed cost over the activated sarcomeres. Therefore, not only the PCSA, representing the cross-bridges that are parallel, should be included into the optimisation criterion, but also a variable related to muscle fibre length, which is related to the number of sarcomeres in series. This has been previously suggested by Happee and Van der Helm (1995) who introduced a metabolic criterion, minimising the active state weighted by muscle volume. Simulations supported this weighting; however, these simulations were unfortunately not validated with metabolic measurements.

The validation issue

Despite the uncertainty related to their validity, the widespread use of cost functions is not surprising because of the difficulties related to proper validation of these cost functions. Validation is difficult since force of even a single muscle can not easily be measured *in vivo*. As an alternative, in general validation is done with electromyography (EMG) measurements, but EMG only provides a relative measure for muscle activation and not a direct measure of muscle force.

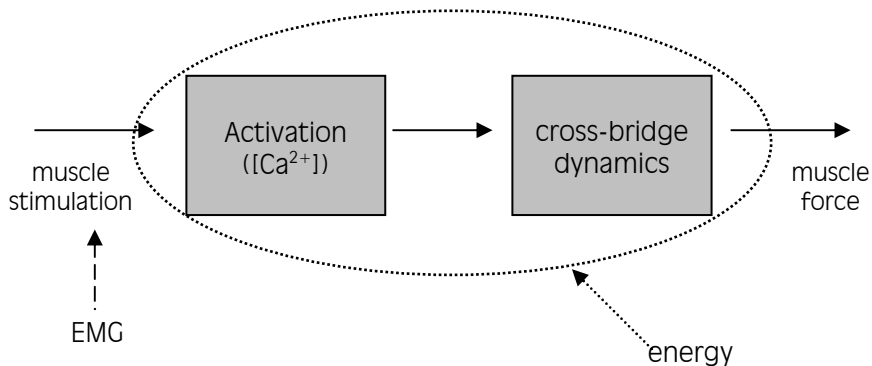


Figure 1.2 Schematic representation of the two main energy-consuming processes of muscle contraction resulting in force production: activation (re-uptake of calcium) and cross-bridge dynamics (detachment of cross-bridges). EMG measurements are related to the muscle stimulation.

The process of muscle contraction and force production (Figure 1.2) starts with an action potential which initiates a calcium flow from the sarcoplasmic reticulum (SR) into the cellular medium. The calcium ions (Ca^{2+}) bind to the troponin molecules, located on the actin filaments, which enables the actin filaments to attach to the myosin filaments. Subsequently, cross-bridges are created which are able to generate force. The Ca^{2+} need to be pumped back into the SR and the cross-bridges need to be detached, which are the two main energy-consuming processes of muscle contraction (Figure 1.2). EMG records only the electrical activity of the action potentials. The exact relationship between the EMG signal and the Ca^{2+} flow or cross-bridge attachment is unknown.

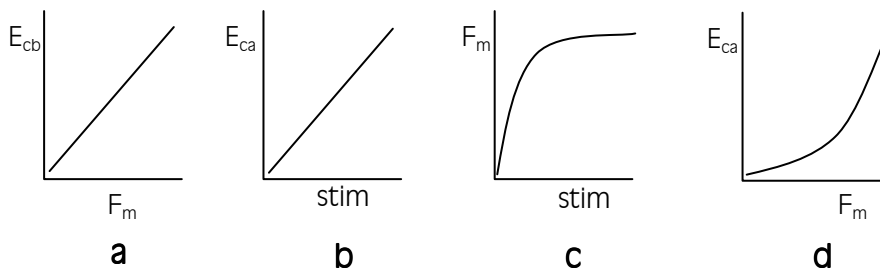


Figure 1.3 E_{cb} (energy consumed by the detachment of cross-bridges) is linearly related to muscle force (F_m) (a). E_{ca} (the energy consumed by the Ca^{2+} re-uptake) is assumed to be non-linearly related to F_m (d), based on the linear relationship between E_{ca} and stimulation frequency (stim) (b) and the non-linear relationship between F_m and stim (c). See text for further explanation.

The energy needed for the detachment of cross-bridges (E_{cb}) is linearly related to the muscle force (F_m) (Huxley, 1957) (Figure 1.3a). The relationship between the energy needed for the Ca^{2+} re-uptake (E_{ca}) is not exactly known, however it can be assumed that this will be a non-linear relationship. From in vitro studies it is known that E_{ca} is linearly related to stimulation frequency (stim) (Figure 1.3b). An increase of stimulation frequency leads to an increase of calcium flow and therefore an increase of E_{ca} . Muscle force on the other hand, is not linearly related to stimulation frequency (Blinks et al., 1978) (Figure 1.3c). At higher stimulation frequencies not all of the released Ca^{2+} is able to bind to the actin filaments and therefore muscle force does not increase directly proportional to stimulation frequency. This means that at higher forces E_{ca} would increase exponentially (Figure 1.3d).

Little is known yet about the relation between E_{cb} and E_{ca} in vivo. In vitro studies have shown that during isometric contractions at optimum muscle length 25 to 40% of the total energetic cost is consumed by the re-uptake of Ca^{2+} (Homsher and Kean, 1978; Wendt and Barclay, 1980; Woledge et al., 1985; De Haan et al., 1986; Lou et al., 1997)

Goal of the study

As mentioned above, it is often assumed that, within given task constraints, movements are performed minimising energy consumption (Hardt, 1978; Van der Helm, 1991; Alexander, 1997). Instead, most cost functions that are used today are mechanical cost functions and although some of them are assumed to be related to physiological costs like energy consumption or fatigue (Dul et al., 1984a, 1984b; Happee and Van der Helm, 1995; Alexander, 1997) clear relationships have not been proven.

The main objectives of the research described in this thesis are:

1. to define a cost function that represents muscle energy consumption and
2. to validate this cost function with a metabolic variable.

A cost function that is based on physiological properties (instead of on muscle behaviour) is preferred since in that way the model can also be used to analyse the relationship between the mechanical and physiological characteristics of muscle function.

This requires:

1. a biomechanical model that represents a complete musculoskeletal system, including all muscles and degrees of freedom. The model should be capable of simulating complex movement tasks.
2. a metabolic parameter that can be measured in vivo and can be used to validate the model predictions performed with the energetic cost function.
3. an experimental set-up to collect the data needed for validation, which should include complex tasks, covering a large variation in moment combinations.

Approach

Modelling

For the research described in this thesis a general biomechanical model is used: the Delft Shoulder and Elbow Model (DSEM), in combination with individual experimental data. The DSEM is a 3D inverse dynamic musculoskeletal model of the upper extremity (Van der Helm, 1994a, 1997b). The model consists of seven bony structures (thorax, scapula, clavicle, humerus, ulna, radius and hand) and 31 shoulder and elbow muscles, divided into 139 muscle elements. Morphological data for the model, such as the geometry of bones and muscles, physiological cross sectional area (PCSA), muscle attachment sites and the rotation centre of the joints, were taken from cadaver studies (Veeger et al., 1991a; Van der Helm et al., 1992; Veeger et al., 1997).

Input for the inverse dynamic version of the DSEM consists of motion data as well as external forces and moments. Output of the model comprises variables such as muscle lengths, moment arms, net joint moments and joint reaction forces. The muscle forces are calculated by means of an optimisation method.

To date the model has been used for applications in the fields of rehabilitation, orthopaedics and ergonomics (Kuijjer et al., 2003; Hoozemans et al., 2004; Magermans et al., 2005; Van Drongelen et al., 2005b, 2006). In addition, the model offers the opportunity to evaluate and preferably validate the effect of different cost functions on individual force predictions (Happee and Van der Helm, 1994).

Near InfraRed Spectroscopy

Since EMG provides neither quantitative information on muscle force, nor on the energy consuming processes of muscle contraction, it would be better to validate a metabolic cost function with a metabolic variable. A possible method to gain information on muscle energy consumption is Near InfraRed Spectroscopy (NIRS). NIRS is a non-invasive technique which can be used to obtain information on the oxygenation of muscle tissue.

In NIRS, Near infrared light is transmitted through the muscle by two fibre-optic cables (optodes), one for the incoming light and one for the outgoing light (Figure 1.4). In the muscle, part of the light will be scattered and part of it will be absorbed by structures, so-called chromophores, in the muscle. By choosing distinct wavelengths of near infrared light and with the knowledge of the chromophores that absorb that specific light, it becomes possible to measure concentration

changes of these chromophores. The main chromophores that absorb near infrared light are oxyhaemoglobin (O_2Hb) and deoxyhaemoglobin (HHb).



Figure 1.4 *In NIRS measurements, two fibre optic cables (optodes) are placed on the skin above the muscle; one for the incoming light and one for the outgoing light. In this way information on the oxygenation of the muscle can be obtained.*

By measuring the absorption changes at at least two wavelengths these changes can be converted into changes in $[O_2Hb]$ and $[HHb]$, making use of the Lambert-Beer law (Colier et al., 1992). The NIRS measurements performed in this thesis have been done by the arterial occlusion method. By applying an arterial occlusion to the limb the venous outflow and arterial inflow is blocked. This is seen as a decrease of $[O_2Hb]$, since the oxygen is consumed by the muscle and no fresh blood is entering the limb (figure 1.5). This decrease of $[O_2Hb]$ is of course accompanied by a corresponding increase of $[HHb]$. The decrease of $[O_2Hb]$ starts linear and finally levels off when the oxygen supply stops and anaerobic energy production becomes more important. From the gradient of the linear part of the $[O_2Hb]$ decrease, the oxygen consumption per unit of time ($\dot{V}O_2$) can be calculated.

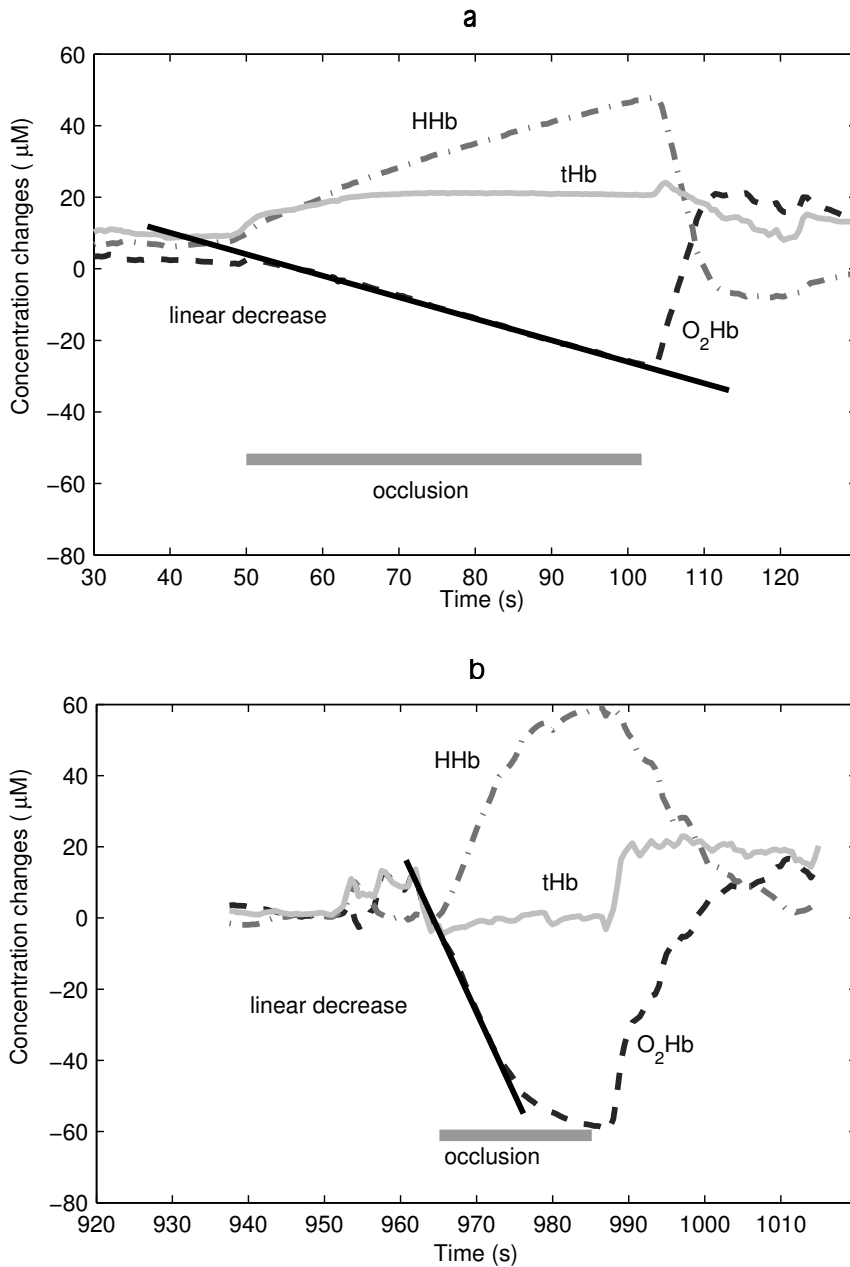


Figure 1.5 Changes in concentrations of oxyhaemoglobin (O_2Hb), deoxyhaemoglobin (HHb) and total haemoglobin (tHb) in response to arterial occlusion during rest (a) as well as during exercise (b). When the occlusion is applied, $[\text{O}_2\text{Hb}]$ starts to decrease linearly and finally levels off (b). $\dot{V}\text{O}_2$ is calculated over the period of linear decrease only. During exercise (b) the oxygen consumption is higher than during rest, which is reflected by the fact that the slope of the decrease is much steeper.

NIRS has mainly been used to monitor oxygenation of the brain, but in the last couple of years it has also become an accepted technique for the determination of local muscle $\dot{V}O_2$ (De Blasi et al., 1993, 1994; Colier et al., 1995). It has been shown that NIRS is able to discriminate between the resting and the exercising states of the muscle and between physically active and less active muscle (Van Beekvelt et al., 2001). No significant differences were found between measurements, repeated at three different days (Van Beekvelt et al., 2002). Our own experiments, in which we repeated measurements for two subjects on two separate days, also showed that NIRS is a reliable method (ICC=0.9). Little is known yet about the relationship between muscle $\dot{V}O_2$ and external force, or muscle activation as measured by EMG.

Experimental set-up

The experimental measurements were to a large extent predefined by the choice to use NIRS. Since an arterial occlusion had to be applied, which can only be done by using an inflatable cuff around the arm, measurements were restricted to elbow muscles. Arterial occlusion was applied for short periods of force contraction (20-60 seconds) which had to be followed by a period of rest of 3-5 minutes. Therefore measurements were very time consuming. In addition, at the most two muscles could be measured simultaneously.

For validation purposes, the experimental task should not only be limited to moment production around one degree of freedom, but should cover a large series of moment combinations. More specifically, our experiments should comprise not only flexion-extension moments, but also pronation-supination moments AND the combination of these two. To investigate the influence of moment arm and muscle length elbow angle had to be varied as well.

The above constraints amounted in the following experimental set-up: Subjects were seated on a chair with their elbow flexed and their forearm in a horizontal and neutral position (Figure 1.6). The subjects had to generate several flexion/extension moments around the glenohumeral joint and pro/supination moments around the radio-ulnar joint as well as combinations of these moments. EMG and NIRS recordings were performed on several elbow muscles.

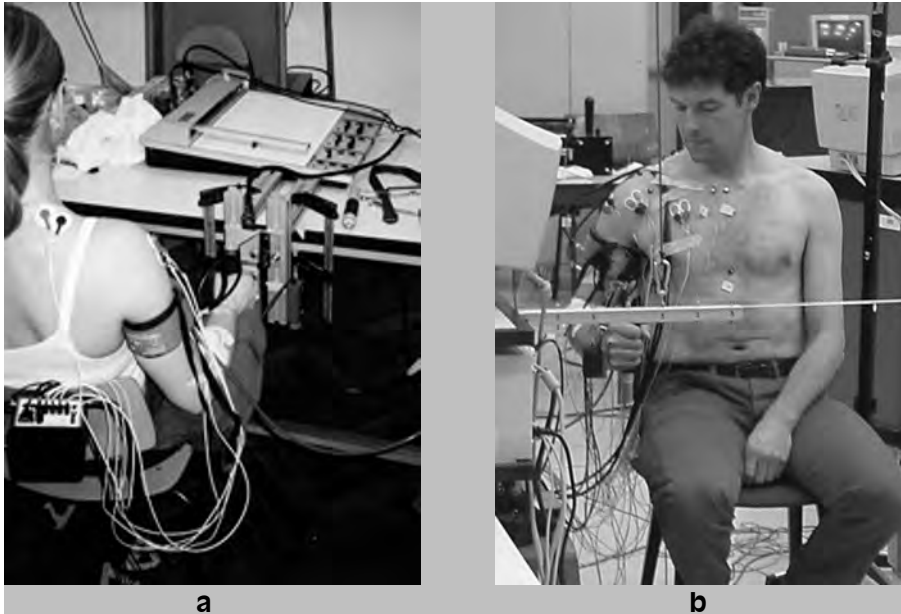


Figure 1.6 *Experimental set-up. Subjects were sitting on a chair with their elbow flexed and their forearm in a horizontal and neutral position. Moments had to be applied to a vertical handle, which was fixed to a six-degree-of-freedom force transducer (a, chapter 2 and 3) or were enforced by holding a vertical beam to which weights could be fixed at various positions (b, chapter 4 and 5).*

Outline of this thesis

In the present thesis we try to define a cost function that represents muscle energy consumption and to develop a method to validate such a cost function with measurements on muscle oxygen consumption determined with NIRS. Up till now cost functions never had been validated with a metabolic variable and validation was generally done with EMG. The relationship between NIRS and EMG is unknown. Since EMG and $\dot{V}O_2$ reflect different processes in the muscle, it is likely that these two variables show different results. Therefore in Chapter 2 we analyse the relationship between EMG and $\dot{V}O_2$ as well as the relation between $\dot{V}O_2$ and external moment.

One of the most commonly used cost functions is the stress cost function, minimising the sum of squared muscle stress ($\sum(F/PCSA)^2$).

Although it has been suggested that this cost function is related to energy consumption clear relationships have never been proven. In Chapter 3 we investigate whether this stress cost function is indeed related to $\dot{V}O_2$. We also propose a new cost function, based on the two major energy consuming processes in the muscle (activation and muscle force). For this energy-related cost function the relationship with $\dot{V}O_2$ is also studied. Chapter 2 and 3 focus on isometric measurements at constant elbow angle and therefore, constant muscle length. Chapter 4 and 5 are based on more extensive experiments in which elbow angle (affecting muscle length and moment arm) is varied. In Chapter 4, we investigate how this influences the load sharing between muscles. Besides the choice of cost function the set of morphological parameters will define the predicted force patterns as well. In Chapter 5, the influence of PCSA and muscle moment arm on the predicted force distribution, using both cost functions, is studied. Furthermore, it is investigated whether differences in force patterns between individual subjects can be (partly) explained by differences in morphology. Finally in chapter 6, the main findings of this thesis are summarised and discussed, and the implications of this thesis for further research are discussed.



Chapter 2

Muscle oxygen consumption, determined by NIRS, in relation to external force and EMG

M. Praagman, H.E.J. Veeger, E.K.J. Chadwick, W.N.J.M. Collier and F.C.T. van der Helm (2003).
Journal of Biomechanics, 36(7), p.905-912

Abstract

Local oxygen consumption in a muscle ($\dot{V}O_2$) can be determined by Near InfraRed Spectroscopy (NIRS). In principle it should be possible to use this measure to validate musculoskeletal models. However, the relationship between $\dot{V}O_2$ and external force, or between $\dot{V}O_2$ and surface electromyography (EMG), as a measure for muscle activity, is hardly known.

The aim of this study was: (1) to evaluate the characteristics of the relationship between $\dot{V}O_2$ and external moments and (2) to determine whether differences exist between the EMG-moment relationship and the $\dot{V}O_2$ -moment relationship.

Subjects (n=5) were asked to perform isometric contractions exerting combinations of elbow flexion and pro/supination moments at force levels up to 70% of their maximum. Simultaneous surface-EMG and Near InfraRed Spectroscopy (NIRS) measurements were performed on the m. biceps brachii caput breve (BB) and the m. brachioradialis (BR). A linear relationship was found between EMG and $\dot{V}O_2$. For BB $\dot{V}O_2$ and EMG were linearly related to both the flexion moment and the pro/supination moment. However, for the BR only a linear relationship with flexion moment was found. As expected, based on the findings above, the relationship between $\dot{V}O_2$ and elbow flexion moment can be described by a linear equation, under the conditions of this study (isometric, and force levels up to 70%).

These findings suggest that load-sharing is independent of force level and that next to EMG, $\dot{V}O_2$ can be used for the validation of musculoskeletal models.

Introduction

In biomechanical studies inverse dynamic models are often used to predict muscle forces. These models make use of optimisation criteria, or cost functions, to calculate the distribution of those forces among the muscles. Unfortunately, muscle forces cannot be easily measured in vivo, which hampers model validation. As an alternative, electromyography (EMG) is often used for model validation, but EMG does not provide direct information about the magnitude of the muscle force. EMG registers the electrical activity of action potentials, which initiate the process of muscle contraction and force production. Due to the action potential, a calcium flow from the sarcoplasmic reticulum is initiated. These calcium ions bind to the troponin molecules, located on the actin filaments, which enables the actin filaments to attach to the myosin filaments. Subsequently cross-bridges are created and are able to generate force. The exact relationship between the EMG signal and the calcium flow or cross-bridge attachment is unknown. Nevertheless it is generally accepted that, for isometric conditions and when the EMG signal is sufficiently smoothed, the relationship between EMG amplitude and applied force is linear (De Luca 1997).

Two processes initiated by the action potential, and resulting in force production, require energy. First of all calcium ions have to be transported back into the sarcoplasmic reticulum by a calcium pump and, secondly, the detachment of cross-bridges requires adenosine triphosphate (ATP). With an increase in the excitation of the muscle, calcium flow also increases, enabling more cross-bridges to attach and resulting in a higher force. However, it is not known whether the energy required to transport calcium back into the sarcoplasmic reticulum increases proportionally with excitation. It might be that at higher excitation levels the increase in energy consumption is higher than the increase in excitation and force. With Near InfraRed Spectroscopy (NIRS) an indication of this energy consumption can be achieved.

NIRS is a non-invasive technique from which information can be obtained about the oxygenation of a biological tissue, such as muscle tissue. Biological tissue is relatively transparent for light in the near infrared region. When the light is transmitted through the tissue, part of it is absorbed and part of it is scattered. The absorption depends on the amount of oxygen that is present in the tissue. By measuring the absorption changes at three different wavelengths (905, 850 and 770 nm), these changes can be converted into changes in the concentration of oxyhaemoglobin (O_2Hb) and deoxyhaemoglobin (HHb), making use of

the Lambert-Beer law (Colier et al. 1992). The Lambert-Beer equation modified for light scattering media describes the relationship between the concentration of a chromophores (c) and recovered light:

$$C = \frac{OD_{\lambda} - OD_{r,\lambda}}{\epsilon_{\lambda} \cdot L \cdot DPF} \quad (2.1)$$

where OD_{λ} (optical density) is the absorption of the light, ϵ_{λ} is the extinction coefficient of the chromophore and L is the distance between the optodes. DPF (Differential Path-length Factor) accounts for the increase in optical path-length due to scattering in the tissue and $OD_{r,\lambda}$ represents the oxygen-independent light losses due to scattering in the tissue.

When measurements are done during arterial occlusion and the DPF is known, it is possible to quantify muscle oxygen consumption. The blood supply to the muscle ceases due to the occlusion, therefore the decrease of $[O_2Hb]$ reflects the oxygen consumption of the muscle. From the gradient of the $[O_2Hb]$ decrease, the oxygen consumption per unit of time ($\dot{V}O_2$) can be calculated. The DPF values for several muscles have been measured in previous studies (Ferrari et al. 1992; Van der Zee et al. 1992; Duncan et al. 1995).

NIRS has been mainly used to monitor oxygenation of the brain, but in the last couple of years it has also become an accepted technique for the determination of local muscle $\dot{V}O_2$ (De Blasi et al. 1993; Colier et al. 1995; Van Beekvelt et al. 2001). NIRS is able to discriminate between the resting and the exercising states of the muscle and between physically active and less active muscle (Van Beekvelt et al. 2001). The relationship between muscle $\dot{V}O_2$ and external force, however, is seldom investigated. Colier et al. (1995) reported a linear relationship between $\dot{V}O_2$ and force for the soleus muscle during isometric contractions up to 20 % maximal voluntary contraction (MVC).

As described before, muscle $\dot{V}O_2$ provides information on a different level of muscle activation to EMG. It therefore is possible that this relationship differs from that between muscle $\dot{V}O_2$ and force. Only a few studies have combined NIRS measurements with EMG measurements, and EMG was mainly used to study muscle fatigue in these studies (Alfonsi et al. 1999; Felici et al. 2001; Yoshitake et al. 2001). Apart from one study in which relative oxygenation was measured (Miura et al. 2000), no attention was paid to the relationship between EMG and muscle oxygenation.

The purpose of the current study is to investigate the relationship between $\dot{V}O_2$ and force as well as between EMG and force for two elbow

flexors during isometric conditions. Measurements focus on the short head of the m. biceps brachii caput breve and on the m. brachioradialis during different isometric contractions at force levels ranging from 10% to 70% of maximal isometric force in a given direction. Flexion moments around the humero-ulnar joint as well as pro- and supination moments around the radio-ulnar joint will be imposed.

The following questions will be answered:

1. Is EMG linearly dependent on flexion moment and/or on pro/supination moment?
2. Is $\dot{V}O_2$ linearly dependent on flexion moment and/or on pro/supination moment?
3. Is there a correlation between EMG and $\dot{V}O_2$?
4. Can EMG be used to predict external flexion moments?
5. Can $\dot{V}O_2$ be used to predict external flexion moments?

Methods and materials

Set-up

Five subjects (3 male, 2 female) (age 22 ± 1 years) participated in this study after giving informed consent. Measurements were performed on two arm muscles, m. biceps brachii caput breve (BB) and m. brachioradialis (BR).



Figure 2.1 *Experimental set-up.*

Moments were measured using a vertical handle, which was fixed to a six-degree-of-freedom force transducer and placed in front of the subject. A plotter was placed in front of the subject to provide feedback on moment magnitudes.

The subjects were seated in a chair with their right arm slightly abducted and flexed forward and their forearm in a neutral and horizontal position, holding a vertical handle with their right hand. This handle was fixed to a six-degree-of-freedom force transducer, placed in front of the subjects (Figure 2.1). Subjects were instructed to perform three different isometric contractions, exerting a flexion moment around the humero-ulnar joint combined with different moments around the radio-ulnar joint: neutral, pronation and supination. All contractions were performed at seven different force levels, from 10 to 70% of their maximal moment. A 2D plotter provided feedback on the generated moments and their directions.

Protocol

The position of the subject's hand on the handle and the position of the chair on the ground were marked and a pointer at the Angulus Acromialis ensured that the subject did not change position during the recordings. Subjects were instructed to perform maximal flexion as well as maximal pro- and supination. On the plotter the flexion moments were marked on the x- axis and the pro- and supination moments on the y-axis (Figure 2.2). The zero-load position was defined as the position in which the subject was holding the force transducer, which implied a correction for the extension moment due to the weight of the arm. The trajectories of the combined moments were defined by the maximal moments of the separate contractions, illustrated by the dashed lines in Figure 2.2. This trajectory was marked on the plotter and the subjects were instructed to follow this line while exerting maximal moment, again this maximum was marked. Finally all the required percentages of the maximal moments the subject had to exert in the subsequent experimental sequence were marked on the plotter.

The experiment consisted of the same protocol for each of the three contractions. First an arterial occlusion was applied while the subject generated no force at all and his arm was resting in an arm support. Subsequently the subject had to perform the tasks consecutively at seven different force levels, from 10 to 70 % of their maximal moment. As soon as the required force level was achieved, an arterial occlusion was applied. The periods of occlusion and force production varied from 15 to 60 seconds depending on the force level (Table 2.1) and each period was followed by a period of rest to recover. At the end an arterial occlusion during rest was applied once again. The $[O_2Hb]$ and $[HHb]$ as well as the external forces and moments were recorded continuously; surface EMG was recorded during the periods of force production only.

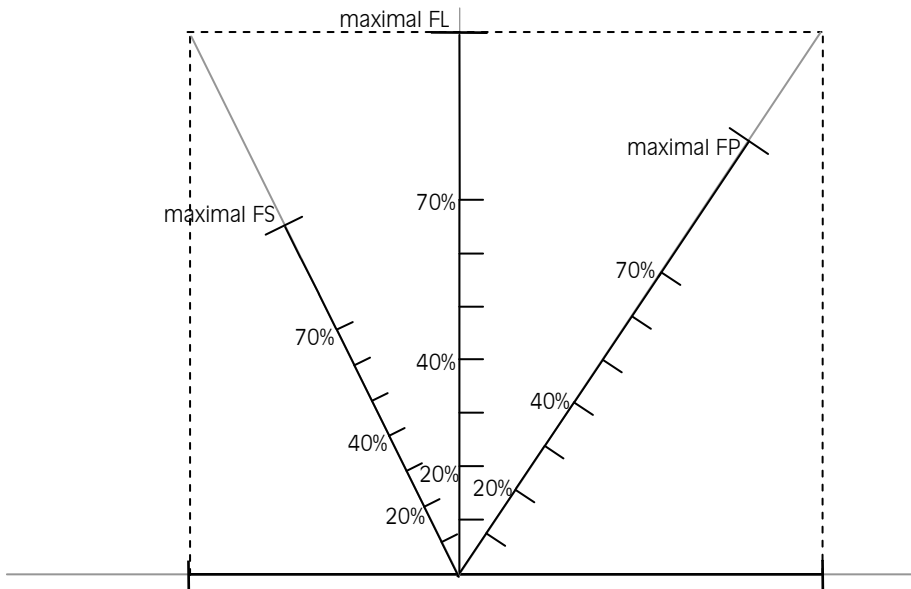


Figure 2.2 Illustration of the feedback information provided on a plotter. Flexion moments were marked on the y-axis and pro/supination moments on the x-axis. The trajectory of flexion-pronation and flexion-supination was defined by the maximal flexion moment and the maximal pro/supination moment. The force levels the subject had to produce were marked as percentages of their maximal moments.

Table 2.1 Duration of occlusion and recovery for each force level.

Force level (%)	Occlusion time (s)	Recovery time (s)
0	60	120
10	30	120
20	30	120
30	30	180
40	20	180
50	20	240
60	20	300
70	15	300

Data recording and processing

A six-degree-of-freedom force transducer (AMTI 500) recorded the forces and moments the subjects applied to the handle. Further, the surface EMG of the muscles was recorded (inter-electrode distance of 17 mm, sample frequency of 1000 Hz, analogue low-pass filter 400 Hz) and the muscle oxygenation was monitored with the help of Near-Infrared Spectroscopy (NIRS). Two continuous-wave near infrared spectrophotometers (OXYMON, Artinis Medical Systems, Arnhem, The Netherlands.) (Van der Sluijs 1998) were used in this study, which made it possible to measure the haemoglobin concentrations of two muscles simultaneously. Two fibre-optic cables (optodes), one for the incoming light and one for the outgoing light, were placed in a holder that was attached to the skin above the muscle (Figure 2.3). The cables were attached to the same segment as the optodes such that the angle of the optodes was fixed and could not change by any movement of the subject. The inter-optode distance was 4 cm and a DPF of 4.3 was used. Occlusion was applied by inflating a thin cuff, placed around the upper arm, to a pressure of at least 230 mmHg. During the occlusion the cuff pressure was monitored with a blood pressure device.



Figure 2.3 NIRS data were measured with fibre optic cables that were attached to the skin above BB and the BR. EMG electrodes were placed on the skin between the cables. A cuff around the upper arm was used to apply an arterial occlusion.

$\dot{V}O_2$ values were determined by performing regression on the linear part of the $[O_2HB]$ decrease immediately after occlusion (Figure 2.4). The slope of the decrease was taken as the $\dot{V}O_2$ of the muscle. The $\dot{V}O_2$ values are expressed as micromoles O_2 per second.

EMG signals were digitally high-pass filtered at 5 Hz, corrected for offset and rectified. Mean EMG values were calculated over the same time period as the oxygen consumption. EMG values were normalised, EMG of BB was expressed as a percentage of the EMG measured at 70% flexion-supination and EMG of the BR was expressed as a percentage of the EMG measured at 70% flexion.

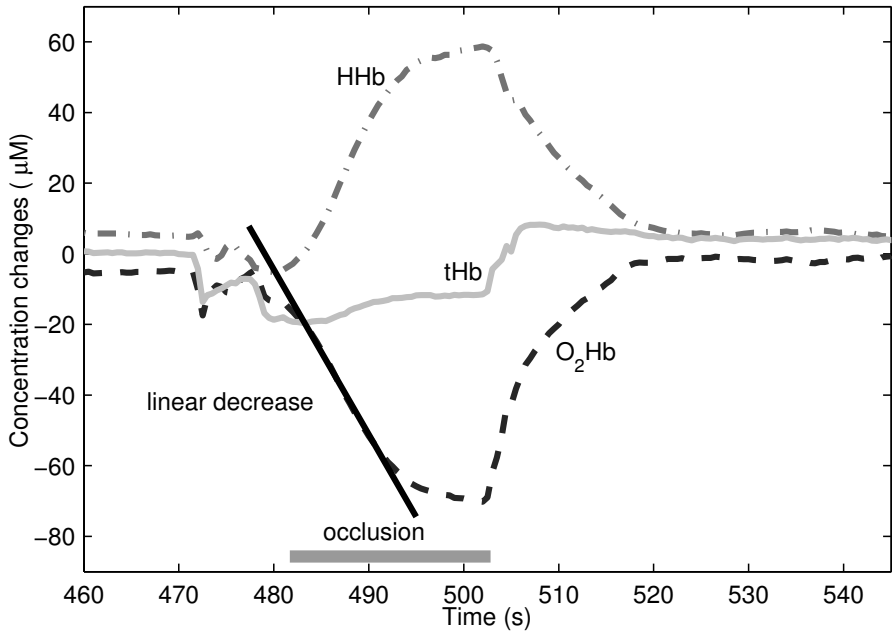


Figure 2.4 Changes in concentrations of oxyhaemoglobin (O_2Hb), deoxyhaemoglobin (HHb) and total haemoglobin (tHb) in response to arterial occlusion during flexion-supination (50% MVC). When the occlusion is applied, $[O_2Hb]$ starts to decrease linearly and finally levels off. $\dot{V}O_2$ is calculated over the period of linear decrease only.

Statistics

Stepwise regression analysis was used, for both muscles, to test whether EMG and $\dot{V}O_2$ were linearly dependent on flexion moment and pro/supination moment. For the evaluation of the relationship between EMG and $\dot{V}O_2$, $\dot{V}O_2$ values were normalised. For each subject and each muscle, $\dot{V}O_2$ values were expressed as percentages of the highest value of that muscle. Correlation between normalised $\dot{V}O_2$ and EMG was

calculated and the relationship between normalised $\dot{V}O_2$ and EMG was evaluated by regression.

Polynomial stepwise regression was used to test whether the relationship between EMG and flexion moment was linear or non-linear and whether EMG can be used to predict flexion moment. This was done for the conditions in which only an elbow flexion moment was imposed. The same was done for the $\dot{V}O_2$ values. Significance level was set to $p < 0.05$.

Results

Elbow flexion moments up to 41.8 ± 10.5 Nm were recorded, while supination and pronation moments varied between -4.0 ± 1.1 Nm and 5.3 ± 1.6 Nm (Figure 2.5).

Since $\dot{V}O_2$ values measured during rest showed little variation during the whole experiment, it was assumed that the recovery periods in between the occlusion periods were long enough and the results were not influenced by fatigue.

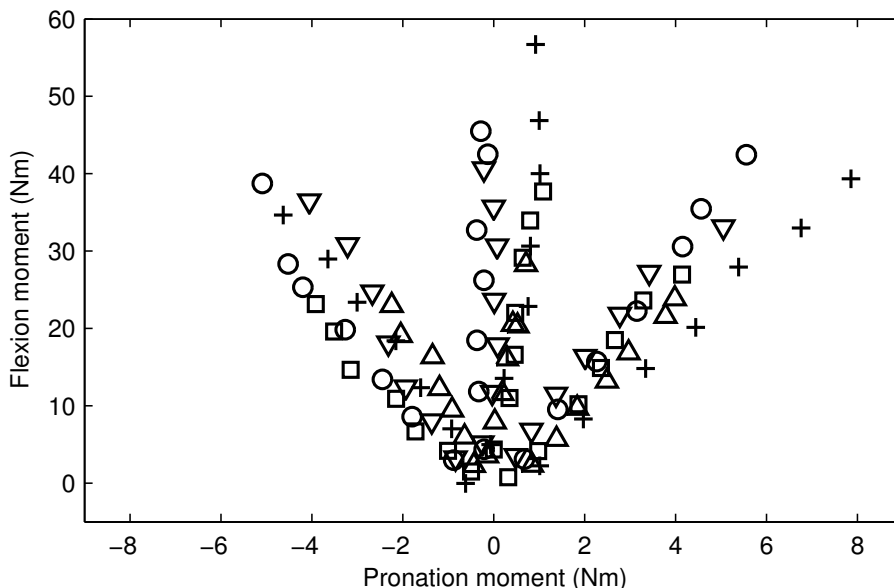


Figure 2.5 External moments produced by the subjects. The five different symbols represent the five different subjects.

As expected, both EMG and $\dot{V}O_2$ increased with increasing load. This applied for all three conditions and for both BB and BR. (Figures 2.6 and 2.7). For BB both $\dot{V}O_2$ and EMG were linearly dependent on flexion moment and pro/supination moment. For BR, EMG and $\dot{V}O_2$ were linearly dependent on the flexion moment only (Table 2.2). A high correlation was found between EMG and normalised $\dot{V}O_2$ values and regression showed a linear relationship for both muscles:

$$\dot{V}O_{2\text{bb}} = 15.32 + 0.55 \text{EMG}_{\text{bb}}, \quad (2.2)$$

($p \leq 0.01$, SE = 12.03 % and $r=0.81$) for BB and:

$$\dot{V}O_{2\text{br}} = 4.48 + 0.87 \text{EMG}_{\text{br}}, \quad (2.3)$$

($p \leq 0.01$, SE=6.98 % and $r=0.94$) for BR.

To evaluate whether EMG or $\dot{V}O_2$ can be used to predict the external flexion moment a polynomial stepwise regression was performed. Three dependent variables were entered: x , x^2 and x^3 , in which x represented EMG or $\dot{V}O_2$. This was only done for the condition with no pro- or supination moment because for the pro/supination moment conditions no distinction can be made between the activation of the muscle used for the flexion moment and the activation used for the pro/supination moment. Entering a cubic term led to a significantly stronger relationship only for the EMG of BB and for the $\dot{V}O_2$ of BR. Quadratic terms did not contribute significantly to the relationships (Table 2.3).

Table 2.2 Regression equations, standard errors of estimate (SE) and correlation coefficients (r) for the relationship between EMG or $\dot{V}O_2$ and flexion moments (Mfl) and pro/supination moments (Mps). The relationship is defined by the equation: $\text{EMG or } \dot{V}O_2 = a + b \cdot \text{Mfl} + c \cdot \text{Mps} + d \cdot \text{Mfl} \cdot \text{Mps}$. *: $p \leq 0.05$.

Muscle	Parameter	a	b	c	d	SE	r
BB	$\dot{V}O_2$ ($\mu\text{M/s}$)	4.97*	0.66*	-1.44*	-	7.69	0.74*
	EMG (%)	4.58	1.85*	-3.79*	-	18.32	0.79*
BR	$\dot{V}O_2$ ($\mu\text{M/s}$)	1.27	0.55*	-	-	5.47	0.78*
	EMG (%)	-2.28	1.55*	-	-	9.97	0.89*

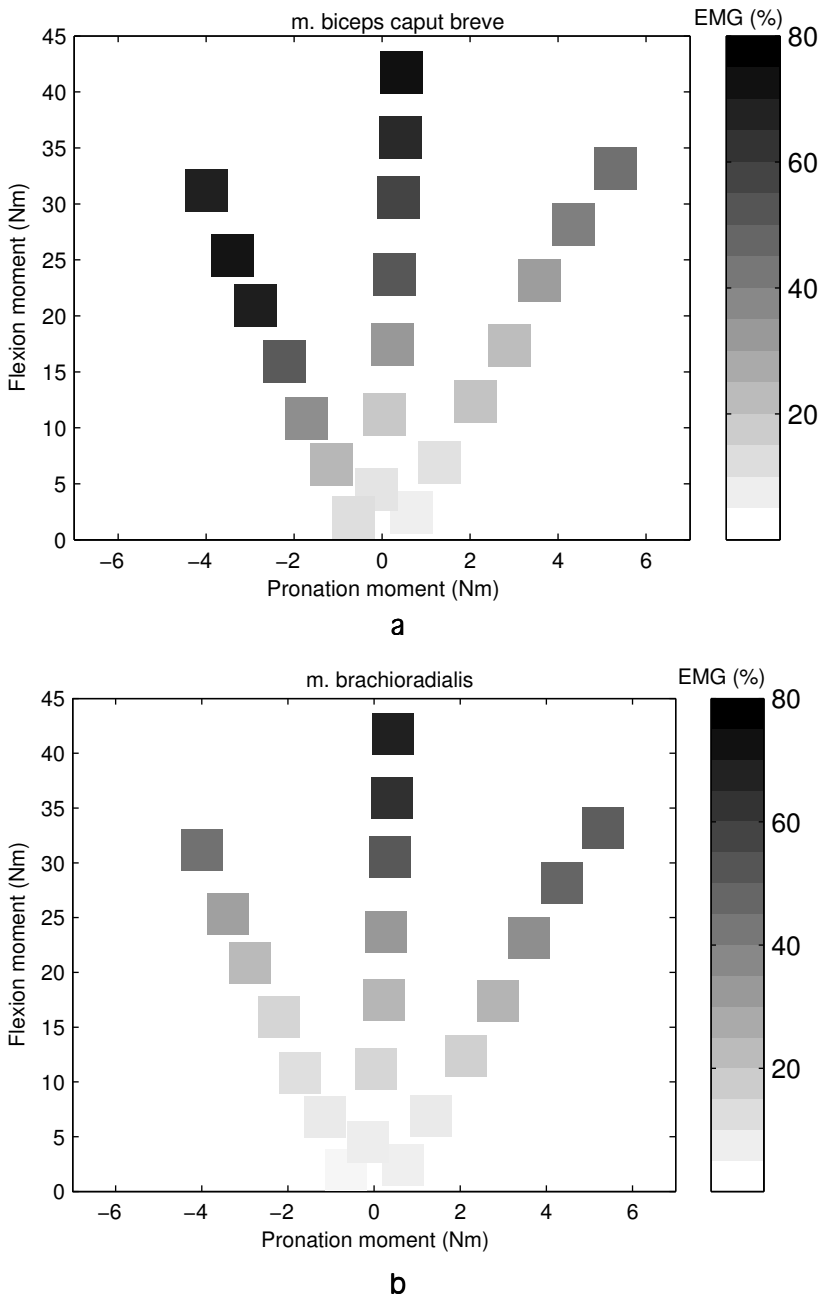


Figure 2.6 EMG values for BB (a) and BR (b), averaged over subjects, plotted against the generated combination of moments. The magnitude of the EMG is represented by a greyscale.

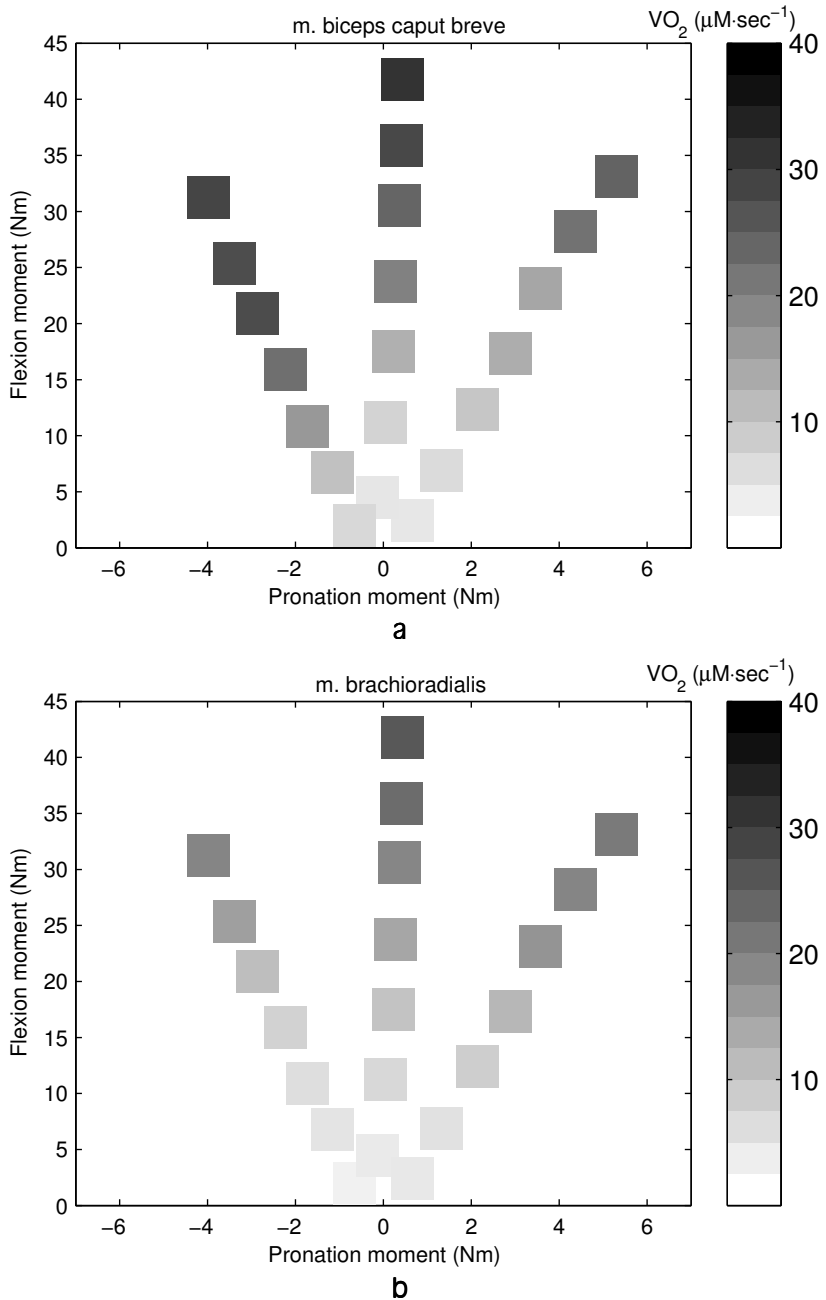


Figure 2.7 $\dot{V}O_2$ values for BB (a) and BR (b), averaged over subjects plotted against the generated combination of moments. The size of the $\dot{V}O_2$ is represented by a greyscale.

Table 2.3 Results of polynomial stepwise regression; correlation coefficients (r) and regression equations for the relationship between flexion moment (Mfl) and EMG or $\dot{V}O_2$. The relationship is defined by $Mfl (Nm) = a + bx + cx^2 + dx^3$, in which x represents EMG or $\dot{V}O_2$. *: $p \leq 0.05$.

x	Muscle		a	b	c	d	SE (Nm)	r
EMG	BB	Linear	8.88*	0.33*	-	-	8.45	0.80
		Non-linear	4.16	0.53*	-	$-1.57 \cdot 10^{-5}$ *	7.79	0.84
	BR	Linear	3.90*	0.53*	-	-	5.66	0.92
$\dot{V}O_2$	BB	Linear	7.89*	0.86*	-	-	9.73	0.73
	BR	Linear	4.09	1.35*	-	-	7.28	0.86
		Non-linear	-0.12	1.93*	-	$-6.23 \cdot 10^{-4}$ *	6.79	0.88

Discussion

In this study muscle oxygen consumption was measured with NIRS during arterial occlusion. Immediately after the occlusion was applied $[O_2Hb]$ started to decrease linearly (Figure 2.4). This linearity indicates that the oxygen consumption was constant (force remained constant) and that there was enough oxygen available in the muscle. The latter implies that the energy needed was mainly provided by oxygen phosphorylation. After some time (depending on the force level) the $[O_2Hb]$ levelled off, indicating a decrease in oxygen consumption. If force were then to remain constant, the contribution of the anaerobic processes would have to increase. $\dot{V}O_2$ values used in the present study were calculated over the period of linear decrease of $[O_2Hb]$ only, in which the energy consumption was mainly dependent on the aerobic processes, complemented with a small (and constant) anaerobic component. It is therefore assumed that the measured $\dot{V}O_2$ gives a good indication of the energy consumption.

NIRS as well as EMG measurements were made on the m. biceps brachii caput breve and the m. brachioradialis. Subjects were seated with the elbow flexed and the forearm in a neutral position and had to generate flexion moments as well as pro- and supination moments. From a mechanical point of view there are several muscles that could be expected to contribute to the required flexion moment: the m. biceps brachii caput breve (BB) and caput longum (BL), the m. brachioradialis (BR) and the m. brachialis (BA). It is expected that pronation moments

will mainly be generated by the m. pronator teres and the m. pronator quadratus. Due to the neutral position of the forearm the BR is not expected to contribute to a pro- or supination moment. Supination moments will be generated by the m. supinator and BB and BL.

It was expected that both the force level and the pro/supination moment would influence the activity of BB and BR. A higher force level would lead to a higher EMG signal as well as a higher $\dot{V}O_2$. Furthermore, it is likely that the imposed pro/supination moment would greatly influence the activity of BB and therefore indirectly the activity of the BR. Due to its supination effect BB would be less active during flexion-pronation and more active during flexion-supination compared to elbow flexion only. If BB (and BL) is less active during flexion-pronation, the other flexors (BR and BA) will have to contribute more to produce the required flexion moment.

From figure 2.6 it can be seen that indeed both the flexion moment and the pro/supination moment influence the EMG amplitude. Regression showed that the size of the EMG signal of BB was linearly related to both the flexion moment and the pro/supination moment (Table 2.2). This implies that EMG increased with flexion moment, but also with supination moment: EMG amplitude was lowest for flexion-pronation and largest for flexion-supination (moment). Although it was expected that BR would compensate for the decrease of the activity of BB during flexion-pronation this was not shown. For BR only a significantly linear relationship with flexion moment was found: the EMG amplitude of BR increased with flexion moment but not with supination moment since BR showed most activity during flexion only. It must be assumed that BA compensated for the loss of flexion moment of BB. The same results were found for $\dot{V}O_2$ (Figure 2.7 and Table 2.2).

EMG reflects the electrical activity of a muscle whereas $\dot{V}O_2$ reflects the energy consuming processes in that muscle (calcium pump and cross-bridge dynamics). Therefore, it would have been possible for these two variables to show different results. However, for the isometric conditions investigated in the current study it turns out that EMG and $\dot{V}O_2$ give comparable results (Figures 2.6 and 2.7). For both muscles, a high correlation between EMG and $\dot{V}O_2$ was found and regression showed a linear relationship (Equations 2.2 and 2.3). This corresponds to findings of Miura et al. (2000) who reported a high negative correlation between integrated EMG and the percentage of O_2Hb . The linear relationship between EMG and $\dot{V}O_2$ together with the linear relationship of both variables with external force suggests that for isometric conditions up to 70 % MVC the energy consuming processes (calcium pump and cross-

bridge dynamics) are linear processes as well. So there seems to be no exponential increase or saturation of energy consumption with increasing external load.

The finding that both EMG and $\dot{V}O_2$ increase linearly with increasing load makes it highly likely that muscle force increases linearly with load as well. This suggests that load sharing is independent of force level. To solve the load-sharing problem many different optimisation techniques have been used (see Tsirakos et al. 1997 for an overview). Non-linear cost functions provide more physiologically realistic results than linear cost functions, since linear cost functions predict sequential recruitment of muscles instead of load sharing. Non-linear functions with a quadratic term are most commonly seen, however several cubic functions are used as well. Quadratic functions predict a linear increase of muscle force with increasing external force, whereas with higher order functions non-linear increases are predicted. If load sharing is independent of force level, as the findings in this study suggest, a quadratic function is appropriate.

To use $\dot{V}O_2$ or EMG for model validation, it is important to know what EMG or $\dot{V}O_2$ tells us about muscle force. In the current study the relationship with external force is evaluated. This was done for the condition in which only elbow flexion was imposed because for the conditions with pro- and supination no distinction can be made between the activation of the muscle used for flexion force and the activation used for pro/supination moment. Linear and non-linear relationships (Table 2.3) with external flexion moment were found. However in the non-linear relationships the non-linear (cubic) term was very small and there was only a small difference in correlation coefficient and standard error between the linear and non-linear equation. This implies that for isometric elbow flexion up to 70% MVC the relationships of EMG and $\dot{V}O_2$ with external force can sufficiently be described by a linear equation. These results correspond to previously reported findings (Lawrence and De Luca 1983; Woods and Bigland-Ritchie 1983; Colier et al. 1995). Since both EMG and $\dot{V}O_2$ showed linear relationships with external force, it is highly likely that both variables are also linearly related to muscle force. This implies that for isometric contractions, besides EMG, $\dot{V}O_2$ could be used for model validation as well.

The current study focused on isometric contractions at different force levels at a constant muscle length. Muscle length influences the number of cross-bridges that are able to bind and according to some studies it influences the calcium flow as well (Stephenson and Wendt 1984; Balnave and Allen 1996). It is therefore likely that muscle length affects

the relationship between $\dot{V}O_2$ and force as well as the relationship between EMG and $\dot{V}O_2$. Further, it is likely that muscle velocity will also affect these relationships. The effect of muscle velocity is hard to determine since it is very difficult to use NIRS for dynamic measurements. The effect of muscle length can, however, be evaluated by measuring $\dot{V}O_2$ during isometric contractions at different muscle lengths. The latter will be done in a future study.

Conclusions

EMG and $\dot{V}O_2$ both increase linearly with load, suggesting that load sharing is independent of force level.

The EMG and $\dot{V}O_2$ of BB are influenced by both the required flexion moment and the pro/supination moment. However, for BR only the flexion moment is of significant influence.

Both the relationship between EMG and flexion moment and the relationship between $\dot{V}O_2$ and flexion moment can be sufficiently described by a linear equation.

These findings indicate that besides EMG, $\dot{V}O_2$ can be used for model validation as well.

Acknowledgements

The authors would like to thank M. van Amerongen and M. Rijs for their assistance in collecting the data.



Chapter 3

The relationship between two different mechanical cost functions and muscle oxygen consumption

M. Praagman, E.K.J. Chadwick, F.C.T. van der Helm, H.E.J. Veeger (2006).
Journal of Biomechanics, 39:(4),758-764

Abstract

Inverse dynamic models often use cost functions to solve the load-sharing problem. Although it is often assumed that energy is minimised, most cost functions are based on mechanically related measures like muscle force or stress. The aim of this study was to analyse the relationships of two cost functions with experimentally determined data on muscle energy consumption. Four subjects performed isometric contractions generating combinations of elbow flexion/extension and pro/supination moments. Muscle oxygen consumption ($\dot{V}O_2$) of the m. biceps brachii caput breve, the m. biceps brachii caput longum, the m. brachioradialis and the m. triceps brachii caput laterale was measured with Near InfraRed Spectroscopy (NIRS). Both cost functions were implemented into an existing inverse dynamic shoulder and elbow model and the individual cost values per muscle were calculated, normalised and subsequently compared to experimental $\dot{V}O_2$ values. The minimum stress cost function led to a good correspondence between $\dot{V}O_2$ and cost for the m. triceps brachii caput laterale but for the flexor muscles cost was significantly lower. A newly proposed energy-related cost function showed, however, a far better correspondence. The inclusion of a linear term and muscle mass in the new criterion led model results to correspond better to experimental results. The energy-related cost function appeared to be a better measure for muscle energy consumption than the stress cost function and led to more realistic predictions of muscle activation.

Introduction

The analysis of muscle function via inverse dynamic modelling requires the use of a cost function for solving the indeterminacy problem (Tsirakos et al. 1997). Unfortunately the relationship between the cost function and the actual control mechanism of the central nervous system is unknown and therefore generally based on assumptions.

Many different cost functions have been proposed (see Tsirakos et al. 1997 for an overview). Although some are based on physiological arguments, most cost functions are chosen rather arbitrarily, mainly due to the fact that validation is difficult since muscle force is difficult to measure in vivo, which leaves EMG patterns available for the comparison of muscle activation.

Especially for sub maximal activities, it is often assumed that movements are performed minimising energy consumption (Hardt 1978; Van der Helm 1991; Alexander 1997), yet only a few energetic cost functions predicting energy consumption have been proposed (Hatze and Buys 1977; Hardt 1978; Alexander 1997). Equations, such as proposed by Hatze and Buys (1977) or Zahalak and Ma (1990) can be used to calculate energy consumption, but require parameters that to date are generally unavailable. Instead most cost functions are mechanical cost functions based on muscle force, often weighted by physiological cross sectional area (PCSA) or maximal force. Although some of these are assumed to be related to physiological costs like energy consumption or fatigue, clear relationships have not been proven. The goal of the current study was to find a cost function that validly represents muscle energy consumption.

The study focuses on two different mechanical cost functions, which require parameters that are available for human muscles and can be used by any inverse dynamic model. The first objective function minimising summed muscle stress to some power p is one of the most commonly used optimisation criteria, although validation efforts (based on EMG) have been less than satisfactory (Buchanan and Shreeve 1996). This cost function was introduced by Crowninshield and Brand (1981) as a criterion that minimises fatigue. Recently Prilutsky (2000) stated that it is likely that this criterion leads to decrease of metabolic energy expenditure as well.

The second objective function, further referred to as the energy-related cost function, is based on the two major energy-consuming processes in the muscle: the re-uptake of calcium and the detachment of the cross-bridges. The metabolic cost is the summed cost over the activated

sarcomeres. Therefore not only the PCSA, representing the cross-bridges that are parallel, is included but also a variable related to muscle fibre length, related to the number of sarcomeres in series.

The aim of the present study was: (1) to determine the relationship of both cost functions with muscle energy consumption and (2) to analyse whether the energy-related cost function gives a better representation of muscle energy consumption than the stress cost function. To validate the cost functions an indication of muscle energy consumption *in vivo* was achieved with Near InfraRed Spectroscopy (NIRS). NIRS is a non-invasive technique, which can be used to monitor tissue oxygenation. Several studies have shown that NIRS is a useful technique for the determination of local muscle $\dot{V}O_2$ (Colier et al. 1995; Van Beekvelt et al. 2001).

Methods and materials

The stress cost function

The first objective function analysed in the present study is minimisation of the summed muscle stress:

$$J_{\sigma} = \text{minimise} \sum_{i=1}^n \left(\frac{F_{mi}}{PCSA_i} \right)^p \quad (3.1)$$

in which F_{mi} is the force produced by the i^{th} muscle and $PCSA_i$ is the physiological cross-sectional area of the i^{th} muscle. In this study squared muscle stress ($p=2$) is used.

The energy-related cost function

The second objective function, proposed in the current study, is

$$J_E = \text{minimise} \sum_{i=1}^n \dot{E}_{mi} = \sum_{i=1}^n (\dot{E}_{fi} + \dot{E}_{ai}) \quad (3.2)$$

in which \dot{E}_m represents the muscle energy consumption and is based on the two major energy-consuming processes in the muscle:

1. Detachment of cross-bridges (\dot{E}_f)
2. Re-uptake of calcium (\dot{E}_a)

Since muscle force is the variable that has to be optimised, E_{mi} is written as a function of muscle force: $E_{mi} = f(F_i)$. In the following equations i is omitted for clarity.

\dot{E}_f is related to the distribution of attached cross-bridges relative to the cross-bridge length (Huxley 1957). Under isometric conditions this

distribution does not change, and is only affected by the number of attached cross-bridges, i.e. the magnitude of force.

When the same muscle force (F_m) is maintained with longer muscle fibres, more sarcomeres are in series and more cross-bridges are attached. Therefore \dot{E}_f must be scaled to muscle fibre length (l_f):

$$\dot{E}_f \approx l_f \cdot F_m \quad (3.3)$$

Eq. (3.3) can be rewritten:

$$\dot{E}_f \approx l_f \cdot F_m = V \cdot \frac{F_m}{PCSA_m} = \frac{m}{\rho} \cdot \frac{F_m}{PCSA_m} \quad (3.4)$$

in which V is muscle volume, m is the muscle mass and ρ is muscle density ($= m/V$).

The second energy consuming process in the muscle is the re-uptake of calcium in the sarcoplasmic reticulum by an active calcium 'pump'. \dot{E}_a is related to the product of muscle volume (V) and the active state (a) of the muscle.

The active state is related to the calcium concentration ($[Ca^{2+}]$) and can be described by the ratio of muscle force (F_m) to maximal isometric muscle force at optimum length (F_{max0}) multiplied by the normalised force-length ($f_l(l_m)$) and force-velocity ($f_v(v_m)$) relationships.

$$\dot{E}_a \approx V \cdot a \approx \frac{m}{\rho} \cdot \frac{F_m}{F_{max0} \cdot f_l(l_m) \cdot f_v(v_m)} \quad (3.5)$$

in which F_{max0} can be described by the product of PCSA and maximal muscle stress.

During isometric contractions $f_v(v_m) = 1$, and can be omitted. Then, a polynomial approximation of \dot{E}_a :

$$\dot{E}_a = f(F_m) = b_0 + b_1 \cdot \frac{m}{\rho} \cdot \frac{F_m}{PCSA \cdot \sigma_{max} \cdot f_l(l_m)} + b_2 \cdot \frac{m}{\rho} \cdot \left(\frac{F_m}{PCSA \cdot \sigma_{max} \cdot f_l(l_m)} \right)^2 + \dots \quad (3.6)$$

As the exact relationship between the re-uptake of calcium and energy consumption is unknown, it is assumed here that cubic and higher order terms can be neglected.

The total energy consumption of the muscle (\dot{E}_m) is composed of terms derived in Equations 3.4 and 3.6. Omitting constants and incorporating constant muscle density ρ in the co-efficients, the following equation can be derived:

$$\dot{E}_m = \dot{E}_f + \dot{E}_a = m \cdot \left\{ a_1 \cdot \frac{F_m}{PCSA} + b_1 \cdot \frac{F_m}{PCSA \cdot \sigma_{max} \cdot f_l(l_m)} + b_2 \cdot \left(\frac{F_m}{PCSA \cdot \sigma_{max} \cdot f_l(l_m)} \right)^2 \right\} \quad (3.7)$$

In the present study all measurements were performed in one position, i.e. at one muscle length, and hence no distinction can be made between the two linear terms, since $b_1/\sigma_{\max} \cdot f_l(l_m)$ is constant. Since muscle optimum length is unknown, the effect of force length relationship could not be accounted for. Then, Eq. (3.7) simplifies to:

$$\dot{E}_m = \dot{E}_f + \dot{E}_a = m \cdot \left\{ c_1 \cdot \frac{F_m}{PCSA} + c_2 \cdot \left(\frac{F_m}{PCSA \cdot \sigma_{\max}} \right)^2 \right\} \quad (3.8)$$

Following previous simulation studies done with the Delft Shoulder and Elbow model σ_{\max} is defined as 100 N/cm² (Veeger et al. 2002a). The relative contribution of the two energy terms is as yet unknown. Here, the values of the constants c_1 and c_2 are chosen such that a fifty-fifty contribution from the linear and non-linear terms at 50% activation was reached. This implied a 1:2 ratio at maximal activation.

The Delft Shoulder and Elbow Model (DSEM)

Both cost functions were implemented in a 3D inverse dynamic model of the complete shoulder and elbow mechanism: the Delft Shoulder and Elbow Model (DSEM) (for a detailed description see: Van der Helm 1994a and 1997b). Data for the model were taken from cadaver studies (Veeger et al. 1991a, 1997; Van der Helm et al. 1992). Kinematic data as well as external forces and moments are needed as input for the model. The output comprises joint contact forces, ligament - and muscle forces, muscle lengths and moment arms.

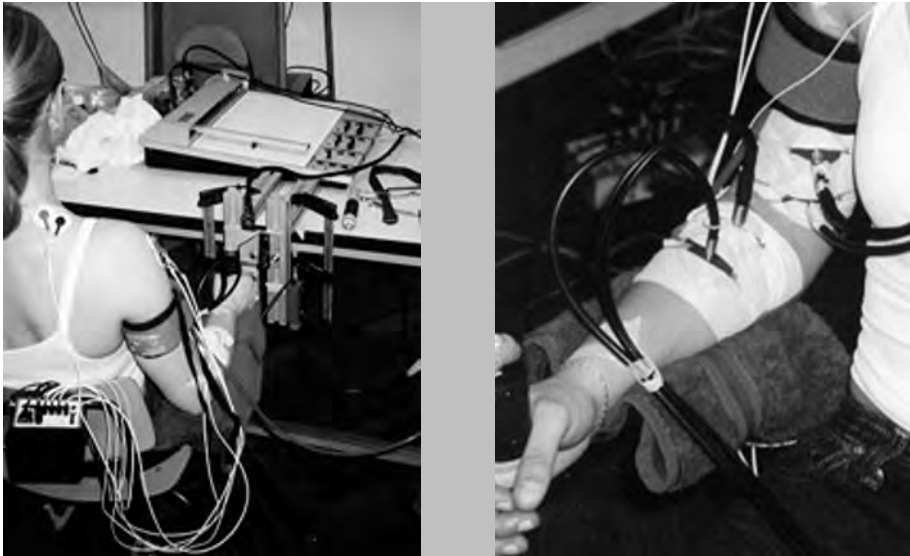
Near InfraRed Spectroscopy

Near InfraRed Spectroscopy (NIRS) is a non-invasive method from which information can be obtained about the oxygenation of a biological tissue, such as muscle tissue. Near Infrared light is transmitted through the muscle tissue by two fibre optic cables, at three different wavelengths (905, 850 and 770 nm) and the absorption of the light is measured. Changes in absorption can be converted into changes in concentration of oxyhaemoglobin (O₂Hb) and deoxyhaemoglobin (HHb), making use of the Lambert-Beer law (Colier et al. 1992). When measurements are done during arterial occlusion it is possible to quantify muscle oxygen consumption (Praagman et al. 2003).

Set-up

Four subjects (2 male, 2 female) (age 28 ± 3 years) participated in this study after giving informed consent. Subjects were seated in a chair with their right arm slightly abducted and flexed forward and their forearm in

a neutral and horizontal position, holding a vertical handle with their right hand (Figure 3.1). This handle was fixed to a six-degree-of-freedom force transducer (AMTI 500), which recorded the forces and moments the subject applied to the handle.



a

b

Figure 3.1 *Experimental set-up. a) Moments were measured using a vertical handle, which was fixed to a six-degree-of-freedom force transducer and placed in front of the subject. b) NIRS data were measured with fibre optic cables that were attached to the skin above BB and BR. EMG electrodes were placed on the skin in between the cables. A cuff around the upper arm was used to apply an arterial occlusion.*

The position of the subject, needed as input to the DSEM, was recorded by measuring the 3D co-ordinates of bony landmarks on the thorax, clavicle, scapula, humerus, ulna and radius, with a three-dimensional digitiser (Pronk 1991). The position of the subject's hand on the handle and the chair on the ground were marked. A pointer at the Angulus Acromialis minimised changes in seating position during recordings. NIRS measurements were performed on four arm muscles, m. biceps brachii caput breve (BB), m. biceps brachii caput longum (BL), m. brachioradialis (BR) and the m. triceps brachii caput laterale (TL). Two continuous-wave, near-infrared spectrophotometers (OXYMON, Artinis

Medical Systems, Arnhem, The Netherlands) (Van der Sluijs 1998) were used (inter-optode distance of 4 cm, Differential Path Factor 4.3), which made it possible to measure the haemoglobin concentrations of two muscles simultaneously (Figure 3.1b). Occlusion was applied by inflating a thin cuff, placed around the upper arm, to a pressure of at least 230 mmHg. Simultaneously surface EMG of the muscles was recorded (inter-electrode distance of 17 mm, sample frequency of 1000 Hz, analogue low-pass filter of 400 Hz).

Task

The subjects were instructed to perform six different isometric contractions, exerting combinations of flexion-extension moments around the humero-ulnar joint and pro-supination moments around the radio-ulnar joint: flexion (FL), flexion-supination (FS), flexion-pronation (FP), extension (EX), extension-supination (ES) and extension-pronation (EP). All contractions were performed at three different force levels: 10%, 25% and 50% of their maximal moment. A 2D plotter, placed in front of the subjects, provided feedback to the subject on the generated moments and their directions.

Protocol

Subjects were instructed to perform maximal flexion and extension moments as well as maximal pro- and supination moments. The magnitudes of the flexion-extension and pro-supination moments were visualised with the use of a 2-D plotter conform a previous protocol (Praagman et al. 2003). For each of the six contractions the protocol was the following: To determine $\dot{V}O_2$ during rest, an arterial occlusion was applied while the subject's arm was resting in an arm support. Subsequently the subject had to perform the tasks at the three different force levels consecutively. As soon as the required force level was achieved, an arterial occlusion was applied. The periods of occlusion and force production varied from 20 to 60 seconds depending on the force level (Table 3.1) and each period was followed by a period of rest to recover. The [O₂Hb] and [HHb] as well as the external forces and moments were recorded continuously, while, EMG was recorded during the periods of force production only.

The whole experiment was carried out twice, once making measurements on BB and BR and once on BL and TL.

Table 3.1 Duration of occlusion and recovery for each force level.

Force level (%)	Occlusion time (s)	Recovery time (s)
0	60	180
10	30	180
25	30	180
50	20	300

Data processing

For each subject the orientations of the skeletal elements were calculated from the measured 3D co-ordinates, following the protocol described in Van der Helm (1997a). The individual 3D orientation of the skeletal elements as well as the measured external forces and moments were input to the DSEM. As mentioned before both cost functions were used for the optimisation. For each subject the model predicted the forces of all shoulder and elbow muscles. In addition the individual cost values were calculated for BB, BL, BR and TL.

$\dot{V}O_2$ was determined by performing regression on the linear part of the $[O_2HB]$ decrease immediately after occlusion. The slope of the decrease was taken as the $\dot{V}O_2$ (micromoles $O_2 \cdot \text{second}^{-1}$) of the muscle. $\dot{V}O_2$ was corrected for rest metabolism by subtracting the $\dot{V}O_2$ measured during rest from the $\dot{V}O_2$ measured during force production.

EMG signals were digitally high-pass filtered at 5 Hz, corrected for offset and rectified. Mean EMG values were calculated over the period of force production. EMG values were normalised to the 50% condition in which the muscle was most active: FS condition for BB and BL, FL condition for BR and EX condition for TL.

To be able to compare between different subjects, $\dot{V}O_2$ and cost were normalised. For each subject and each muscle, values were expressed as percentages of the highest value of that muscle.

Correlation was used to test whether $\dot{V}O_2$ values corresponded to EMG. Based on the results of a previous study (Praagman et al. 2003), in which a linear relationship was found between EMG and $\dot{V}O_2$, it was expected that EMG and $\dot{V}O_2$ values would be similar. If this was indeed the case, EMG measurements could be used to check the accuracy of the $\dot{V}O_2$ measurements.

Linear regression and correlation were performed to evaluate the relationship between $\dot{V}O_2$ and cost. The level of significance, for all analyses was set at $p < 0.05$.

If the cost function is a measure of energy consumption it is expected that normalised $\dot{V}O_2$ values would be equal to normalised cost values. The conditions for which the difference between $\dot{V}O_2$ and cost was larger than 10% were further analysed and divided into four categories:

- A. the model predicted no muscle activity while $\dot{V}O_2$ did show activity (false negatives);
- B. $\dot{V}O_2$ showed no activity while the model did predict activity (false positives);
- C. the magnitudes differed but the activation patterns were in general comparable;
- D. cost differed from $\dot{V}O_2$ but not from EMG.

While for the first three categories the differences are probably due to the model or the cost function, for the last category it is likely that the difference is caused by an error in the $\dot{V}O_2$ recording. Therefore values in category D were excluded from further analysis. In the current study we focussed on the first two categories since these indicated conditions for which model predictions were definitely incorrect.

Results

Extension and flexion moments generated by the subjects varied between -19.4 Nm (± 3.6) and 16.2 Nm (± 3.4) and supination and pronation moments varied between -2.5 Nm (± 0.8) and 3.1 Nm (± 1.6). A typical example of muscle forces predicted by the model is shown in Figure 3.2. Both EMG and $\dot{V}O_2$ increased linearly with increasing load. As expected, a high and significant correlation ($R=0.86$) was found between normalised EMG and normalised $\dot{V}O_2$.

Optimising stress led to a good correspondence between $\dot{V}O_2$ and cost for TL (Table 3.2 and Figure 3.3). However for the three flexor muscles a considerable amount of false positives and false negatives was found (Figure 3.3 and 3.4). Using the energy-related cost function instead of the stress cost function a far better correspondence between cost and $\dot{V}O_2$ was achieved (Table 3.2 and Figure 3.3). The number of conditions in which the difference between $\dot{V}O_2$ and cost was above 10% was decreased and the remaining differences were mainly differences in magnitude and not in activation pattern. There were only a few false positives and false negatives left (Figure 3.3 and 3.4), and the overall correlation coefficient increased (Table 3.2).

Table 3.2 Regression equation, correlation coefficient (*R*) and root mean square error (RMS) for the relationship between $\dot{V}O_2$ and cost (predicted with the stress (J_σ) or the energy-related cost function (J_E)) defined by $\dot{V}O_2 = a \cdot \text{cost} + b$, for all individual muscles as well as for the overall data set. *: $p \leq 0.05$.

Muscle	Cost function	a	b	R	RMS
BB	J_σ	0.96*	7.89*	0.91*	12.15
	J_E	0.92*	3.83*	0.94*	9.91
BL	J_σ	0.80*	10.71*	0.70*	22.10
	J_E	0.88*	7.39*	0.86*	15.67
BR	J_σ	0.85*	5.55*	0.83*	15.04
	J_E	0.92*	1.12	0.95*	8.79
TL	J_σ	0.96*	1.40	0.96*	8.11
	J_E	0.96*	0.82	0.93*	11.30
All	J_σ	0.89*	6.53*	0.85*	16.21
	J_E	0.92*	3.36*	0.91*	12.18

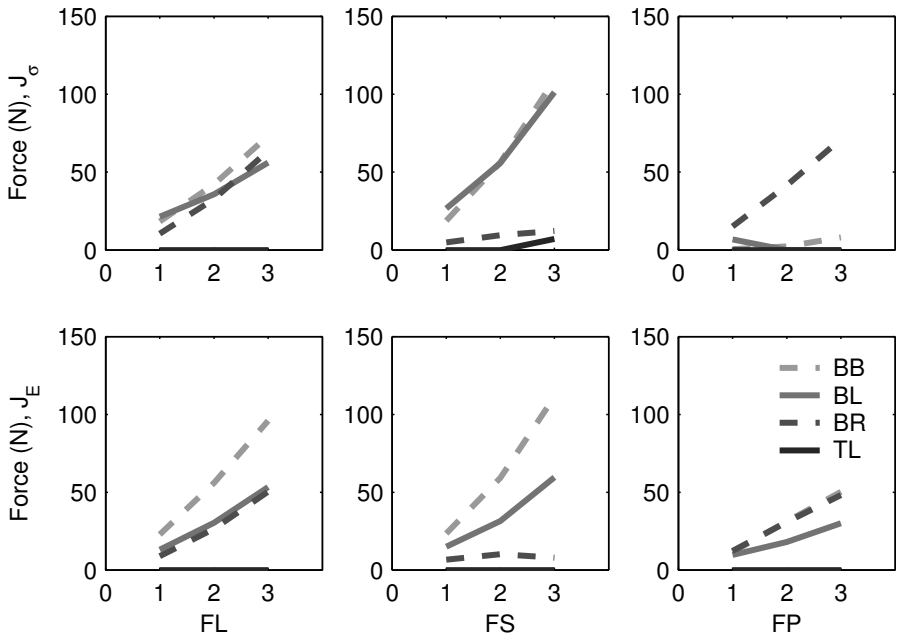


Figure 3.2 Predicted muscle forces of BB, BL, BR and TL, during flexion (FL), flexion-supination (FS) and flexion-pronation (FP). The upper three figures show the muscle forces predicted with the stress cost function and the lower three figures show the muscle forces predicted with the energy-related cost function.

Muscle load sharing

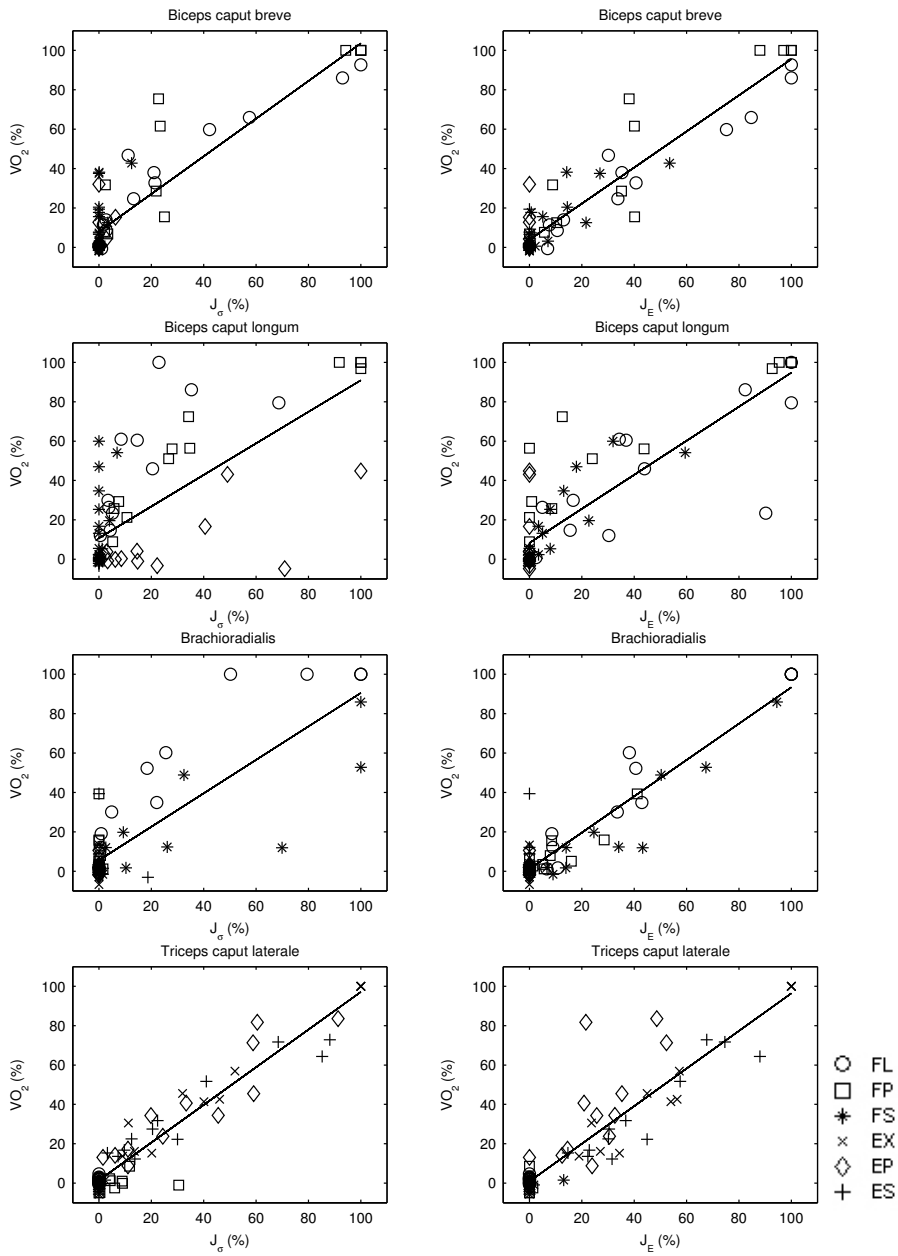


Figure 3.3 $\dot{V}O_2$ ($n=4$) plotted against cost predicted with the stress cost function (left) and the energy-related cost function (right). The different symbols represent the different contractions.

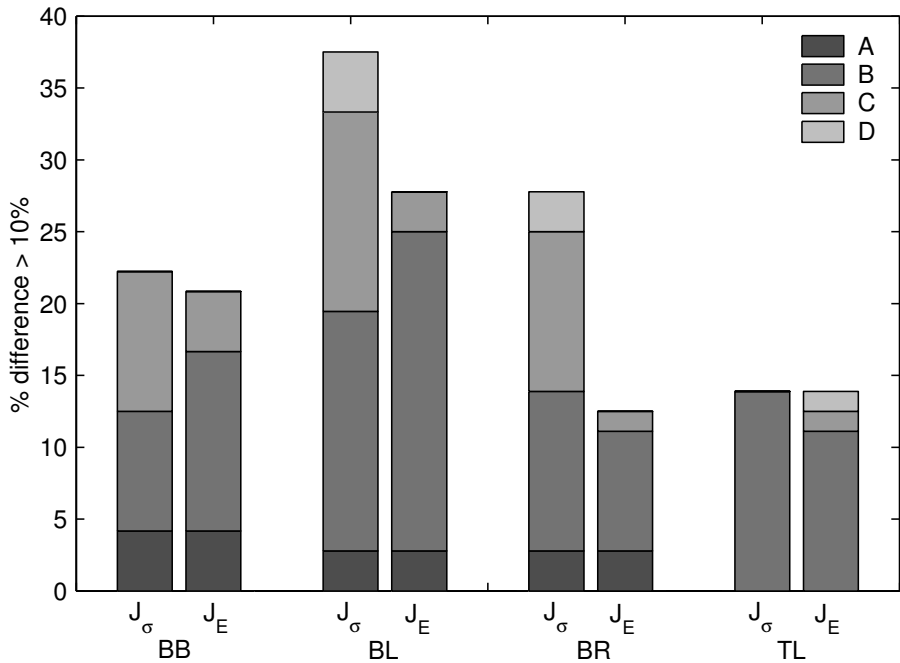


Figure 3.4 The amount of conditions (%) in which the difference between $\dot{V}O_2$ and cost exceeds 10% (see methods section) for the stress cost function (J_σ) and the energy-related cost function (J_E), divided into four categories: (A) error in $\dot{V}O_2$ recording, (B) difference in magnitude but not in activation pattern, (C) model predicted no activity while $\dot{V}O_2$ did show activity, (D) $\dot{V}O_2$ showed no activity while the model did predict activity.

Discussion

In this study the correspondence to $\dot{V}O_2$ of two different cost functions was evaluated. Both cost functions were based on mechanical properties related to muscle force and can be used by any inverse dynamic model. There are, however, two main differences between the commonly used stress cost function and the new energy-related cost function: (1) the energy-related cost function consists of not only a quadratic term but also a linear term and (2) the energy-related cost function represents both the cross-bridges in parallel and in series by including not only PCSA but also muscle mass. The stress cost function accounts only for the cross-bridges in parallel. Since the metabolic cost of a muscle is the summed cost over the sarcomeres, it was expected that the energy-related cost function would be a better representation of energy

consumption than the stress cost function. When the stress cost function is minimised, the predicted load sharing depends, although in a complex, non-linear way, on the relationship between moment arm and squared PCSA (Prilutsky, 2000). Using the energy-related cost function, it is not only muscles with large moment arms and large PCSA's that are preferred but also those with small masses and short fibre lengths. In addition the linear component will affect the load sharing since a linear term leads to sequential recruitment whereas quadratic terms lead to synergism.

In this study no significant differences between EMG and $\dot{V}O_2$ were found. This corresponded to an earlier study in which we found a linear relationship between EMG and $\dot{V}O_2$ during isometric contractions (Praagman et al. 2003). In the present study EMG was used to filter possible errors in the $\dot{V}O_2$ determination (see Methods).

Predicted cost values were compared to $\dot{V}O_2$ values measured during isometric contractions in which combinations of flexion-extension moments and pro- and supination moments were generated. It is unrealistic to expect complete agreement between $\dot{V}O_2$ and cost for two reasons: (1) the position of the subjects was not recorded continuously therefore it is possible that minor changes in position occurred during the experiment and (2) the model is based on one anthropometrical data set obtained in a cadaver study (Veeger et al. 1997) while subjects vary in morphology and anthropometrics. For this reason only differences above 10% have been analysed.

During the experiment, subjects were seated with the elbow flexed and the forearm in a neutral position. From a mechanical point of view flexion moments are supposed to be mainly generated by both heads of the m. biceps brachii (BB and BL), the m. brachialis and the m. brachioradialis (BR). Extension moments will be mainly produced by m. triceps brachii. Due to the neutral position of the forearm it was expected that BR would not contribute to the required pro/supination moments. Supination moments were expected predominantly to be produced by BB, BL and the m. supinator, and pronation moments by the m. pronator quadratus and m. pronator teres. External pro/supination moments will of course influence the flexion function of BB and BL. Due to this interaction, changes in the activity of BB and BL may alter the total load sharing and hence have an effect on both BR and triceps brachii.

The stress cost function showed a strong relationship between $\dot{V}O_2$ and predicted force for the mono-articular TL but not for the bi- and even tri-articular flexor muscles. The cases in which the model predicted no

muscle activity while $\dot{V}O_2$ did show activity or vice versa (the false positives and false negatives) were further investigated. It appeared that pro/supination moments had a disproportionately large effect on the optimisation, compared to flexion/extension moments. BB and BL are not activated during FP due to their undesired supination moment. During FS BR does not contribute to the required flexion moment since the m. biceps brachii is preferred due to its desired supination moment. Although this does not seem very surprising from a mechanical point of view, these findings were in contrast to the NIRS and EMG measurements, which did show activity of these muscles (Figure 3.2 and 3.3). The model also predicted activity of BL during ES despite its undesired flexion moment. NIRS measurements showed this for only two of the four subjects. This effect of favouring PS over FE by the stress cost function appears to coincide with the favouring of larger muscles over the contribution of smaller muscles, as found by Herzog and Leonard (Herzog and Leonard 1991) on the leg muscles of an adult cat. With the energy-related cost function most of the above-mentioned problems disappeared. By including a linear term and muscle mass in the criterion the load-sharing changed in several ways. The contribution of the relatively small pronator and supinator muscles increased. BB for instance contributed to the flexion moment during FP since the undesired supination moment could be compensated for by the relatively 'low cost' m. pronator quadratus. This favouring of smaller muscles also led to a decrease in force in BB and BL, and an increase in force in BR and the supinator muscle during FS, reflecting what was seen in the NIRS measurements. The increase in activity of the m. supinator also resulted in non-activity of BL and BB during ES. This did not completely correspond to the experimental results in which, as mentioned above, activity of BB and BL during ES was seen for two subjects. Since this effect was not recorded for all subjects it is well possible that these differences were caused by individual differences in morphology, which the model cannot account for. An EMG study by Buchanan et al. (1989) also showed variation in activity of the m. biceps brachii during extension-supination among different subjects. Although muscle length remained constant in these experiments and force-length characteristics were not yet taken into account, it was found that including muscle mass and indirectly, fibre length, into the criterion had a major effect on load sharing. When muscle length changes the effect of muscle mass may change and the linear term may become more important. Therefore in a future study muscle length will be varied.

In static conditions muscles with short muscle fibres are preferred above muscles with larger fibres. However in dynamic conditions this preference may change. Muscles with shorter fibres will have a larger relative contraction velocity than muscles with longer fibres (when they have the same moment arm and joint angular velocity) and therefore will be in a less optimal part of the force-velocity curve. Therefore it can be expected that the activation patterns will change going from static to dynamic contractions.

The energy-related cost function consisted of a linear as well as a quadratic term; the contribution of each term was defined by the constants c_1 and c_2 . Changing the constants and therefore the ratio between the two terms will of course influence the load sharing. In the current study these constants were chosen arbitrarily. It is expected that more improvement can be achieved by optimising these constants.

In conclusion it can be said that the newly proposed energy-related cost function appeared to be a better measure for muscle energy consumption than the stress cost function and led to more realistic predictions of muscle activation. Further research on the effect of muscle length and the ideal ratio between the linear and quadratic term is expected to lead to further refinement of this energy-related cost function.

Acknowledgements

We would like to thank W.N.J.M. Colier for his advice on the NIRS measurements and for the use of the NIRS devices.



Chapter 4

The effect of elbow angle and external moment on load sharing of elbow muscles

M. Praagman, E.K.J. Chadwick, F.C.T. van der Helm, H.E.J. Veeger.
Submitted for publication

Abstract

To study the occurrence and underlying principles of load sharing we investigated how external flexion/extension (FE) and pro/supination (PS) moments influenced the activation and oxygen consumption $\dot{V}O_2$ of elbow muscles and whether this was dependent on elbow angle.

Two different experimental data sets were obtained. In the first set (n=6) electromyography (EMG) of elbow flexors (m. biceps brachii, caput breve (BB) and caput longum (BL), m. brachioradialis (BR), m. brachialis (BA)) and extensors (m. triceps brachii caput longum (TR), caput laterale (TL) and caput mediale (TM), m. anconeus (AC)) was recorded during all possible (49) combinations of FE and PS moments at three different force levels, which were repeated at four different elbow angles (50°, 70°, 90° and 110°). In the second set (n=4) both EMG and $\dot{V}O_2$ of three muscles (BB, BR and TL) were measured during a subset of the above mentioned conditions.

Results showed that joint angle, and therefore moment arm and muscle length influenced both the activation level of the muscle as well as the load sharing between muscles. The principles behind load sharing however were difficult to quantify, since it was impossible to distinguish all the individual aspects that affect muscle activity.

The relationship between EMG and $\dot{V}O_2$ could be described as a linear relationship and joint angle did not appear to have a major effect on this linear relationship. Although, in general, subjects showed comparable muscle activation patterns, there were also some striking inter-individual differences. These inter-individual differences might be explained by two different factors: 1. subjects use different optimisation strategies or 2 differences might reflect the role of inter-individual differences in morphology.

Introduction

Humans appear to follow comparable musculoskeletal control principles in movement tasks. A striking phenomenon is that, given a particular force task, an inter-individually compatible pattern of load sharing occurs between muscles, while this does not appear to be mechanically necessary. Although frequently studied (Hardt, 1978; Dul et al., 1984b; Buchanan et al., 1989; Kaufman et al., 1991b; Challis, 1997), the principles behind this load sharing phenomenon are still unknown. A leading thought is that the total energy cost of the particular activity is minimised by keeping individual muscle contributions low and thus preventing fatigue and the detrimental effects on efficiency related to the occurrence of fatigue (Alexander, 1997). The energy cost of a muscle can be assumed to depend on the two major energy-consuming processes in a muscle, namely the *activation dynamics* (Ca^{2+} restoring in the Sarcoplasmic Reticulum) and the *contraction dynamics* (detachment of cross-bridges). Given the assumption that total energy consumption might be minimised in a given task, it is not clear to what extent changes in task conditions will influence load sharing. It is obvious that changing joint angle will influence both the moment arm and muscle length of a muscle crossing that joint, but it is absolutely obscure what effect that might have on load sharing. It can be argued that muscles with larger moment arms and near to their optimum length are the most advantageous muscles to be used and therefore their activation and energy consumption would be highest in this position. On the other hand, since the advantageous moment arm and optimum length would require less muscle force and activation to exert the required moment, one could also assume that the activation and energy consumption of that particular muscle might be lower.

Musculoskeletal models heavily depend on valid cost functions to estimate load sharing. A considerable number of cost functions has been used (see Tsirakos et al., 1997 for an overview). Most cost functions are based on muscle force, often scaled by physiological cross sectional area or maximal force. Since predictions of energy consumption are difficult, most cost functions attempt to approximate energy consumption through mechanical variables such as muscle stress (assuming a direct correlation between energy consumption and muscle stress). Validations of these cost functions have been generally done by EMG (Kaufman et al., 1991a; Happee, 1994; Van der Helm, 1994b; Buchanan and Shreeve, 1996; Raikova and Prilutsky, 2001).

Praagman et al. (2006) performed direct measurements of the energy consumption of individual muscles using Near InfraRed Spectroscopy (NIRS). Two mechanical cost functions (the stress cost function and a newly proposed energy related cost function) were compared with *in vivo* measured muscle oxygen consumption. In that study it was shown that the energy-related cost function showed better results than the stress cost function. Comparisons between modelling results and experimental data for muscle oxygen consumption indicated, especially for the stress cost function, a large number of "false negatives": the model estimated NO muscle activity where a muscle was active, based on experimental observations. The use of an energy related cost function led to fewer false negatives. It was therefore concluded that the latter cost function appeared to be a promising improvement (Praagman et al., 2006). In this previous study, we based our comparisons on data for only one arm position and limited combinations of elbow flexion-extension and forearm pronation-supination moments. However, from results by Jamison and Caldwell (1993) it can be inferred that, despite the complexity of measurements, these results can not readily be extrapolated to all possible combinations of joint moments. Also, the muscle force-length relationship could not yet be accounted for, while, as said before, it is likely that load-sharing is influenced by joint angle.

Energy consumption and activation might differentiate and do not show the same relationship for each joint angle. It is therefore not certain that muscle activation, as measured with (surface) EMG and energy consumption will show a linear relationship under all conditions, although this relationship was shown to exist for a single joint position (Praagman et al., 2006). As a consequence, the most appropriate method to quantify muscle energy consumption is still NIRS.

Muscle function is often studied around a single joint or degree-of-freedom, ignoring the interaction with adjacent joints. For example, the activation of m. biceps brachii not only influences elbow flexion, but also forearm supination and glenohumeral anteflexion. To perform a simple elbow flexion torque, it is therefore inevitable that the role of a- and antagonistic wrist, forearm and shoulder muscles should be taken into account (Buchanan et al., 1989; Jamison and Caldwell, 1994). A study by Jinha et al.(2006a) has shown that muscle activity predictions using a one or two degrees of freedom modelling approach did not lead to valid predictions when more degrees of freedom were present in the system. This implies that a valid study on *in vivo* muscle coordination should:

1. involve all relevant degrees-of-freedom and

2. involve all relevant combinations of external force conditions.

The consequence of the above should be that validation can only take place using models of sufficient reality and experimental data with sufficient information. This study describes the collection of the data necessary for model cost function validation.

The purpose of the current study was to investigate the principles of load sharing between muscles in a multiple degrees of freedom joint system, i.e. the elbow. An extensive data set was obtained, including variation in muscle length and moment arms, which can be used for validation of the previously introduced cost functions. To account for possible differences between activation dynamics and energy consumption, both EMG (indication of muscle activation) and muscle oxygen uptake (as indication for energy consumption) were measured for selected muscles. To study the mechanism of load sharing, sufficient combinations of flexion/extension and pro/supination moments around the elbow and forearm were measured. Inclusion of these moments would enable to study the effect of the interaction between different degrees of freedom. It was investigated in what way the activation of elbow flexors and extensors was influenced by the different external moments and whether this was influenced by elbow angle. We further investigated the influence of elbow angle on both the load sharing between muscles and the relationship between $\dot{V}O_2$ and EMG within muscles.

Methods

Two related experiments were performed. In experiment I, subjects had to perform a full set of 49 combinations of flexion/extension and pro/supination moments. EMG measurements were performed on four elbow flexors: m. biceps brachii caput breve (BB), m. biceps brachii caput longum (BL), m. brachialis (BA) and m. brachioradialis (BR), and four elbow extensors: m. triceps brachii caput longum (TR), m. triceps brachii caput laterale (TL), m. triceps brachii caput mediale (TM) and m. anconeus (AC).

In experiment II, EMG and muscle oxygen consumption ($\dot{V}O_2$) were measured for three elbow muscles (BB, BR and TL). $\dot{V}O_2$ was measured using Near InfraRed Spectroscopy (NIRS). Measurements with NIRS took place during arterial occlusion of the upper arm and therefore required relatively long periods of rest after each period of force production. Measurements of experiment II were therefore much more time-

consuming than measurements of experiment I, in which EMG was measured only. To ensure a protocol of acceptable length a selection of the moment combinations performed in the first experiment was studied. Even using these selected conditions, experiments still took four days per subject.

In experiment I, six subjects (4 females, 2 males, age 19.2 years (SD 2.3), height 1.71 m (SD 0.07), body mass 64.3 kg (SD 2.7)) participated. Experiment II comprised four male subjects (age 29.4 years (SD 7.3), height 1.75 m (SD 0.06), body mass 70.2 kg (SD 6.9)). Prior to the experiments, all subjects were informed on the intent, procedures and risks of the experiments and then signed an informed consent review form. The protocols of both experiments were separately reviewed and approved by the local ethical committee.

Data collection

EMG was recorded during periods of force-production only (inter-electrode distance of 2 cm, analogous low-pass filter of 400 Hz, sample frequency 1000 Hz). Changes in concentration of oxyhaemoglobin (O_2Hb) and deoxyhaemoglobin (HHb) of the muscles were recorded continuously with two continuous-wave, near infrared spectrophotometers (OXYMON, Artinis Medical Systems, Arnhem, The Netherlands) (Van der Sluijs, 1998). An inter-optode distance of 4 cm was used and the differential path length factor was set to 4.0. Measurements were done during arterial occlusion, applied by inflating a thin cuff, placed around the upper arm, to a pressure of at least 230 mmHg. $\dot{V}O_2$ values were determined by taking the slope of the linear part of the $[O_2Hb]$ decrease immediately after occlusion. For a detailed description see Chapter 2.

Set-up

Subjects were seated on a chair with their elbow flexed at a fixed angle and their forearm horizontal and in a neutral position (Figure 4.1). There was no elbow or arm support. Subjects had to generate pure moments around the elbow joint (flexion (FL) and extension (EX)) and radio-ulnar joint (pronation (PR) and supination (SU)), as well as combinations of these moments (flexion-supination (FS), flexion-pronation (FP), extension-supination (ES) and extension-pronation (EP)). The subjects held a special tool with their right hand, consisting of a stick with a horizontal bar on top to which on several positions weights (0.75, 1.5, 3 or 4.5 kg) could be applied (directly or through a pulley), enforcing the external moments the subject had to withstand (Figure 4.1). This

resulted in flexion/extension moments around 5, 10 and 15 Nm and pro/supination moments around 1, 2 and 3 Nm. Subjects were instructed to hold the tool in a fixed position keeping the bar horizontal. Feedback was given by means of a horizontal cord in front of the subject.



a

b

Figure 4.1 *Experimental set-up. Subject was sitting on a chair with the elbow flexed and forearm in a horizontal and neutral position. The subject had to hold the tool with his right hand, keeping the bar on top horizontal (a). Visual feedback on the position of the tool was given by a horizontal cord. Flexion moments were enforced by hanging weights right under the stick while extension moments were enforced by loads applied to the middle of the bar using a pulley system. Pro/supination moments were imposed*

During experiment I, the periods of force production lasted 5 seconds. A full set of 49 flexion/extension and pro/supination moment combinations was measured (Figure 4.2). The moment combinations protocol was repeated at four different elbow angles: 50, 70, 90 and 110° of flexion (where 0° is full elbow extension), leading to a total of 196 trials per subject. The elbow angle was imposed by measuring the angle between forearm and upper arm with a goniometer. The order of the elbow angles was randomly defined. Since the forearm stayed

horizontal, a decrease of flexion angle in the elbow led to an increase of ante flexion angle of the glenohumeral joint. For each subject, all measurements were performed on one single day. The 3D co-ordinates of bony landmarks on the thorax, clavicle, scapula, humerus and forearm, were recorded for each elbow angle, using a 3D digitizer (Veeger, 1993). A head rest together with a pointer at the angulus acromialis and the epicondylus lateralis were used to ensure the subject stayed in the same position.

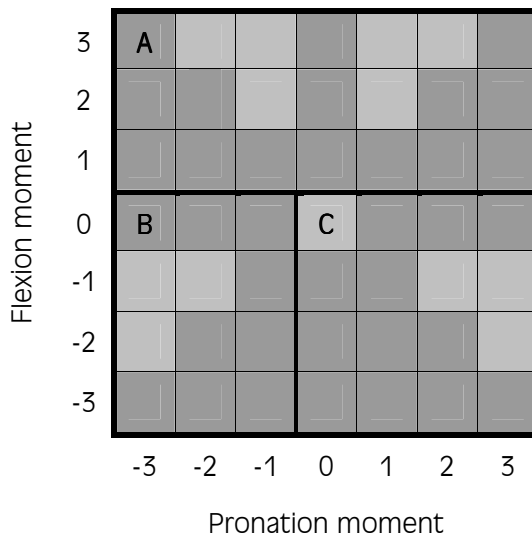


Figure 4.2 Schematic overview of all different moment combinations the subjects had to perform. All loads could be applied at three different force levels (level 1, 2 and 3) leading to a total of 49 combinations. In the first experiment, this complete set of moment combinations was measured at one single day. During the second experiment, a selection of these conditions, represented by the dark grey cells, was measured, divided over three different days (boxes A, B and C). TL was measured during all three sets, BB was measured during set A and B and BR was measured during set A only.

During experiment II, the periods of force production and especially the periods of rest between sessions had to be longer due to the NIRS measurements. The periods of force production varied between 20 and 30 seconds and were followed by a recovery period varying from 3 to 5 minutes depending on the force level. The arm of the subject was resting during the recovery period. A selection of the moment combinations measured in the first experiment was used, which was

divided into three sets (A, B and C, respectively 15, 9 and 12 trials, see Figure 4.2) measured on three separate days. TR was measured during all three sets, BB during sets A and B and BR during set A only. Since with the NIRS device only two muscles could be measured at once, set A was performed twice (on two separate days), once for BB and BR and once for TR. Each day the relative set was repeated four times, once for each elbow angle (50, 70, 90 and 100° of flexion). In total each subject had to perform 204 trials. The order of the elbow angles was randomly defined. EMG of all these muscles was measured on all 4 days. The position of the subject was monitored at 25 HZ by recording the 3D co-ordinates of bony landmarks on the thorax, clavicle, scapula, humerus and forearm, using an automated video based recording system (Optotrak™, Northern Digital Inc., Canada). During the experiment, the actual elbow angle was controlled on-line using markers on top of the acromion, the epicondylus lateralis and the processus styloideus ulnae.

Data processing

Orientations of the body segments of the subjects were calculated from the measured 3D co-ordinates of the bony landmarks following the protocol described in Van der Helm (1997a). EMG signals were digitally high-pass filtered at 5 Hz, corrected for offset and rectified. Mean EMG (EMG_{mean}) values were calculated over the period of force production. Muscle $\dot{V}O_2$ was determined by performing regression on the linear part of the $[O_2HB]$ decrease immediately after occlusion. The slope of the decrease was taken as the $\dot{V}O_2$ (micromoles $O_2 \cdot \text{second}^{-1}$) of the muscle. $\dot{V}O_2$ was corrected for rest metabolism by subtracting the $\dot{V}O_2$ measured during rest from the $\dot{V}O_2$ measured during force production. The measurements were standardised for each subject and each muscle. To prevent the detrimental effect of outliers, we standardised our results relative to the 75% percentile and not to the maximum value obtained during the experiment. So with EMG_{mean} the measured value and $EMG_{mean(75)}$ the 75% percentile of all of the EMG_{mean} measurements for that subject and that muscle, our standardised data became

$$EMG_{(75)} = 0.75 * EMG_{mean} / EMG_{mean(75)} \quad (4.1)$$

and similar

$$\dot{V}O_{2(75)} = 0.75 * \dot{V}O_{2\ mean} / \dot{V}O_{2\ mean(75)} \quad (4.2)$$

Statistics

A multiple regression model was used to test to which extent the EMG amplitude was dependent on external moment and elbow angle. Since muscle force can only be positive, or zero, four moment variables were defined: flexion (Mf), extension (Me), pronation (Mp) and supination (Ms). If for a particular condition the moment direction was not requested it was set to zero. In other cases, it was set to the - coded - moment level (1 – 2 – 3, for flexion/extension force level 5, 10 and 15 Nm and pro/supination moments 1, 2 and 3 Nm).

With the natural logarithm of $EMG_{(75)}$ as the dependent variable, and these external moments as independent variables, stepwise regression was used. (The logarithmic transformation was suggested by the data: residuals after regression turned out to be rather skewed if the original data were used. After this transformation, they show a normal distribution.) External moment variables were included into the model if they led to a substantial increase [0.05] of the R-squared. Next, angle specific moment variables were defined and it was investigated whether a substantial increase could be achieved including these variables in our model. In fact this means that interaction effects between angle and the external moments were included in the considerations.

The analyses were carried out for the data of experiment I. Subsequently, the resulting model was used to predict EMG results for the second experiment and correlations between predicted and measured EMG were determined.

Concerning the relationship between $\dot{V}O_2$ and EMG, a stepwise regression was performed with $\dot{V}O_{2(75)}$ as dependent and $EMG_{(75)}$ and $EMG_{(75)}^2$ as independent variables. To investigate whether elbow angle significantly influences the relationship between EMG and $\dot{V}O_2$ a second regression model was used in which $EMG_{(75)}$ was redefined into four elbow angle categories (115° – 100° – 80° – 60°). The subdivision in elbow angles was accepted when R-squared improved with more than 0.05.

Results

Position data

The actual elbow angles differed somewhat from the imposed elbow angles: 55, 80, 100 and 120° for experiment I and 60, 80, 100 and 115 ° for experiment II, where 0° is full extension.

EMG data (experiment I)

EMG amplitude of all four flexor muscles increased with flexion moment (Figure 4.3). Regression analysis (Table 4.1) showed that this influence of flexion moment depended on the elbow angle: the EMG level increased with decreasing flexion angle. For both heads of biceps brachii (BB and BL) the EMG level also increased with supination moment whereas the EMG signal of BR increased with pronation moment (Table 4.1 and Figure 4.3). In contrast to expectations, the EMG signal of the mono-articular elbow flexor BA was also influenced by supination moment as well as extension moment (Table 4.1).

As expected, for all extensor muscles a linear relationship with extension moment was found (Figure 4.4). Regression showed that this relationship was not influenced by elbow angle except for AC: the EMG level decreased with decreasing flexion angle (Table 4.1). There was also a significant influence of supination moment found for all four extensor muscles. It was also shown that activity of AC and TL was influenced by pronation moment and that the EMG signal of TL was linearly related to flexion moment. As was found for the elbow flexors, the effect of flexion moment was influenced by elbow angle: EMG amplitude of TL increased with decreasing elbow angle.

Table 4.1 Results of stepwise regression. Regression coefficients and R-squared for the relationship between the natural logarithm of $EMG_{(75)}$ (experiment I) and external moment (flexion/extension and pro/supination) and elbow angle. External moment variables were included into the model if they led to a substantial increase (0.05) of the R-squared. If, for a particular moment, angle had a significant contribution (increase of the R-squared ≥ 0.05), angle specific variables were defined for this moment. (See text for further explanation).

	R ²	cons	SU ₁₂₀	SU ₁₀₀	SU ₈₀	SU ₅₅	PR ₁₁₂	PR ₁₀₀	PR ₈₀	PR ₅₅	EX ₁₂₀	EX ₁₀₀	EX ₈₀	EX ₅₅	FL ₁₂₀	FL ₁₀₀	FL ₈₀	FL ₅₅
BB	.73	-2.5			.76										.41	.48	.62	.79
BL	.72	-2.4			.66										.46	.59	.67	.82
BR	.73	-1.7						.31							.52	.53	.58	.66
BA	.65	-1.9			.49						.26				.28	.34	.45	.61
TR	.72	-1.9			.29						.68							
TL	.64	-1.8			.28			.24			.44				.08	.15	.30	.48
TM	.73	-2.3			.37						.80						.24	
AC	.62	-1.7			.41			.41		.39	.34	.26	.17					

Muscle load sharing

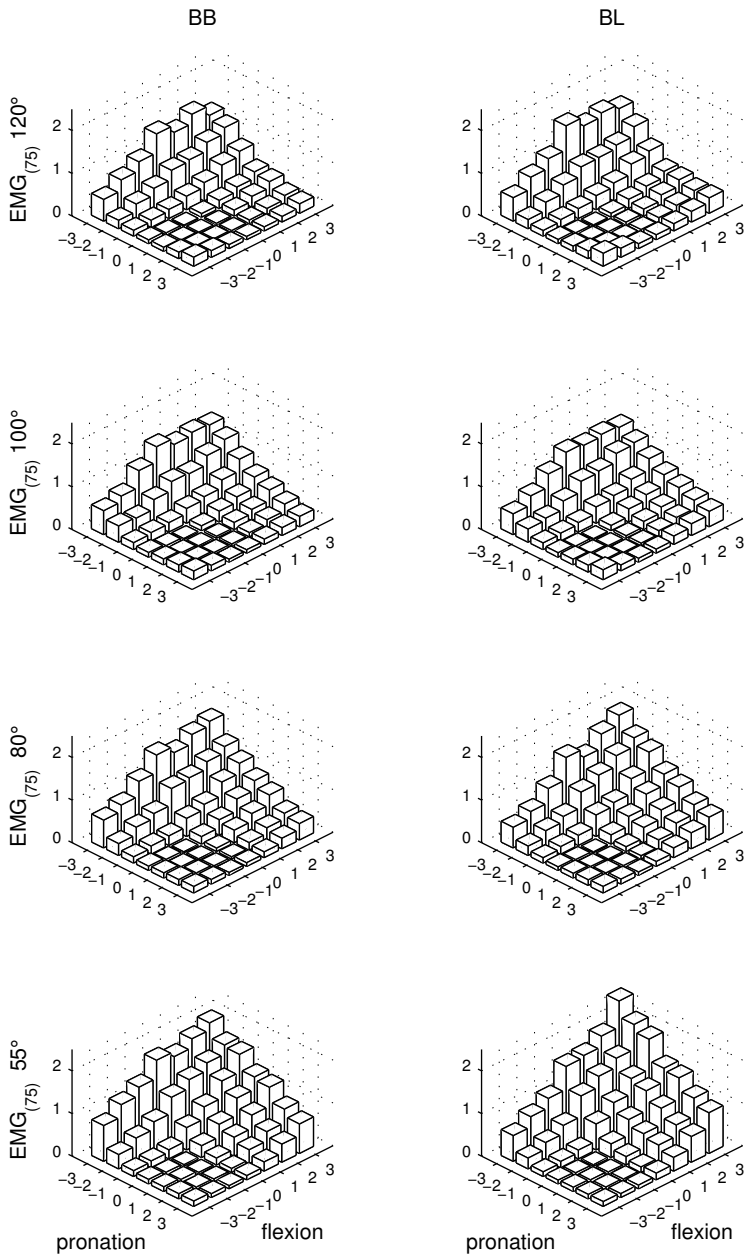
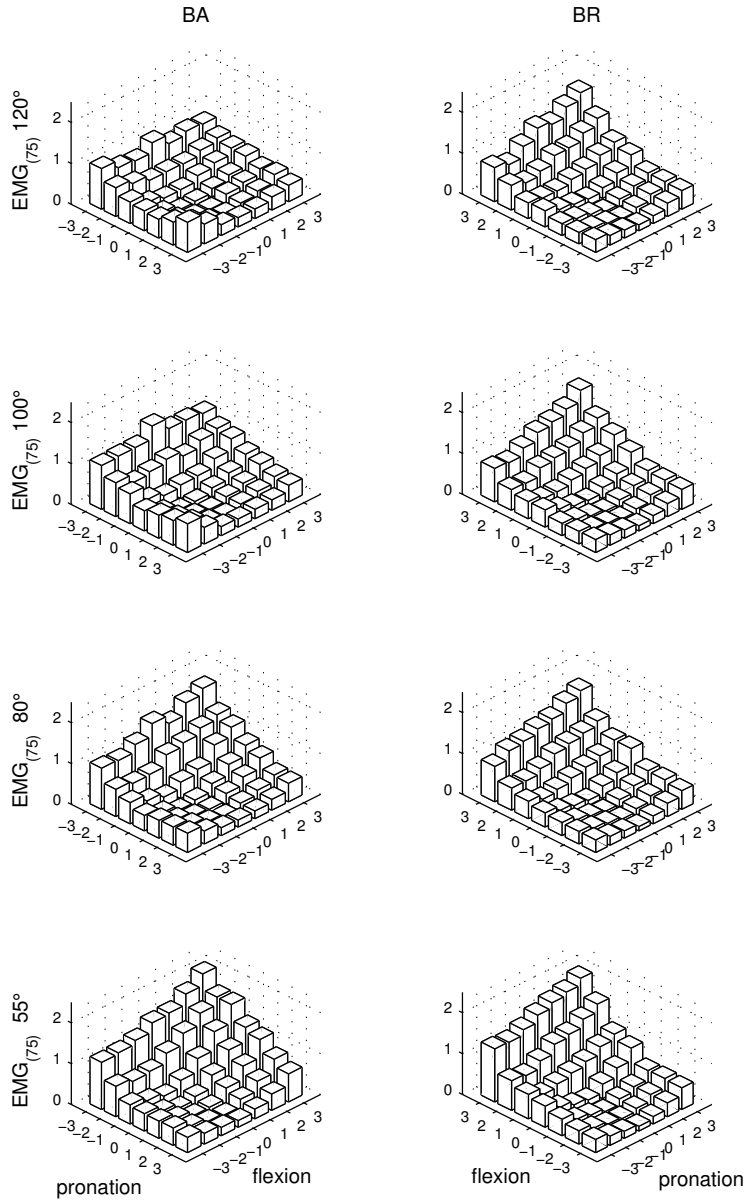


Figure 4.3 Normalised EMG values of the four measured flexor muscles (experiment I) averaged over subjects ($n=6$) plotted against the flexion moments and pronation moment for each muscle and each elbow angle.

The effect of elbow angle and external moment



Muscle load sharing

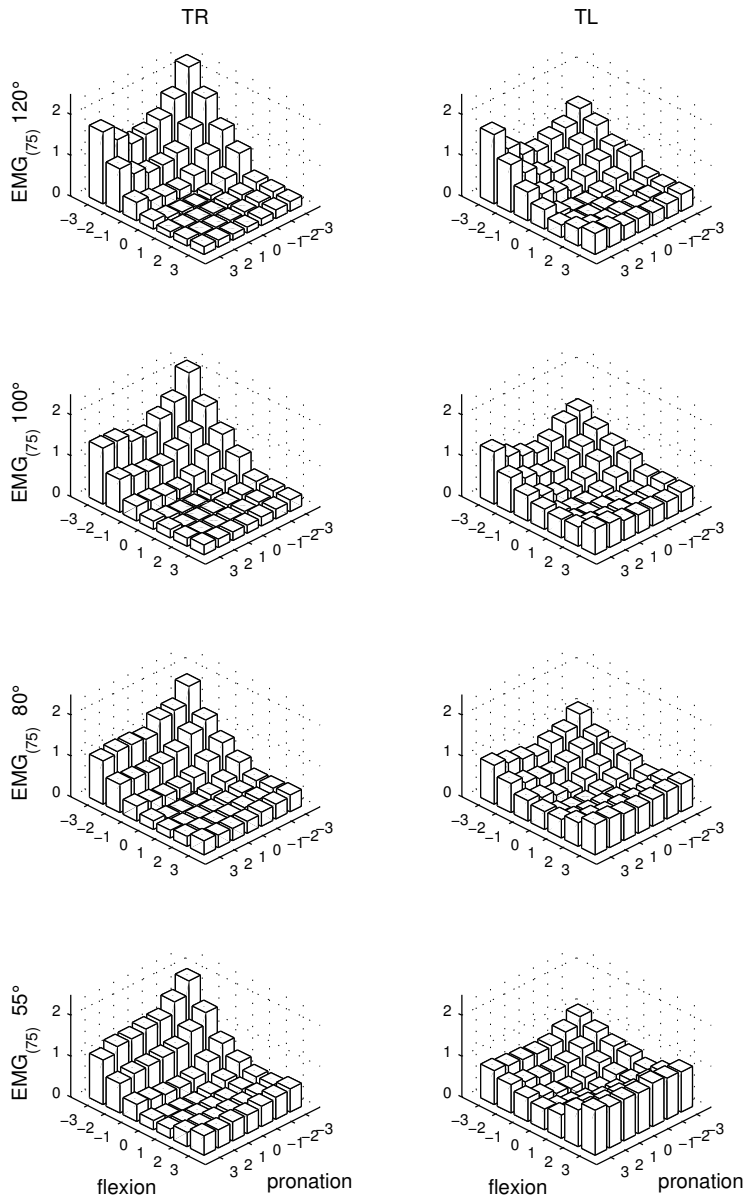
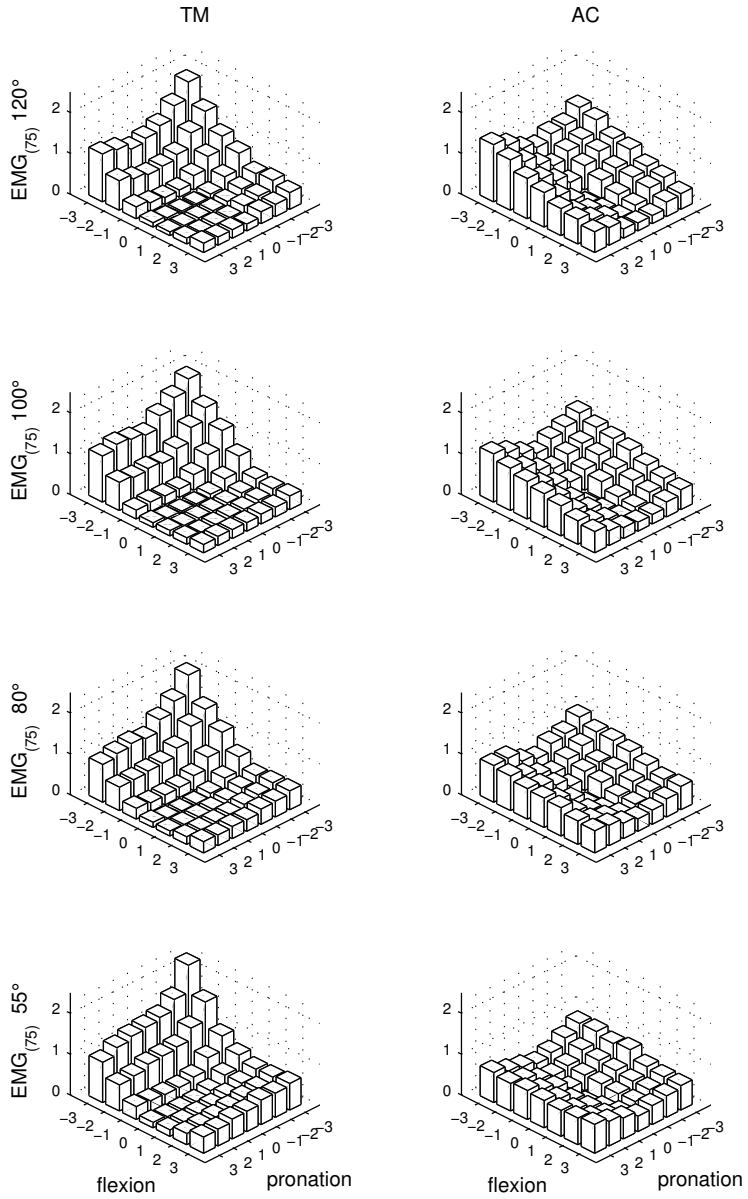


Figure 4.4 Normalised EMG values of the four measured extensor muscles (experiment I) averaged over the subjects ($n=6$) plotted against the flexion moments and pronation moment for each muscle and each elbow angle.

The effect of elbow angle and external moment



EMG data (experiment II)

Application of the regression model obtained in experiment I produced a good prediction of EMG amplitude for the EMG data of experiment II (R-squared of 0.72 and 0.68 and 0.55 for respectively BB, BR and TL).

Residual analysis

Analysis of variance showed that 25% to 46% of the residual sum of squares could be explained by the effect of subject and subject-moment (such as FL, FP, FS.) interaction. More specific analysis of the residuals showed that for some of the moment conditions residuals were indeed relatively large compared to other conditions and that a large part of these residuals could be explained by subject variance. This was especially the case for the data of TL during FL in experiment I and for BB during ES in experiment II.

Load sharing (experiment I)

Relative EMG contributions between BB and BR changed over the different moment combinations (Figure 4.5), which indicated a change in load sharing. As was seen before in Figure 4.4, supination led to an increase of BB and pronation led to an increase of BR. Second, relative EMG amplitude (i.e. load sharing) was also influenced by elbow angle, which was in turn different for the different moment combinations: during FP the EMG amplitude of BR was larger than that of BB, though the relative contribution of BB increased with elbow extension. For the extensors TR and TL, load sharing was only influenced by moment and not by elbow angle (Figure 4.6). During extension tasks the contribution of TR and TL was comparable, whereas during flexion tasks some activity of the bi-articular TL was found, but not, or hardly for the mono-articular TR. Elbow angle has no influence on the distribution between the two muscles (Figure 4.6).

Looking at the load sharing between flexor (BB) and extensor (TL) muscles (Figure 4.7) it was seen that during the supination tasks (ES and FS) this load sharing changed over elbow angle. As expected, TL was especially active during EP and ES. During EP the activity of TL decreased with elbow extension and there was no activity of BB. During ES on the other hand, there was a rather large contribution of BB activity, which increased with elbow extension. As seen before TL was also active during FP and FS. During FP, the contribution of TL was even higher than that of BB. During FS the contribution of BB was much larger than that of TL, however, the contribution of TL increased with elbow extension.

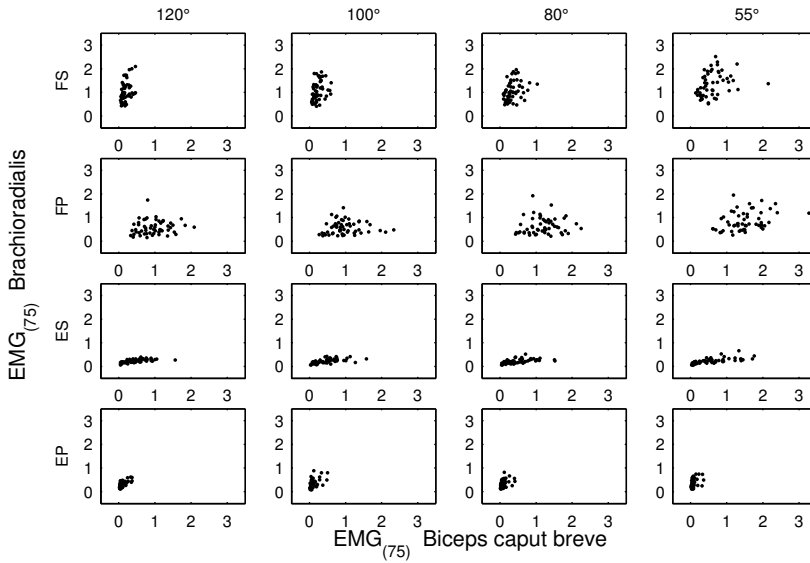


Figure 4.5 Load sharing. $EMG_{(75)}$ values of *m. brachioradialis* (BR) plotted against *m. biceps caput breve* (BB). The columns represent the four different elbow angles (120°, 100°, 80° and 55° of flexion) and the rows show the results of the four different moment combinations (FP, FS, ES and EP).

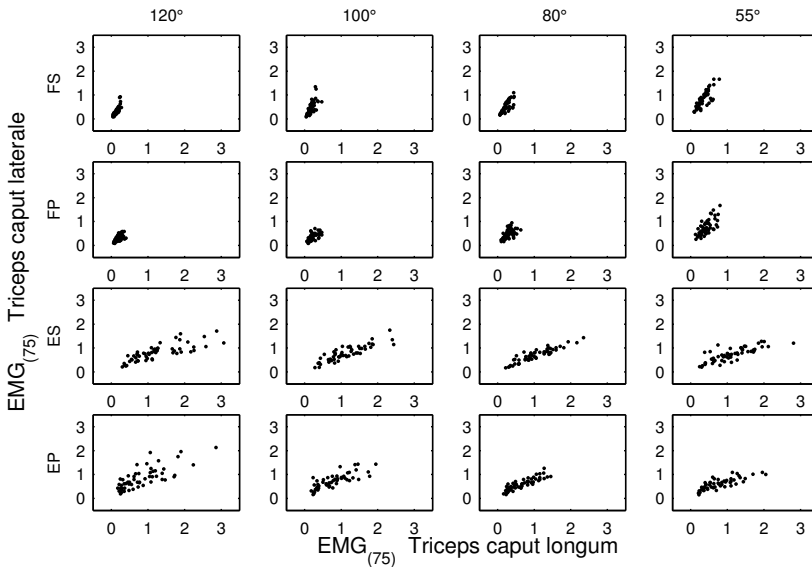


Figure 4.6 Load sharing. $EMG_{(75)}$ values of the *m. triceps caput laterale* (TL) plotted against the *m. triceps caput longum* (TR). The columns represent the four different elbow angles (120°, 100°, 80° and 55° of flexion) and the rows show the results of the four different moment combinations (FP, FS, ES and EP)

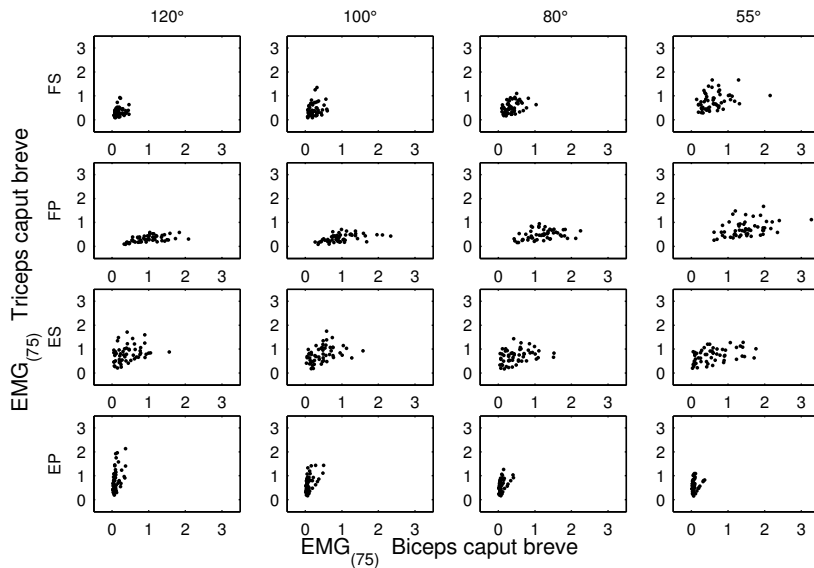


Figure 4.7 Load sharing. $EMG_{(75)}$ values of the *m. triceps caput laterale* (TL) plotted against the EMG_{75} values of the *m. biceps caput breve* (BB). The columns represent the four different elbow angles (120°, 100°, 80° and 55° of flexion) and the rows show the results of the four different moment combinations (FP, FS, ES and EP).

Relationship between $\dot{V}O_2$ and EMG (experiment II)

Corresponding to previous results (Pragman et al., 2003) it was found that the relation between EMG and $\dot{V}O_2$ could be described by a linear relationship. For BB and BR, the model only marginally improved when a quadratic term was added.

For BB and TR, the linear relationship was not influenced by elbow angle (Figure 4.8). For both muscles, angle specific variables did not give an improvement of fit (Table 4.2). For BR angle specific variables increased the R-squared from 0.63 to 0.71.

Table 4.2 Regression equations and R-squared for the relationship between $\dot{V}O_{2(75)}$ and $EMG_{(75)}$ defined by: $\dot{V}O_{2(75)} = \text{constant} + b * EMG_{(75)}$ or $\dot{V}O_{2(75)} = \text{constant} + b1 * EMG_{(75)} + b2 * EMG_{(75)}^2$ or $\dot{V}O_{2(75)} = \text{constant} + b1 * EMG_{(75)115} + b2 * EMG_{(75)110} + b3 * EMG_{(75)80} + b4 * EMG_{(75)60} + b5 * EMG_{(75)}^2$

Muscle	R ²	constant	EMG ₍₇₅₎₁₁₅	EMG ₍₇₅₎₁₀₀	EMG ₍₇₅₎₈₀	EMG ₍₇₅₎₆₀	EMG ₍₇₅₎ ²
BB	0.83	0.18			0.65		
	0.85	0.11			0.90		-0.12
	0.83	0.18	0.64	0.67	0.71	0.62	
BR	0.63	0.06			0.88		
	0.64	-0.07			1.32		-0.32
	0.71	0.05	0.74	0.85	0.93	1.05	
TL	0.60	0.008			0.92		
	0.60	0.001			0.94		-0.02
	0.62	0.002	1.03	0.93	0.86	0.75	

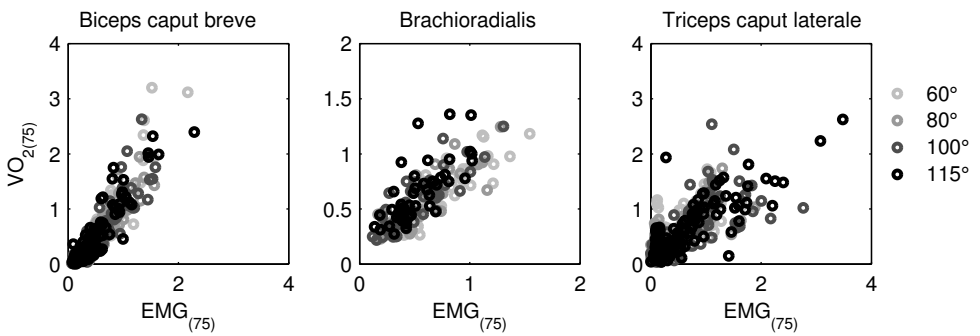


Figure 4.8 Normalised $\dot{V}O_2$ values plotted against normalised $EMG_{(75)}$ values for the *m. biceps caput breve* (BB), the *m. brachioradialis* (BR) and the *m. triceps caput laterale* (TL).

Discussion

Inverse dynamic models use cost functions in order to predict the individual contribution of muscles to a particular external moment. The exact principles behind this load sharing are (yet) unknown, making it difficult to find the right cost function. In the current study, data on muscle activation of elbow muscles was collected which can be used for model cost function validation. Not all of the functioning of elbow muscles is yet understood. For studying elbow muscles it is necessary to collect experimental data that includes sufficiently detailed information to account for the effect of combination of flexion/extension (FE) and pro-/supination (PS) moments as well as for the effect of elbow angle. In addition, these data should be sufficiently accurate to be used in an inverse dynamic model, such that muscle moment arm and length can be accounted for as well.

Previous studies on elbow function often focussed on flexion-extension (FE) tasks only, neglecting or not controlling the effect of pro/supination (PS) (Soechting and Lacquaniti, 1988; Leedham and Dowling, 1995; Van Bolhuis and Gielen, 1997; Kasprisin and Grabiner, 2000). Investigating the function of *m. biceps brachii caput breve*, the effect around the shoulder is often accounted for (Soechting and Lacquaniti, 1988; Van Bolhuis and Gielen, 1997), indicating that shoulder moment plays an important role as well, whereas, unfortunately, the supination moment is neglected. As can be learned from studies on compensatory motion in spastic children (Kreulen et al., 2006), it is, however, evident that the supination moment of *m. biceps brachii* is also of large significance and interacts strongly with its elbow flexion function.

The results of elbow studies are not unambiguous. Differences could possibly be due to inadequate control of degrees of freedom. Studies in which pro/supination was included (Buchanan et al., 1986; Van Zuylen et al., 1988; Buchanan et al., 1989; Caldwell and Van Leemputte, 1991; Hebert et al., 1991; de Serres et al., 1992; Jamison and Caldwell, 1993; Bechtel and Caldwell, 1994; Jamison and Caldwell, 1994), however, also do not show explicit muscle activation patterns. Experimental results show:

1. load sharing during elbow/flexion is (of course) influenced by the presence or absence of (external) pro- or supination moment and vice versa (Buchanan et al., 1989; Hebert et al., 1991; de Serres et al., 1992; Jamison and Caldwell, 1993; Bechtel and Caldwell, 1994; Jamison and Caldwell, 1994) and also by elbow angle (Van Zuylen et al., 1988; de Serres et al., 1992),

2. Muscle activation patterns seem to be task dependent as well as subject specific (Buchanan et al., 1989; Bechtel and Caldwell, 1994; Buchanan and Lloyd, 1995),
3. Muscles sometimes show 'seemingly inappropriate muscle actions' (Buchanan et al., 1989), presumably meant to compensate for unwanted additional muscle moments of other muscles (Van Zuylen et al., 1988; Buchanan et al., 1989; Jamison and Caldwell, 1993).

The question remains how load sharing is organised and whether the differences in results presented in the literature are task specific, or subject specific, or both.

In the current study, an extensive data set on activation of elbow muscles, including variations in elbow angle and a wide range of moment combinations as well as different force levels, was collected. The use of EMG and NIRS allowed for the measurement of indicators for both muscle activation and muscle energy consumption. Since the local $\dot{V}O_2$ measurements were extremely time consuming, these measurements had to be restricted to a limited set of moment combinations as well as to a limited number of muscles and subjects. Therefore, another experiment was performed in which only EMG was measured enabling measurements of a larger number of muscles and subjects and a complete set of external moments.

Influence of external moment

The aim of imposing a broad set of combinations of elbow flexion-extension and forearm pro/supination was to quantify the effect of external load and elbow angle on the relative contribution of muscles (at varying lengths). Results of the current study showed, that muscle activity (EMG) was, as expected, strongly influenced by external moment.

Although the relationship between EMG and external moment often can be satisfactorily described by a linear relationship (see Praagman et. al., 2003), the EMG data in the current study seemed to be better described by a logarithmic relationship, in the sense that residuals showed a better normal distribution.

The major part of the recorded EMG activity could be explained mechanically, though in different ways. First, muscles are directly influenced by the in- or decrease of a particular external moment if that muscle can actually contribute to that particular moment (e.g., the increase of biceps activity with increasing supination). Second, it can also be influenced indirectly by the activity of another muscle that contributes to the particular moment (synergistic- as well as antagonistic load sharing). If a muscle produces moments around more than one

joint axis, a change in activity due to a change in the moment required on the one axis automatically leads to a change in the generated moment around the other axis as well. The latter leads to an increase or decrease of one (or more) of the synergists for the second axis (synergistic load sharing). However, if the moment generated around the second axis is not wanted at all, this moment needs to be compensated by an antagonistic muscle (antagonistic load sharing) (Veeger and Van der Helm, 2007).

As expected, activity of all flexor muscles increased with increasing flexion moment. Since BB and BL generate not only a flexion- but also a supination moment, it is not surprising that the activity during flexion further increased with increasing supination moment and decreased with increasing pronation moment. The latter influences the contribution of other elbow flexors such as BR as well: due to the decrease of biceps activity during flexion-pronation an increase of BR can be seen, since the flexion moment that had to be generated remained the same (synergistic load sharing). In spite of the fact that extensor muscles cannot produce any pro- or supination moment, their activity was influenced by supination moment. There was an increase in activity with increasing supination moment. This could be explained by a compensation for the flexion moment generated by BB and BL which is generated when these muscles contribute to the required supination moment. If this additional flexion moment is either unwanted (i.e., during extension-supination or pure supination) or larger than the required flexion moment, a compensating extension moment is needed. The latter can be generated by the m. triceps brachii, resulting in co-contraction (antagonistic load sharing).

A small part of the experimental data could not be explained by one of the above mentioned load sharing principles. During experiment I, co-contraction of TL was also seen during flexion. The activity of TL was not only influenced by the extension moment and supination moment but also by the flexion moment (Table 4.1). This type of activity cannot be explained by the load sharing principles mentioned above. TL does not contribute to the requested flexion moment and there is no side-effect that needs to be compensated for. It is possible that this type of co-contraction was caused by stability requirements. By applying the external moments by weights (and a pulley system) at a bar an unstable situation was created (compared to using a fixed force transducer (Chapter 2 and 3). Moreover, it was seen (residual analysis) that there were large differences in the amount of co-contraction between the different subjects, suggesting that strategies leading to co-contraction are quite subject-specific instead of general. This finding is not unique. In a study on the activity of back muscles, Van Dieën (1996) showed that

25% of the subjects showed a diverged pattern which was due to a higher level of co-contraction of the abdominal muscles.

Influence of elbow angle

Elbow angle had a significant effect on EMG level and relative muscle activation. Variation in elbow angle (from 55 to 120° of elbow flexion), changed both muscle lengths and moment arms of the elbow muscles, which both can influence relative and absolute muscle activation. It is well known that when a muscle has to produce a given force at a length shorter than optimum length, the activation needed to generate this force increases due to the increased overlap of sarcomeres. It is also obvious that the force that a muscle has to generate to produce a given moment is inversely related to its moment arm. Both factors might influence the relative muscle activity. It seems reasonable to expect that if a muscles' length becomes sub-optimal or its moment arm decreases, the energy consumption increases since more activation/force is needed to produce the same force/moment. However, this is seen from a single muscle perspective, assuming that the power produced by the muscle stays the same and that load sharing would not change over the different elbow angles. Taking a multiple muscle system as starting point, a more optimal length or larger moment arm will make a muscle 'cheaper' or more economic, which could possibly lead to a change in force sharing: an increase in activity of the particular muscle and a simultaneous decrease of activity of one (or more) of the synergists.

The results of the current study showed that elbow angle indeed influenced the activity of some muscles (Table 4.1). But results can not be easily related to the actual changes in muscle length or moment arm, as both can vary in a different way. For instance, increase of BR activity with decreasing elbow angle could be related to a decreasing moment arm. The maximal moment arm is found between 100° and 115° (Murray et al., 1995; Veeger et al., 1997). Length, however, becomes more favourable with decreasing elbow angle at first and has its optimum around 80°. For BB both optimum length and moment arm are found around 80° of elbow flexion. Nevertheless, results of the current study show that BB activity during flexion increased with decreasing flexion angle (Table 4.1), and no optimum (maximum or minimum) was found at 80°. It has to be noticed that as the anteflexion angle of the glenohumeral joint increased with decreasing elbow angle, the increase in BB activity might as well be attributed to the increasing anteflexion angle. Further by influencing the activity of one muscle, a change in moment arm or length likely indirectly influences its synergists as well.

In line with previous findings (de Serres et al., 1992), our results show that load sharing changes over elbow angle (Figures 4.5 and 4.7).

However, it can not be derived from our data whether the contribution of a muscle increases or decreases if it becomes more favourable, since it is impossible to distinguish all the individual aspects that affected the muscle activity. To unravel the exact effects a musculoskeletal model would be needed, in order to gain better insight into the specific effects of the different factors that influence load sharing.

Subject specific patterns

Although overall results were quite comparable between subjects, for some specific conditions there seemed to be large differences between subjects in activation patterns of particular muscles. These inter-individual differences were found for pure antagonistic muscle activity (TL during FL) as well as for antagonistic load sharing (BB during ES). As mentioned before, this finding was in line with previous studies (Buchanan et al., 1989; Bechtel and Caldwell, 1994). Assuming that people use the same load sharing principle, such individual muscle activation patterns could possibly be due to a high sensitivity to inter-individual differences in morphology.

Relationship between EMG and $\dot{V}O_2$

Another research question of this study was whether the linear relationship between $\dot{V}O_2$ and EMG as was found earlier (Praagman et al., 2003) for a constant elbow angle would also hold for different elbow angles and a larger range of moment combinations.

The current study confirmed our earlier finding (Praagman et al., 2003) that the relationship between $\dot{V}O_2$ and EMG can be satisfactorily described by a linear equation. No substantial improvement was found by adding a quadratic term (Table 4.2). Introducing elbow-specific EMG variables also did not lead to a better fit, except for BR (Table 4.2). Based on morphological data (Klein Breteler et al., 1999) it can be concluded that within the range of elbow angles (60°-115° of elbow flexion) used, the corresponding change in muscle fibre length was by far the largest for BR (almost 60% compared to about 30% for BB and TL). It is therefore, possible that the relationship between $\dot{V}O_2$ and EMG is influenced by change in muscle fibre length but only at major length changes.

In musculoskeletal modelling it was shown that cost functions linearly related to muscle force (i.e., minimisation of sum of muscle forces or sum of muscle stress) resulted in sequential muscle recruitment (Dul et al., 1984b). Using linear cost functions it is most advantageous to use the muscle with the largest moment arm to produce the required muscle moment, since the least muscle force is required. The linear

relationship between $\dot{V}O_2$ and EMG suggests that muscle activation and muscle energy consumption are linearly related. Since muscle force is linearly related to energy consumption as well, this would mean that minimisation of energy consumption (which is in general expected to be the principle behind load sharing) would lead to sequential recruitment. From experimental evidence it is clear that load sharing does *not* lead to sequential recruitment. It can therefore be argued that energy consumption is indeed minimised or that the linear relationship between $\dot{V}O_2$ and EMG is based upon two opposing non-linear relationships; EMG-activation and activation- $\dot{V}O_2$, leading to a linear relationship between EMG and $\dot{V}O_2$.

Conclusions

Joint angle, and therefore moment arm and muscle length influence both the activation level of the muscle as well as the load sharing between muscles.

The principles behind load sharing, however, are difficult to quantify, since it is impossible to distinguish all the individual aspects that affect muscle activity. To solve this complex problem a biomechanical model is needed at least.

The relationship between EMG and $\dot{V}O_2$ could be described by a linear relationship, it is yet unknown whether all processes lying in between are linear processes as well.

Although, on average, subjects show comparable muscle activation patterns, during conditions in which more than one moment was required and the particular muscle counteracted to one of these moments, there are some striking inter-individual differences as well.

These inter-individual differences might be the consequence of two different factors: 1. subjects use different optimisation strategies or 2. they might reflect the role of inter-individual differences in morphology.

Acknowledgements

The authors would like to thank J. Praagman for his advice on the statistical analyses.



Chapter 5

The effect of PCSA and moment arm distributions on the load sharing of arm muscles

M. Praagman, J. Praagman, E.K.J. Chadwick, F.C.T. van der Helm, H.E.J. Veeger.
Submitted for publication

Abstract

The use of cost functions in inverse dynamic models, to predict individual muscle forces, is based on experimentally observed general movement patterns and the assumption that people use the same optimisation strategy. Experimental studies on muscle activity however, show that there are inter-individual differences in activity, which have to be accounted for. Assuming that people use the same optimisation strategy it could be maintained that these individual differences are caused by differences in morphology. As biomechanical models are in general based on a single anthropometrical data set, it is certain that such differences in muscle activity will not be reflected by these models. The goal of this study was to investigate whether observed inter-individual differences in load sharing could be caused by morphological differences between subjects and whether interaction exists between morphology and optimisation criteria.

Two different cost functions were studied: the standard stress cost function and an energy-related cost function. 16 PCSA and moment arm values of several arm and forearm muscles in an inverse dynamic model of the shoulder and elbow (the Delft Shoulder and Elbow Model) have been varied. An approximative optimisation strategy was used to find for each subject the individual morphological parameter set (PCSA and moment arm) that was expected to correspond best with experimental data (EMG and muscle oxygen consumption), collected in a previous study.

Predicted load sharing was strongly dependent on cost function as well as on morphology. The energy-related cost function showed a better fit to experimental results than the stress cost function. Modelling results improved by fitting the morphological parameters to the experimental data of individual subjects; however this was only effective when the energy-related cost function was used. It can be concluded that inter-individual variability in the experimental results could be partly explained by morphological differences.

Introduction

Musculoskeletal models need cost functions to estimate the relative and absolute contribution of individual muscles, or muscle parts, to a particular external force or moment. Generally, more than one muscle combination can, mechanically speaking, be used to exert this external force. The human body appears to apply some form of load sharing principle to activate a specific combination of muscles. It is as yet uncertain how load sharing can be realistically simulated. Several cost functions have been proposed (see Tsirakos et al., 1997 for an overview) but validation is hampered by the fact that muscle force is not easily measured *in vivo* and that information on muscle contraction often is restricted to EMG patterns, i.e. the activation signal.

Most cost functions are mechanical cost functions based upon muscle force, often weighed by maximal force or physiological cross sectional area (PCSA). Therefore the model outcome depends not only on the kinematics, external force and the choice of cost function, but also on the model's morphology. Data on the morphology of most models are based on cadaver measurements, which are scarce (Veeger et al., 1991a) and often incomplete (Yamaguchi et al., 1990).

An inverse dynamic model of the shoulder and elbow has been developed by Van der Helm (1994a, 1997b). In a previous study we used this model to evaluate the effect of different cost functions on individual force predictions (Praagman et al., 2006). Two different cost functions were investigated: the 'standard' sum of squared stress cost function and a new metabolic energy-related cost function. Cost values predicted by the model were compared to measured muscle oxygen consumption ($\dot{V}O_2$) values for several arm muscles. Analyses focused on two different measures: first the overall fit (correlation and root mean square error (RSME) values) between model predictions and experimental results and secondly the number of so-called 'false negatives' and 'false positives' (conditions in which the model predicted NO muscle activity where a muscle was active, based on experimental observations and vice versa). Comparisons between modelling results and experimental data for muscle oxygen consumption indicated a large number of "false negatives", especially for the standard stress cost function. These were mainly seen for muscles which span more than one degree of freedom (Praagman et al., 2006). It appeared that pro/supination moments had a disproportionately large effect on the predicted activity of these muscles, compared to flexion/extension moments. The use of an energy related cost function led to fewer false

negatives. It was concluded that the energy related cost function resulted in more realistic prediction of force patterns and therefore appeared to be a promising improvement (Praagman et al., 2006).

Although previous measurements focused on several combinations of flexion/extension and pro/supination moments, comparisons were based on data for one arm position only. This implies that length effects could not be taken into account, while it is to be expected that muscle fibre length will be of influence. Moreover, muscle force-length characteristics were not incorporated in the cost functions that were used in our previous study (Praagman et al., 2006). Recent cadaver studies (Klein Breteler et al., 1999) allows the construction of a unique model parameter set that also includes muscle optimum length and therefore can account for the force-length characteristics of the muscles. In addition, new experiments were performed in which elbow angle, and therefore muscle length, was varied (for a detailed description of this data set see Chapter 4) and in which a larger set of moment combinations was obtained.

When posture (in our case the elbow flexion angle) is changed, the length of the muscle as well as its moment arm is affected. It is unclear what effect this change in elbow angle will have on the distribution of forces over muscles around the joint involved: From a single muscle perspective it could be expected that muscle activity *decreases* at optimum length/optimum moment arm as the muscle can achieve the same force/moment with less activity. Conversely, from a multiple-muscle point of view completely opposite expectation can be extracted: as the muscle becomes 'cheaper' its contribution might *increase*, since use of that muscle has become 'cheaper'. Which of these (or a combination of these) two principles forms the conceptual basis of the muscle activation pattern could not easily be revealed from our previous study (Chapter 4). The use of a biomechanical model might give a better insight into the trade-off between these principles.

Although, on average, subjects show the same muscle activation patterns, inter-individual differences in activation patterns have been reported (Buchanan et al., 1989; Bechtel and Caldwell, 1994). Our previous study also showed for some conditions differences between subjects (Chapter 4). Assuming that people use the same optimisation strategy (which is the basis of any cost function) it could be maintained that these individual differences are caused by differences in morphology. As the model is based on one anthropometrical data set it is certain that such differences will not be reflected by the model. This raises the question to what extent the correspondence between model

predictions and experimental data will improve with the inclusion of personalised morphological scores. In that case for any given subject a different combination of for instance PCSA's and moment arms should lead to a better fit between experimental and model data.

The goal of this study is to investigate whether morphological differences can explain the recorded differences in muscle recruitment between subjects. Also the interaction between morphology and optimisation criteria will be investigated.

Since no actual morphological measurements of our subjects were available we used another approach, starting from the generic model and searching those values for the morphological parameters that give the best fit with the experimental data. 16 PCSA and moment arm values of several arm and fore-arm muscles in the model have been varied in a range based on several cadaver studies (An et al., 1984; Murray et al., 1995, 2000; Veeger et al., 1997; Ettema et al., 1998; Klein Breteler et al., 1999). By changing parameters in different directions and for several muscles, numerous combinations will be possible. An approximative optimisation strategy was used to find for each subject the individual parameter set that was expected to correspond best with the experimental data. The fit between the experimental data and the model with this optimal morphological parameter set can be seen as the maximum improvement that could be attained by inclusion of individual morphology in the model. All procedures were performed for two different cost functions; a stress cost function as well as an energy-related cost function (Praagman et al., 2006).

Methods

The Delft Shoulder and Elbow Model

The Delft Shoulder and Elbow model (DSEM) is a 3D inverse dynamic model of the shoulder and arm (for a detailed description see Van der Helm, 1994 and 1997b). Parameters for the model included, besides from standard information on geometry and PCSA based on cadaver measurements (Klein Breteler et al., 1999), also the force-length relationship of the muscles (Klein Breteler et al., 1999). Kinematic data as well as external forces and moments are needed as input for the model. The output comprises joint contact forces, ligament - and muscle forces, muscle lengths and moment arms. In the current study two different cost functions were compared, the well known stress cost function

(Crowninshield and Brand, 1981) and an energy-related cost function (Praagman et al., 2006).

The stress cost function J_σ was defined as:

$$J_\sigma = \text{MIN} \sum_{i=1}^n \left(\frac{F_{mi}}{\text{PCSA}_i} \right)^2 \quad (5.1)$$

in which F_{mi} is the force produced by muscle i and PCSA_i is the physiological cross-sectional area of muscle i .

The energetic cost function J_E was defined as:

$$J_E = \text{MIN} \left[a_1 \cdot F_m \cdot l_{f_{\text{opt}}} + m \cdot \left\{ b_1 \cdot \frac{F_m}{\text{PCSA} \cdot \sigma_{\text{max}} \cdot f_l(l_m)} + b_2 \cdot \left(\frac{F_m}{\text{PCSA} \cdot \sigma_{\text{max}} \cdot f_l(l_m)} \right)^2 \right\} \right] \quad (5.2)$$

in which $l_{f_{\text{opt}}}$ is the optimal fibre length, m is muscle mass, σ_{max} is the maximal muscle stress and $f_l(l_m)$ are the normalised force-length characteristics. σ_{max} is defined as 100 N/cm² (Fick, 1910) and the constants a_1 , b_1 and b_2 are respectively set to 1, 100 and 400.

J_E represents the muscle energy consumption and is based on the two major energy-consuming processes in the muscle: detachment of cross-bridges and re-uptake of calcium. The detachment of cross-bridges is represented by the first linear term. F_m is linearly related to the number of attached cross-bridges (Huxley, 1957) and has to be scaled to optimal fibre length. The second and third term represent the re-uptake of calcium, which although the exact relationship is unknown, is assumed to be non-linearly related to muscle energy-consumption

Although this cost function is essentially comparable to the function that was used in (Praagman et al., 2006), the function has been reformulated to include the (now available) force-length characteristics of the muscles.

Experimental set-up and data collection

The experimental data were collected in a previous study (Chapter 4) and comprised data on muscle oxygen consumption ($\dot{V}O_2$) of three arm muscles: m. biceps brachii caput breve (BB), m. brachioradialis (BR) and m. triceps brachii caput laterale (TL). Four male subjects (age 29.4 years (SD 7.3), height 1.75 m (SD 0.06), body mass 70.2 kg (SD 6.9)) participated. Subjects were seated on a chair with their elbow flexed at a fixed angle and their forearm horizontal and in a neutral position (Figure 5.1). No elbow or arm support was used. Subjects had to generate moments around the humero-ulnar joint (flexion (FL) and extension (EX)) and radio-ulnar joint (pronation (PR) or supination (SU)), as well as combinations of these moments (flexion-supination (FS), flexion-

pronation (FP), extension-supination (ES) and extension-pronation (EP)). All moments had to be performed at three different force levels. In total 36 of the 49 possible moment combinations were performed (Figure 5.2).

The subjects held a special tool with their right hand. This tool consisted of a stick with a horizontal bar on top to which, on several positions, weights (0.75, 1.5, 3 or 4.5 kg) could be applied (directly or through a pulley), enforcing the external moments the subject had to withstand. This resulted in flexion/extension moments of 5, 10 and 15 Nm and pro/supination moments of 1, 2 and 3 Nm. Subjects were instructed to hold the tool in a fixed position keeping the bar horizontal. Feedback was given by means of a horizontal cord in front of the subject (Figure 5.1).



a

b

Figure 5.1 *Experimental set-up. Subject was sitting on a chair with the elbow flexed and forearm in a horizontal and neutral position. The subject had to hold the tool with his right hand, keeping the bar on top horizontal (a). Visual feedback on the position of the tool was given by a horizontal cord. Flexion moments were enforced by hanging weights right under the stick while extension moments were enforced by loads applied to the middle of the bar using a pulley system. Pro/supination moments were imposed by hanging weights on different distances left or right from the stick (b).*

Measurements were repeated in a random order at four different elbow angles: 60, 80, 100 and 115° of elbow flexion (where 0° is full elbow extension). Muscle oxygen consumption ($\dot{V}O_2$) was measured with Near InfraRed Spectroscopy (NIRS) during arterial occlusion. The position of the subject was monitored at 25 HZ by recording the 3D co-ordinates of bony landmarks on the thorax, clavicle, scapula, humerus and forearm, using an automated video based recording system (Optotrak™, Northern Digital Inc., Canada). A detailed description of the experimental set up and data can be found in Chapter 4.

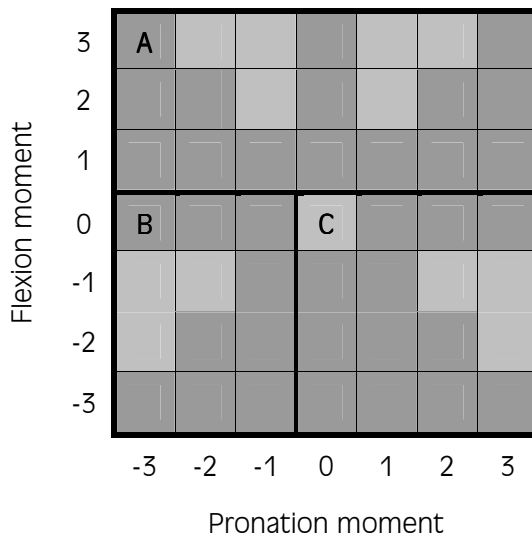


Figure 5.2 Schematic overview of all different moment combinations the subjects had to perform. All loads could be applied at three different force levels (1, 2 and 3) leading to a total of 49 possible combinations. A selection (36) of these conditions, represented by the dark grey cells, was measured, divided over three different days (A, B and C). TL was measured during all three sets, BB was measured during set A and B and BR was measured during set A only.

Experimental data processing

Per subject muscle oxygen consumption values were normalised to the highest value measured for that muscle. For BB, BR and TL individual cost values were calculated and normalised in the same way.

Orientations of the body segments of each subject were calculated from the measured 3D co-ordinates, following the protocol described in Van der Helm (1997a). The individual 3D orientation of the body segments as well as the measured external forces and moments of all subjects and all

conditions (4 subjects x 4 elbow angles x 36 conditions = 576 datasets) were used as input to the DSEM.

Model simulations

Two different simulations were performed. First, simulations were done with the 'standard' model based on the original cadaver morphology, using the 'standard' morphologic parameters in combination with the J_c and J_E . Second, each simulation was repeated with an individualised morphology set for each cost function.

Derivation of individual morphology sets

For the individualised morphology 16 model parameters were taken into account: the PCSA's of both heads of m. biceps brachii (BB, BL), m. brachioradialis (BRD), m. brachialis (BRA), combined lateral and medial head of m. triceps brachii (TLM), m. pronator teres (PT), m. pronator quadratus (PQ) and m. supinator (SUP) as well as flexion-extension (FE) momentarms of combined heads of m. biceps brachii (BB/BL), BRD, PT and TLM and pro-supination (PS) moment arms of BIC, PT, PQ and SUP. Based on variations of these parameters as reported in the literature (An et al., 1984; Murray et al., 1995; Veeger et al., 1997; Ettema et al., 1998; Klein Breteler et al., 1999; Murray et al., 2000), they were restricted to vary between 50% and 150% of their nominal values. In addition the PCSA's of BB, BL and BA were restricted to a maximal inter-individual difference of 50%.

The aim was to find for each individual the values of these 16 parameters that result in the best fit between the results of the DSEM (cost values) and our empirical measurements ($\dot{V}O_2$). The implicit nature of the DSEM (it can not be described by one single function) makes the calculation of this optimal solution very difficult and time consuming if not impossible. Therefore an approximation strategy has been used. First explicit compact models have been build that reproduce the outcomes of the DSEM as good as possible. These models describe the outcome of the DSEM as function of the 16 morphological parameters and can be used to predict the outcome of the DSEM at any possible combination of these parameters. Next optimisation was carried out using these compact models and the resulting morphology approximates the solution of the original optimisation problem (Figure 5.3).

To find good compact models the simulations with the DSEM were repeated for 160 different sets of the morphological parameters. These 160 sets of parameters were chosen according to a space filling latin hyper cube (Morris and Mitchell, 1995), which guarantees that the 160

sets represented an optimal spread over the 16-dimensional parameter space.

Next, per muscle for each of the measured conditions (in total 300 conditions: 4X24=96 for BB, 4X15=60 for BR and 4X36=144 for TL) a compact model was fitted that described these 160 outcomes of the DSEM as a function of the 16 morphology parameters. Subsequently these explicit compact models were used to calculate the parameter values that resulted in the best fit between the outcomes of the compact models and the experimentally obtained oxygen data. For each subject this led to our approximate optimal individual morphology set.

Two types of model structures were used to define the compact models:

1. a second order polynomial model :

$$Y = \beta_0 + \beta_1 X_1 + \dots + \beta_{16} X_{16} + \beta_{1,1} X_1^2 + \beta_{1,2} X_1 X_2 + \dots + \beta_{16,16} X_{16}^2 \quad (5.3)$$

2. a kriging model:

$$K(x_1, \dots, x_{16}) = \alpha + \sum_j \beta_j \cdot \exp \left[-\theta_j \sum_i (x_i - x_{j,i})^2 \right] \quad (5.4)$$

in which the morphological parameter sets are represented by j (1:160) and the specific parameter by i (1:16). α , β and θ are chosen to maximise the fit between the DSEM output and $K(x_1, \dots, x_{16})$ over all 160 test sets.

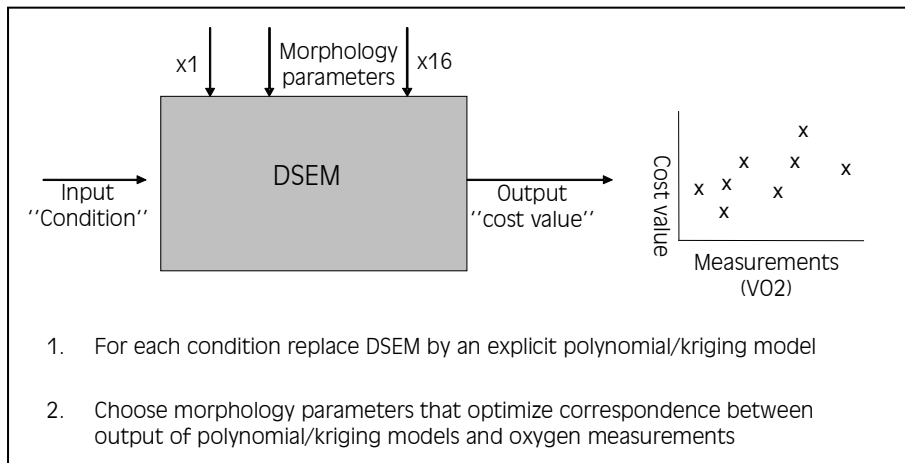


Figure 5.3 Schematic representation of the approximative optimisation strategy used to predict the optimal individual morphology (see text for further detail).

Kriging models stem from statistical geology but have shown to be valuable in modelling the outcomes of computer experiments also (Sacks et al., 1989). Generally speaking, they often can better cope with non-linearity in the data than polynomial models.

The whole procedure described above was done for both the J_o and J_E . If for a particular subject and cost function the individual morphology set predicted by the kriging models led to a substantial better fit between cost values and oxygen consumption than the morphological parameters predicted by the polynomial functions, these kriging models were used.

Data analysis

Measured oxygen consumption values were normalised per subject and per muscle to the highest value measured for that subject and muscle. The same was done for the cost values of the individual muscles predicted by the DSEM.

Linear regression was performed to evaluate the relationship between $\dot{V}O_2$ and cost, expressed as correlation coefficient and RMSE value. Further analysis focused on the number of false negatives and false positives: conditions for which the DSEM did not predict any muscle activity while experimental measurements did show that the particular muscle was active and vice versa.

For each muscle (BB, BR and TL) average values (over the four subjects) of the normalised cost values and normalised $\dot{V}O_2$ values were also calculated. These average cost values were plotted against the mean oxygen consumption values and correlation coefficients and RMSE values were calculated.

All of the above described analyses were performed for the DSEM predictions performed with both cost functions (J_o and J_E) and with both morphological data sets (standard morphology as well as the individually optimised morphology).

Results

Due to technical problems the $\dot{V}O_2$ measurements of BR for one of the subjects failed. Therefore, results of BR are based on 3 subjects only.

Flexion moments as well as pronation moments will be defined as positive (negative flexion moments are extension moments and negative pronation moments are supination moments).

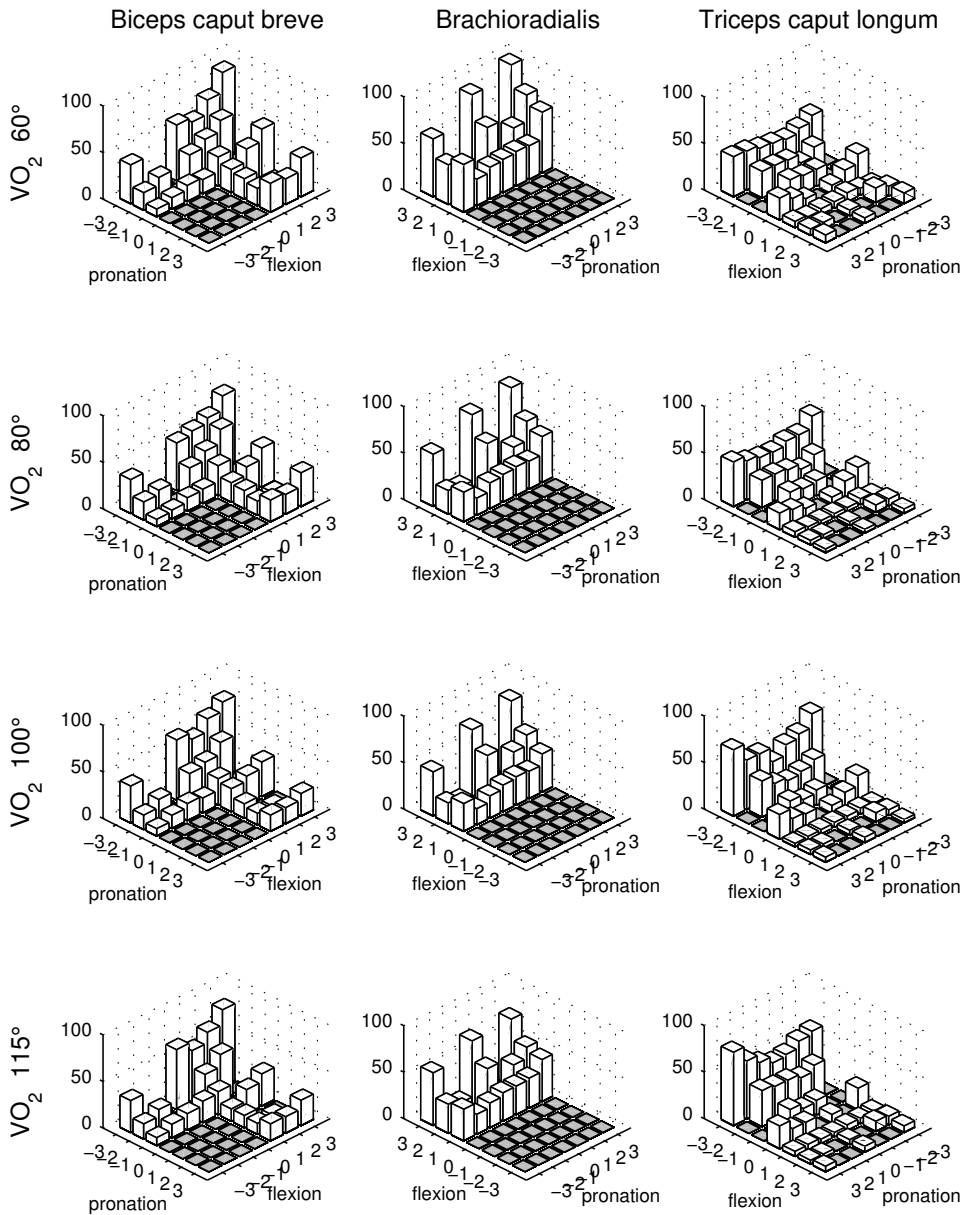


Figure 5.4 Normalised VO_2 values averaged over the subjects plotted against internal flexion and pronation moment, for *m. biceps caput breve* (BB), *m. brachioradialis* (BR) and *m. triceps caput laterale* (TL) for four elbow angles (60°, 80°, 100° and 115°).

The experimental data showed that muscles were not only active when they could contribute to (one of) the requested moments but also in some conditions in which they could not contribute to the requested moments (TL was found to be active in tasks involving pronation, but without extension) or even had an opposing effect on (one of) the requested moments (BB was found to be active in tasks involving supination and extension) (Figure 5.4). There were also considerable differences between subjects (Figure 5.5).

Differences between subjects in $\dot{V}O_2$ patterns were seen especially for BB and TL. Figure 5.5 shows these differences for the m. biceps caput breve. Subj1 deviated most from the other subjects and the largest differences were seen between subj1 and subj3. Subj1 showed much more biceps activity during SU and ES whereas subj3 showed more activity during PR. For TL differences were seen during ES, EP, SU and PR.

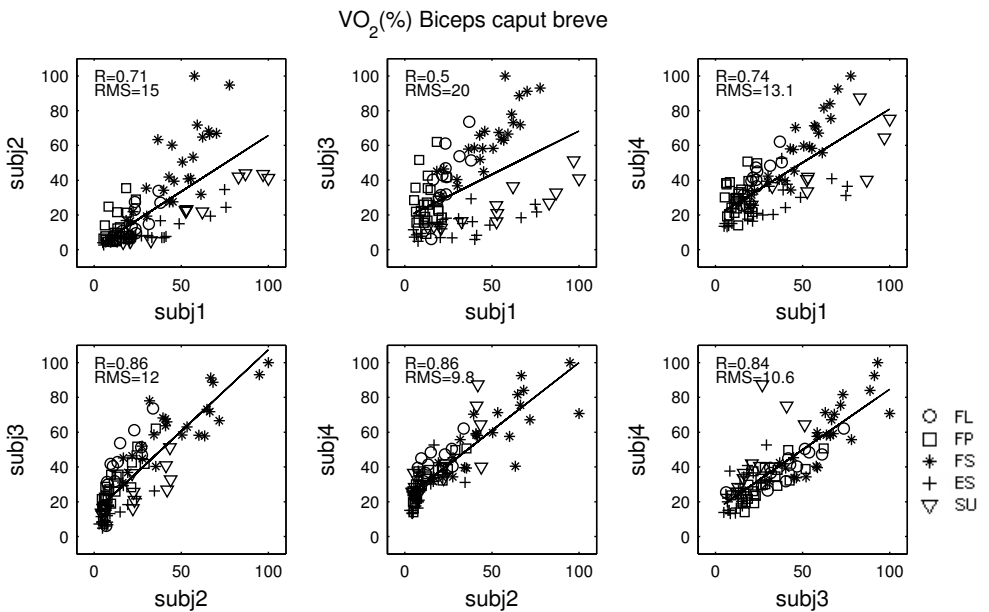


Figure 5.5 Normalised $\dot{V}O_2$ values of m. biceps caput breve of the different subjects plotted against each other.

Model predictions

Standard morphological data set

Optimisation using J_o led to a large number of false negatives for all three muscles (Figure 5.6 and Table 5.1). For BB and BR the correlations between experimental results and model predictions were on average low, though results for TL were better (Figure 5.6 and Table 5.2). Also, correlations differed strongly between subjects (Table 5.2).

Optimisation using J_E still showed false negatives for BB and TL (Table 5.1). As can be seen in Figure 5.6, for TL false negatives were found during pronation (Δ) and for BB during extension-supination (+), regardless of the choice of cost function. Furthermore, the activity of BB during supination (∇) predicted by the model was much lower than seen in the experimental data. During flexion-pronation (\square) the model predicted more activity for BB than was seen in the experimental data.

For BR however, results with J_E were considerably improved (Figure 5.6). The number of false negatives dropped to 1%, where using J_o false negatives were found for flexion-supination (Table 5.1). The correlation between model predictions and measurements improved considerably using J_E , which was also due to improvements in the predictions for flexion and flexion-pronation (Table 5.2).

Individualised morphology

Optimisation of the morphology to the measurements led to an individually optimised morphological parameter set for each subject and each cost function (Table 5.3).

As expected the individual morphological parameter sets differed between the subjects. These different parameters sets led to a considerable increase in differences in model predictions between the subjects (Figure 5.7 and 8), reflecting part of the differences seen in the experimental data (Figure 5.5 and 8). Consequently the optimised morphology led to a better fit between model predictions and measured $\dot{V}O_2$ values (Figure 5.12 compared to Figure 5.6). Improvements (cost values that corresponded better to experimental results than the original cost values) were highest for BB and J_E . For both cost functions correlations between $\dot{V}O_2$ and cost improved for BB, but only for J_E the false negatives disappeared as well (Table 5.1, Figures 5.9 and 5.12).

Even with the optimised morphology J_o still predicted a large number of false negatives for BR (Table 5.1, Figures 5.10 and 5.12). J_E already showed very good results for BR with the standard morphology. Although for some individuals the correlations decreased (Table 5.2) and

some false negatives were seen (Table 5.1) with the optimised morphology, averaged results were still very good (Figure 5.12).

For TL the optimised morphology did not really change results for J_o and only slightly improved for J_E (Table 5.1 and 5.2, Figures 5.11 and 5.12).

Table 5.1 The total number (%) of false negatives found for J_o and J_E using the standard morphological data set as well as the optimised morphological data set

	Standard morphology		Optimised morphology	
	J_o	J_E	J_o	J_E
BB	25%	19%	26%	10%
BR	46%	1%	40%	14,4%
TL	17%	25%	20%	23%

Table 5.2 Correlation coefficient (R) and root mean square error (RMS) for the relationship between $\dot{V}O_2$ and cost (predicted with J_o and J_E) defined by $\dot{V}O_2 = a \cdot \text{cost} + b$. Values are calculated for each subject as well as for the data averaged over all subjects (\bar{x}).

		Standard morphology				Optimised morphology			
		J_o		J_E		J_o		J_E	
		R	RMS	R	RMS	R	RMS	R	RMS
BB	Subj1	0.38	21.4	0.24	22.5	0.5	20.0	0.69	16.8
	Subj2	0.72	14.7	0.65	16.1	0.87	10.50	0.89	9.5
	Subj3	0.83	13.0	0.85	12.2	0.82	13.13	0.91	9.3
	Subj4	0.79	11.8	0.74	13.0	0.85	10.2	0.86	9.7
	Subj \bar{x}	0.78	12.2	0.71	13.85	0.85	10.5	0.91	7.9
BR	Subj1	0.67	14.4	0.76	12.7	0.87	9.7	0.89	8.7
	Subj2	0.68	19.4	0.91	11.0	0.47	23.5	0.86	13.5
	Subj4	0.42	16.3	0.67	13.5	0.41	16.4	0.63	14.0
	Subj \bar{x}	0.60	15.12	0.76	12.21	0.68	13.9	0.85	9.9
TL	Subj1	0.87	10.3	0.81	12.1	0.86	10.3	0.85	10.7
	Subj2	0.84	9.9	0.83	10.1	0.74	12.2	0.83	10.2
	Subj3	0.68	11.7	0.84	8.8	0.80	9.6	0.83	9.0
	Subj4	0.94	7.3	0.82	12.3	0.94	7.5	0.91	9.1
	Subj \bar{x}	0.92	6.67	0.91	7.15	0.93	6.3	0.94	6.1

Table 5.3 Scale factors of PCSA and moment arm of the optimised individual parameter sets.

		J_{σ}					J_E				
		subj1	subj2	subj3	subj4	mean	subj1	subj2	subj3	subj4	mean
PCSA	BB	1,19	1,17	1,19	1,04	1,15	1,34	1,40	1,24	1,35	1,33
	BL	0,82	0,69	0,69	0,62	0,71	0,84	1,00	0,74	0,85	0,86
	BR	0,63	0,50	1,50	1,35	0,99	0,88	0,50	1,44	1,50	1,08
	BA	1,00	0,67	0,94	0,71	0,83	1,34	1,50	0,74	1,08	1,17
	TLM	0,90	1,50	0,50	1,41	1,08	0,50	0,50	0,64	0,68	0,58
	PT	0,50	0,84	0,96	1,10	0,85	0,50	1,49	0,83	0,77	0,90
	PQ	1,50	0,52	0,86	0,66	0,88	0,56	0,52	1,40	0,64	0,78
	SU	0,83	1,15	0,50	1,40	0,97	0,50	0,50	0,66	0,59	0,56
FE moment arm	BB/BL	0,68	1,31	1,48	1,37	1,21	0,50	0,50	1,50	1,33	0,96
	BR	0,64	0,57	0,50	0,74	0,61	0,75	1,11	1,10	0,91	0,97
	PT	1,37	1,13	1,16	1,46	1,28	0,95	0,50	1,50	0,50	0,86
	TR	1,27	0,81	0,50	0,91	0,87	0,50	1,50	1,50	1,50	1,25
PS moment arm	BB/BL	1,14	0,61	1,24	1,35	1,08	1,50	1,26	1,40	1,50	1,42
	PT	0,76	0,61	1,30	0,69	0,84	1,16	1,37	1,27	1,35	1,29
	PQ	0,79	0,50	0,50	0,93	0,68	0,50	0,50	0,50	0,50	0,50
	SU	1,13	1,50	1,25	1,19	1,27	0,50	0,50	0,50	0,50	0,50

Standard morphology

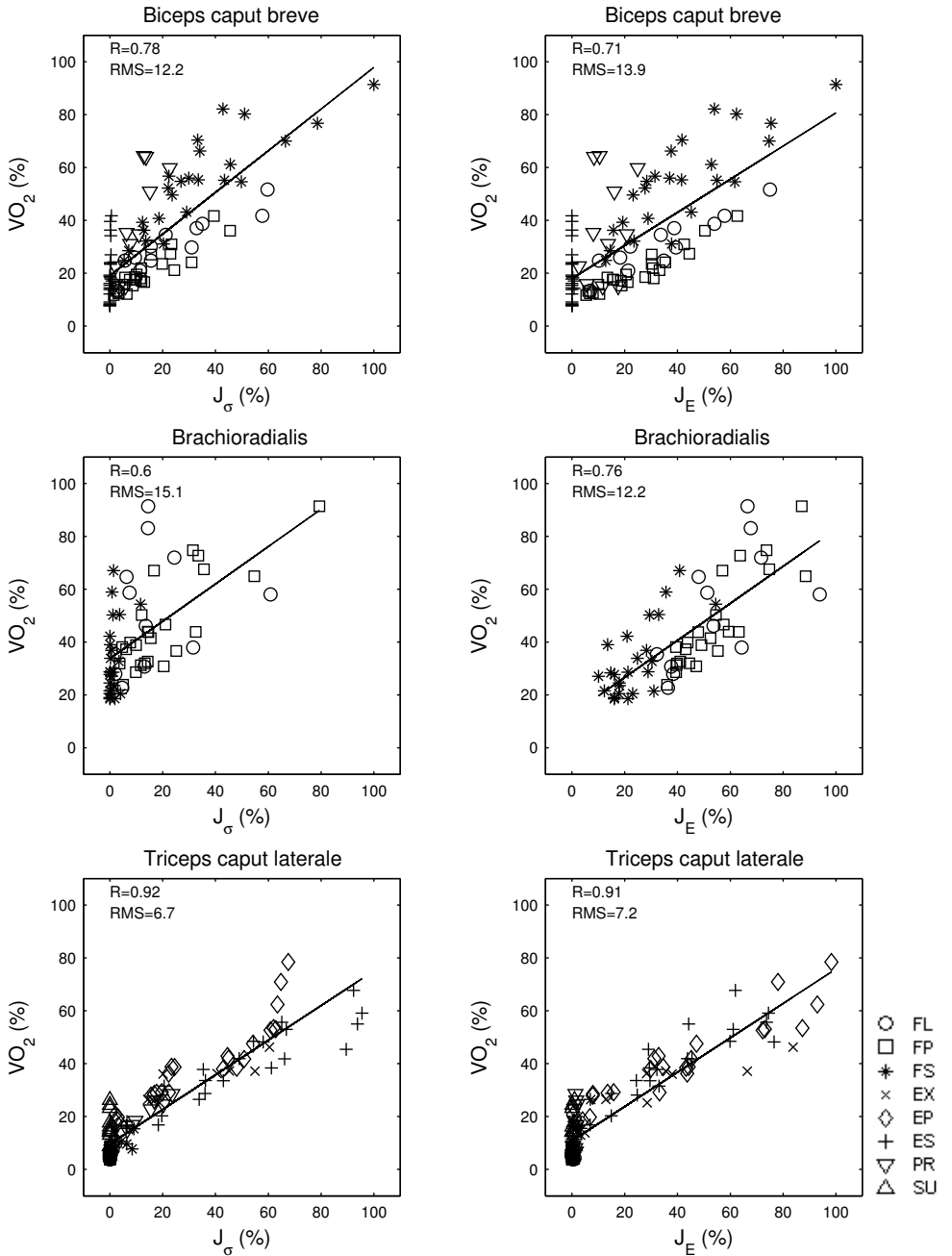


Figure 5.6 Measured $\dot{V}O_2$ plotted against predicted cost values (averaged over all subjects) for the simulations done with J_{σ} (left) and with J_{E} (right)

J_E (%) (standard morphology) Biceps caput breve

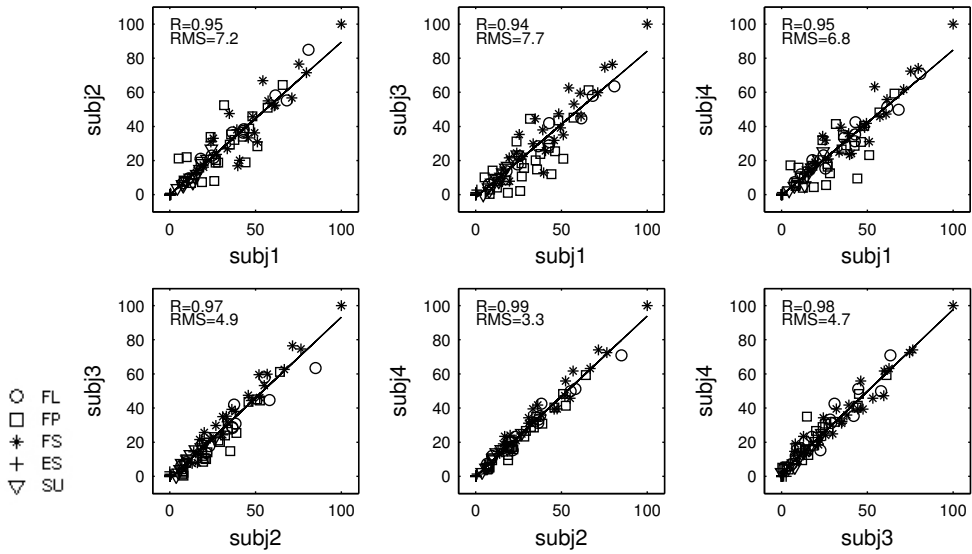


Figure 5.7 Cost values of BB predicted by the model using the standard morphology and the energy-related cost function. Different subjects plotted against each other

J_E (%) (individualised morphology) Biceps caput breve

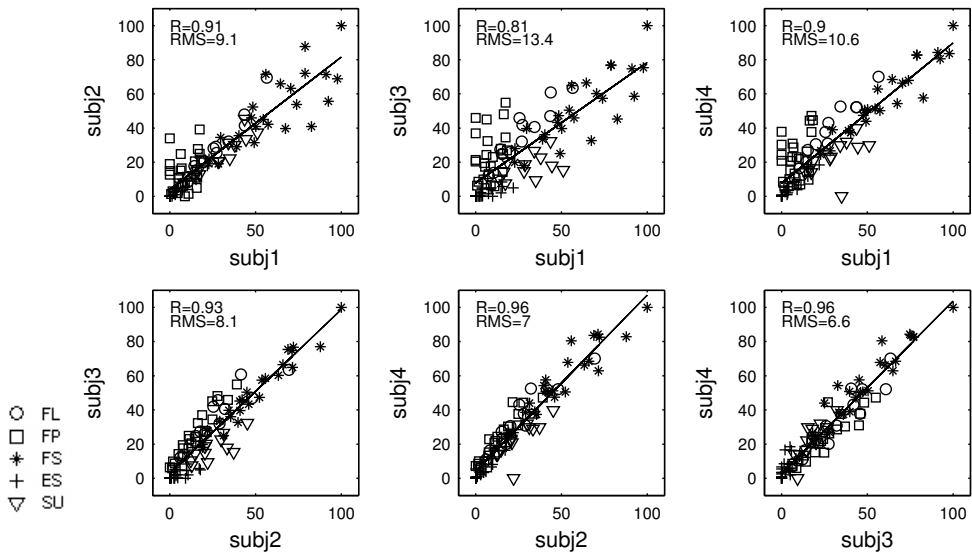


Figure 5.8 Cost values of BB predicted by the model using the individualised optimised morphology and the energy-related cost function. Different subjects plotted against each other

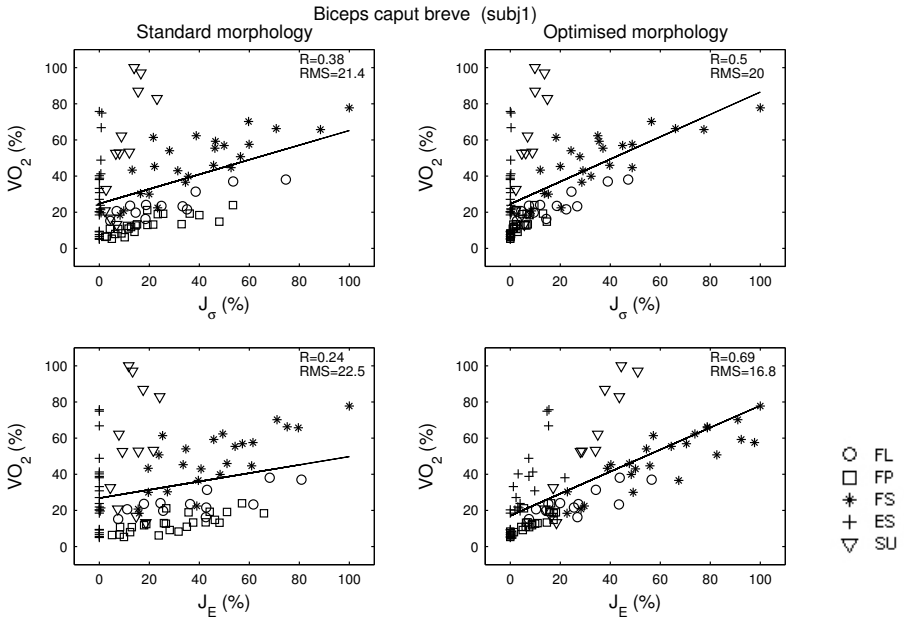


Figure 5.9 Results for subject 1 for *m. biceps caput breve*. $\dot{V}O_2$ plotted against cost value simulated with the standard morphology parameter set (left) and the individualised parameter set (right).

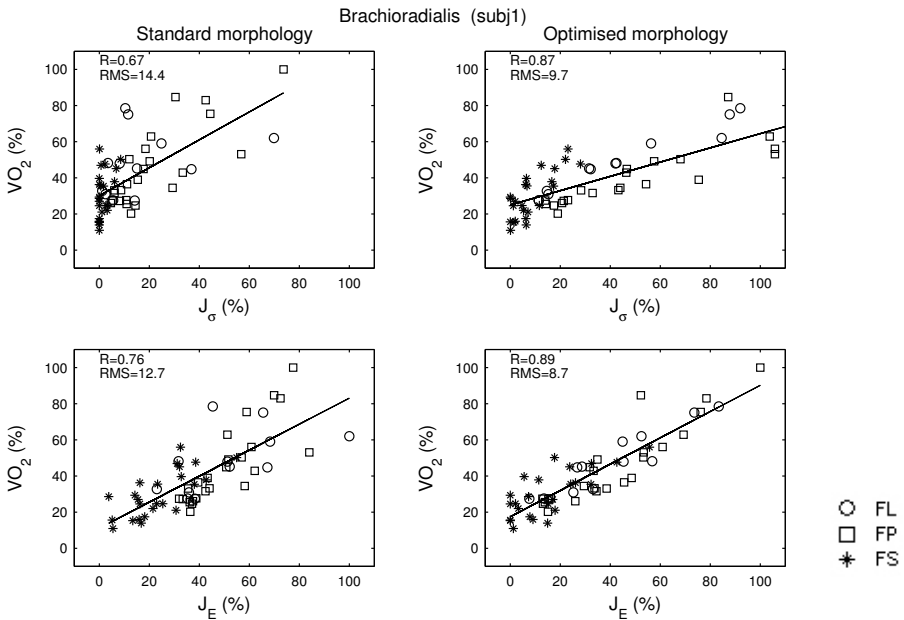


Figure 5.10 Results for subject 1 for *m. brachioradialis*. $\dot{V}O_2$ plotted against cost value simulated with the standard morphology parameter set (left) and the individualised parameter set (right)

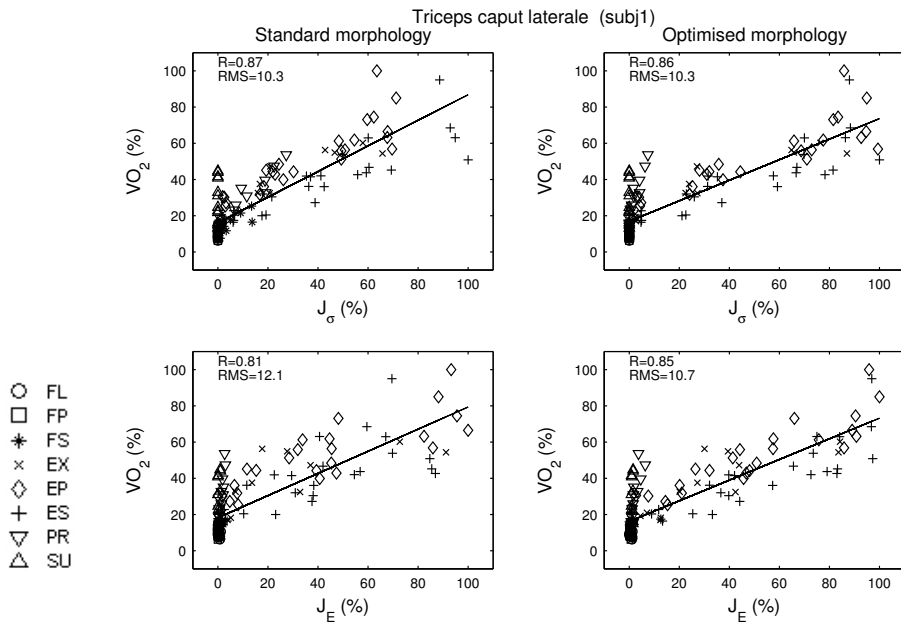


Figure 5.11 Results for subject 1 for *m. triceps caput laterale*. $\dot{V}O_2$ plotted against cost value simulated with the standard morphology parameter set (left) and the individualised parameter set (right)

Individualised morphology

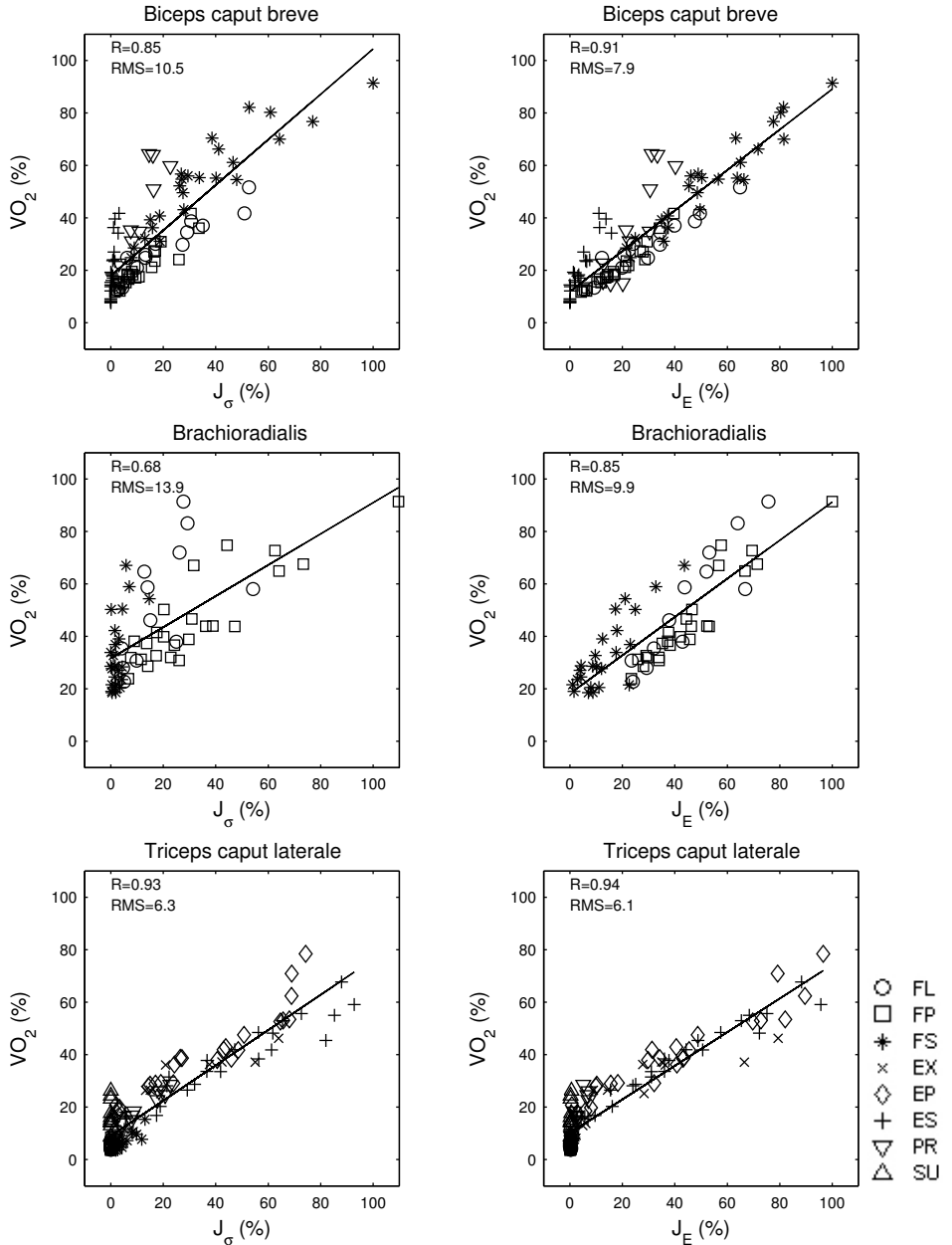


Figure 5.12 Measured VO_2 plotted against predicted cost values (averaged over all subjects) for the simulations done with the individual parameter sets. Results for J_{σ} (left) and J_E (right).

Discussion

Cost functions

In our previous study (Praagman et al., 2006) for the first time a mechanical cost function was defined which is directly based on muscle energy consumption and which was also validated with a metabolic variable. To date, it has often been assumed that optimising stress is comparable to optimising energy consumption although there is no direct relationship between the two. We performed model simulations using two different cost functions: the traditional sum of squared stress cost function (J_{σ}), and the energy-related cost function (J_E), in which the energy consumption due to the calcium dynamics and cross-bridge coupling was approximated. Since both J_{σ} and J_E are used as a function that minimizes overall energy consumption, the cost per individual muscle was compared to *in vivo* measured muscle oxygen consumption, as a direct validation of these cost functions.

In our previous study it was already shown that J_E was a better measure of muscle energy consumption than the stress cost function J_{σ} (Praagman et al., 2006). In the current study these findings were not only confirmed for a larger range of isometric force conditions and elbow angles, but J_E also worked out to be more sensitive to tuning of morphological parameters.

The cost function J_E was developed as a representation of calcium dynamics (\sim active state), and cross-bridge dynamics (force generation). The calcium dynamics are related to muscle volume (approximated by muscle mass). Whereas force generation through cross-bridges, is directly related to the PCSA and to the length of the muscle, also resulting in a volume weighing (see Eq. 5.2). It is assumed that longer muscles with the same PCSA will require more energy for the same force level. The active state related part of J_E is sensitive to the force-length relationship, since the same force would require less activation at optimum length than below or above optimum length. In isometric conditions the force-related part of J_E is not sensitive to the force-length curve since the force is directly related to the number of cross-bridges coupled in parallel sarcomeres, which is linearly related to energy turnover.

The stress cost function J_{σ} (Eq.5.1) is not sensitive to the length of a muscle, and hence not to the force-length relationship. Since the metabolic cost of a muscle is the summed cost over the sarcomeres in parallel and in series, it can be expected that J_E would be a better representation of energy consumption than J_{σ} .

Effect of morphological parameters

Changes in posture will induce changes in muscle length as well as in moment arm and this applies to all muscles crossing a joint. The exact consequences of these changes on muscle activity are unknown. As mentioned before, for a change in elbow angle leading to a muscle length and moment arm nearer to the muscle's optimum length or maximal moment arm, it can be expected that the muscle's activity decreases ('single muscle perspective') as well as increases ('multiple muscle perspective').

In a separate analysis we have investigated these effects by varying the moment arms one by one for each single muscle. The results were mixed: some muscles increased in force level, others decreased. It appeared that the model predictions are very sensitive to morphological changes, especially for the energy cost function, which could explain the inter-individual differences in the experimental study (Chapter 4)

Standard morphological parameter set

The morphological data set used in this study was more complete than the previous one (Praagman et al., 2003), because also muscle optimum length and the force-length relationship was incorporated. The sensitivity of the cost function to morphological parameters showed that morphology of the model indeed is a very important factor in optimisation.

Using the standard morphology of the model, J_E showed less false negatives in comparison to J_o which were mainly visible for BR (Table 5.1, Figure 5.6). Correlations between cost function and oxygen consumption (Table 5.2) were also much higher for this muscle, while correlations did not really differ for TL and were slightly lower for BB. It seemed that the force prediction of BR was highly influenced by its moment arm for pro/supination, which underlines the importance of taking into account a sufficiently large number of degrees of freedom when performing a model validation study. Especially during Flexion-Supination (FS), the forearm was positioned such that (according to the model) BR had a small moment arm for pronation. Using J_o this leads to inactivity of BR during FS. However, with J_E not only moment arm and PCSA but also muscle mass and fibre length are of influence. This leads to activity of BR (low mass) during FS despite its unfavourable moment arm, reflecting what is seen in the experimental data.

In contrast to our previous study, for BB model predictions done with J_E were not better than predictions done with J_o . Model predictions of BB

and TL showed some differences to the predictions in our previous study, which can be explained by the fact that in this study more force conditions, were included and a different morphological parameter set was used than in the previous study.

The conditions pronation (PR) and supination (SU) were not examined in the previous study. Therefore false negatives for TL during PR and SU as well as the discrepancy between $\dot{V}O_2$ and cost values of BB during SU were not revealed before.

False negatives for BB were predominantly found for extension-supination (ES). Apparently, the m. biceps brachii is activated because of its moment arm for supination despite its unwanted flexion moment. The degree of activity during ES varied largely between the subjects. In our previous study, biceps activity during ES was only seen by some of the subjects (Praagman et al., 2006). False negatives possibly can be prevented if the moment arm of the m. supinator is smaller, and hence the m. biceps brachii is more favourable for supination even considering its antagonistic flexion activity. Another option is an enlargement of the m. biceps' moment arm for supination. Again, differences in morphology might explain the differences in muscle oxygen consumption as found between subjects in this study.

Optimised morphological parameter sets

To investigate in what way the two different cost functions are influenced by the morphological parameters, PCSA and moment arm model simulations were repeated with individualised parameters sets for moment arm and PCSA which fitted best on the experimental data. It was expected that the model predictions using the individualised parameter sets would lead to a better individual fit with the experimental data.

Only for J_E , the use of an optimised individual parameter set led to a substantial better fit, since false negatives for BB (in flexion-supination) disappeared with J_E (Figures 5.9 and 5.12). The optimal parameter sets for J_E did indeed show the already suggested reduction of the m. supinator's moment arm for supination and enlargement of the m. biceps's moment arm for supination. Apparently, the proportion of the moment arms between m. biceps brachii and m. supinator has effect on activity of the m. biceps brachii during ES, which was quite variable between subjects. It is striking that a change in moment arms for one degree of freedom has such profound effects around other degrees of freedom.

The use of an optimised individual parameter set for J_0 did not lead to substantial improvements. J_0 still showed false negatives for BB and BR and a low correlation with experimental results for BR (Figure 5.12).

Neither cost function, nor optimisation of morphology had a major effect on the prediction of TL activity (Figure 5.11 and 5.12). In contrast to the bi- and even tri-articular BR and BB, the mono-articular TL is not directly influenced by pro- or supination moments. Experimental findings however, do show that TL is indirectly influenced by pro/supination moments. TL was found to be active during PR and SU as well as during FS, which was only partly predicted by the model. It is as yet unclear whether this gap between prediction and experimental results can be closed through adjustments in the chosen cost function (such as tuning of the constants $a1$, $b1$ and $b2$), or by including additional constraints such as joint stability.

Not all subject variation can be explained by the differences in PCSA and moment arm. There are of course more morphological parameters that vary between subjects and therefore might be worth tuning, for instance the exact locations of muscle attachment sites (Kaptein and Van der Helm, 2004).

Large-scale musculoskeletal models vs. simplified models

In modelling studies multiple degree of freedom systems are often replaced by a system that contains only a subset of all the possible degrees of freedom (Dul et al., 1984b; Challis and Kerwin, 1993; Raikova, 1996; Van den Bogert et al., 1999; Kistemaker et al., 2007). This, in itself understandable simplification of the musculoskeletal systems can lead to unjustified conclusions. Jinha et al. (2006b) showed that representing a three degrees-of-freedom system as a one or two degrees of freedom system will produce force-sharing solutions that cannot be extrapolated to the original system, and vice versa. We realised that function around the elbow joint is controlled by muscles of which some also have a function around the proximal and distal joints and that this chain effect continues. Therefore, we used in our study on load sharing of elbow muscles a model that was as complete as possible. We used a model of the shoulder and elbow (Van der Helm, 1994a) that included eight degrees-of-freedom (Van der Helm, 1997b). In this way it has become less likely (but can not be excluded) that model simplifications will negatively affect extrapolation to the experimental, i.e. real, condition.

False negatives were predominately found for conditions including a moment for which the particular muscle has no or even the opposite effect. In these conditions muscles seem to be activated due to a

compensating effect for one of the other muscles or due to their effect on another degree of freedom. However, model simulations did not always predict this kind of activity. It appeared that both the choice of cost function and the morphology play a major role. These results emphasize the importance of including all degrees of freedom when validating a cost function. Not only by using a complete musculoskeletal model but also by measuring a wide range of all possible moment combination.

Many elbow studies however focus on flexion-extension moments only and pay little or no attention to the pro/supination moments (Lacquaniti and Soechting, 1986; Leedham and Dowling, 1995; Van Bolhuis and Gielen, 1997). This study showed that when validating an inverse dynamic model of the elbow and its cost function, this can not be based on predictions for flexion and extension only.

Conclusions

- The predicted load sharing is strongly depended on cost function as well as on morphology. Clearly the stress cost function (J_σ) does not predict realistic results and the energy-related cost function (J_E) shows a better fit to experimental results.
- Modelling results can be improved by fitting the morphological parameters to the experimental data of individual muscles. This can not only explain part of the inter-individual variability in the experimental results, but also leads to a better morphological parameter set for individual subjects than the 'generic' model morphology that is based on one specimen only. Fitting individual morphological data is only effective when J_E is used and has no effect on predictions of J_σ .
- A large-scale musculoskeletal model is necessary for validation using oxygen consumption and EMG, since the muscle activity is often the result of 'indirect' activity of the muscles compensating undesired moments from muscles, which are active around other degrees of freedom.





Chapter 6

Epilogue



Introduction

The general aim of this thesis was to develop a new, and better, cost function for an inverse dynamic model of the human shoulder and arm. Previously, mainly physiological research on wheelchair propulsion has shown that a relationship exists between wheelchair lay-out and the efficiency with which wheelchair users were able to propel their chair (Van der Woude et al., 2001). The hypothesis was developed that the technique that was adopted by the users was in fact the most suitable, i.e. most efficient, technique based upon the human morphology (Veeger et al., 1991). Standard biomechanical models and cost functions do not calculate energy consumption; not on the level of the organism, nor on the level of an individual muscle. As a consequence, it is at least uncertain whether these models can be used for the evaluation of the causes for differences in efficiency. A model that uses a (validated) physiological cost function, i.e. a function that calculates energy consumption per muscle, is more likely to predict the efficiency.

In a musculoskeletal system, more muscles are present than strictly necessary to generate the joint moments. In other words, the same joint moment can be generated by multiple combinations of muscle activation. Humans appear to 'solve' this indeterminacy in a more-or-less standard manner (Bernstein, 1967). In general, it is assumed that this standard manner is established by adhering to certain optimisation principle. This principle, in mechanical terms labelled as cost, is used in inverse dynamic modelling to mathematically solve the unknown muscle forces related to load sharing. It is of great importance for all inverse dynamic models to find and use a cost function that adequately describes the optimisation principle that the (human) musculoskeletal system uses *in vivo*.

In a very useful review article, Tsirakos et al. (Tsirakos et al., 1997) discussed the different cost functions that have been used in the past years. Although this review was published a decade ago, the overview is still up-to-date. Most cost functions have been based on mechanical parameters, such as muscle force scaled by maximal force or PCSA (Physiological Cross Sectional Area), i.e. muscle stress. No cost functions were described that were based on the calculation of muscle energy consumption. Since then, none were published either.

Multi-joint systems

Normally there are multiple muscles available to produce a certain external moment. In general, a combination of these muscles is used to produce the required moment (load sharing), but the combination could not always be understood on the basis of (simple) mechanical properties (Buchanan et al., 1986; Buchanan et al., 1989; Caldwell and Van Leemputte, 1991; Hebert et al., 1991; Jamison and Caldwell, 1993; Jamison and Caldwell, 1994). It appears that these load sharing patterns are difficult to predict since the principles behind it are unknown. For validation of inverse musculoskeletal models that intend to predict muscle contributions, it is important to use broad experimental findings covering different force levels and moment combinations but also different joint angles. In many studies, cost functions have only been validated over a small number of degrees of freedom involved, mainly around the main degrees of freedom to be controlled and without combining control over more than one degree of freedom. In addition, 'validity' has generally been checked by comparing whether a muscle is 'on' or 'off'. Although extremely complex, it is, however, obvious that validation should also focus on the amplitude of the cost or muscle force.

In an inverse dynamic analysis the muscle activation or force depends on both the level and direction of the external moment. Experimental results showed that muscle activation increased with force level (Chapter 2 and 4) and that the amount of muscle activation depended on moment combination as well. As expected, muscles are active when they can contribute to the required external moment(s). The m. biceps brachii for instance, contributes to a flexion or supination moment or a combination of these two. In addition, experiments showed that muscles were also activated when they contribute to only one of the requested moments even when they have an opposing effect on one of the other requested moments, like m. biceps brachii activity during extension-supination (Jamison and Caldwell, 1993, Chapter 4). Third, muscles can also be influenced indirectly by an external moment. Using the m. biceps brachii for producing the supination moment during pure supination requires activity of for instance the m. triceps brachii to compensate for the undesired flexion moment. This thesis shows that differences between model predictions and experimental results mainly occur in two types of situations:

1. the activated muscle contributes to one of the requested moments only and counteracts the other moment,

2. the muscle does not directly contribute to one of the requested moments at all.

Whether a biomechanical model will predict muscle activation in these situations depends heavily on the used cost function as well as on the parameters that determine the force production capability such as the muscle moment arms, PCSA or force-length relationship.

Finding the right optimisation criterion (cost function) is difficult since the exact principles behind load sharing are unknown. Results of this thesis show that it is hard to unravel these principles as load sharing seems to be influenced by many different factors which can not be easily separated.

The human body consists of many bi- and poly-articular muscles, such as m. brachioradialis and m. biceps brachii. When studying, for instance, elbow muscles (like m. biceps brachii) the effect of the bi-articular muscles around the shoulder joint can not be neglected. Even a mono-articular muscle such as m. brachialis will indirectly be influenced by the moment around the shoulder, as one of its synergists (m. biceps brachii) is partly determined by the shoulder moment.

Studies have shown that reducing the degrees of freedom of a musculoskeletal model, e.g. from 3D to 2D, or by neglecting the proximal or distal joint, leads to different predictions of muscle activation patterns, and therefore does not lead to realistic results (Jinha et al., 2006). In our experiments as described in Chapters 4 and 5 we varied elbow angle, in order to vary muscle length. In our set-up the forearm was kept horizontal in order to keep the external moment around the elbow constant. Consequently, the shoulder angle (and therefore external moment) changed as well. It is, unfortunately, impossible without complex external compensation torques to vary elbow angle at a constant shoulder angle while remaining the external elbow moments constant. This also emphasises the necessity to use a large-scale shoulder and elbow model in our study as this model did take into account the effects around the shoulder.

Single muscle versus multiple muscle perspective

In Chapters 4 and 5 elbow angle was varied since we wanted to investigate the effect of muscle length on load sharing as well as on the optimisation. Inevitably, the variation in elbow angle also led to a change in moment arm, while both variables are likely to influence muscle activity and load sharing. An exclusive change in muscle length is essentially impossible, making it impossible to study the effect of muscle length on its own.

The maximal force that can be produced by a muscle depends on its actual muscle length, and is by definition highest at optimal length. Likewise, the moment that can be produced by a muscle depends on the actual moment arm, which is defined by the elbow angle. Given this, at first glance, it is obvious that elbow angle will influence muscle activation. This relationship between angle and activation is, however, not at all that trivial. Viewed from a single muscle perspective one could argue that the activation of a muscle **decreases** with optimal length and/or increasing moment arm. After all, at optimal length or maximal moment arm a muscle can produce the same force/moment with a lower activation/force. Taking a multiple muscle system as starting point, the argument could be that a more optimal length or larger moment arm will make a muscle 'cheaper', or more economic, which would then lead to a change in load sharing: an **Increase** in activity of the muscle in question and a simultaneous decrease of activity of one (or more) of the synergists.

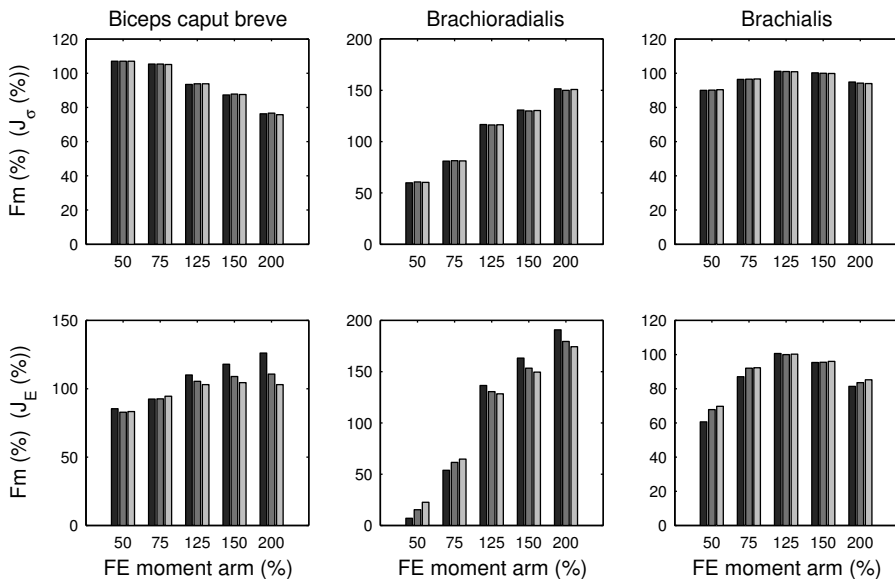


Figure 6.1 Predicted muscle force (F_m) during pure elbow flexion plotted against the altered FE moment arm (ranging from 50% to 200% of the normal moment arm). F_m is expressed as a percentage of the muscle force predicted at the normal moment arm. Different shades of grey represent different force levels. Results are given for three elbow flexors (*m. biceps caput breve*, *m. brachioradialis* and *m. brachialis*) predicted with the stress cost function (above) as well as with the energy-related cost function (below).

Based on these considerations it would have been possible to find a minimum as well as a maximum of EMG and muscle oxygen consumption ($\dot{V}O_2$) at optimal length or maximal moment arm. Results of Chapter 4 showed that EMG and $\dot{V}O_2$ magnitude did change with elbow angle, but unfortunately these changes could not easily be related to changes in moment arm or muscle length. We had to conclude that it is likely that a combination of the two earlier described effects takes place; a muscle's contribution to the external moment increases as it becomes "cheaper", but activation decreases as well since the muscle is able to produce the same force with less activation. Moreover, changes in elbow angle always lead to changes of muscle length and moment arms in more than one muscle and even in different directions, making it very difficult to unravel all the individual effects. Model simulations in which only one moment arm of one single muscle was changed at the time showed that the effect of this change in moment arm was not only dependent on the used cost function but also differed largely between different muscles (Figure 6.1). Therefore, from these model simulations it neither could be concluded whether a muscle's activity increases or decreases when it becomes more favourable.

Validation of cost functions

A cost function that is presumed to be related to energy consumption needs to be validated with a metabolic parameter instead of just EMG. The use of Near InfraRed Spectroscopy (NIRS) in this thesis, to measure muscle oxygen consumption, is an innovative development in cost function validation. Predicted cost values were validated with measured muscle oxygen consumption for individual muscles. Our energy-related cost function was compared to the well-known, and on large scale used, stress cost function. Comparison was done by means of several variables: correlation coefficients, RMSE values and false positives and negatives.

Correlation coefficients give a moderate indication of the correspondence between model predictions and experimental results but can easily be influenced by outliers. Therefore RMSE values were presented as well. The amount of muscle oxygen consumption should correspond to the amount of predicted cost. Very sensitive measures of the quality of the model are the false positives and false negatives; conditions for which the model predicts NO muscle activity at all while experiments do show that the muscle is active and vice versa. False positives and false

negatives occur when load sharing is calculated between muscles covering multiple degrees of freedom, in which the relative moment arms and PCSA's become very important.

Both Chapters 3 and 5 made it clear that the stress cost function has major shortcomings. Comparison of cost values predicted by the model to experimentally determined muscle oxygen consumption values showed a relatively large amount of false negatives and positives. This finding indicated that the stress cost function was not a good representation of energy consumption and that, apart from the question whether energy is indeed optimised, it did not predict realistic muscle activation patterns. Results of the energy-related cost function, on the other hand, seemed to be very promising at first sight (Chapter 3). It showed a large decrease of false negatives and positives compared to the stress cost function and on average higher correlations and lower RMSE values. The inclusion of muscle mass turned out to be an important factor leading to an increase of the contribution of smaller muscles, like the pronator and supinator muscles, which resulted in activation patterns that corresponded better to experimental results. Nevertheless, when a broader spectrum of moment combinations was studied for a number of different elbow angles (Chapter 5), for both cost functions new false negatives were revealed.

The fact that new moment conditions revealed new false negatives, stressed the significance of including a wide range of force tasks into the experimental set-up, covering all degrees of freedom. Not only the apparent conditions should be measured, such as flexion tasks for flexor muscles, but also the more unpredictable conditions such as extension-supination for *m. biceps brachii* or pronation for *m. triceps brachii*. This thesis showed that false negatives especially occurred during such paradoxical conditions. This implies that judgements on the legitimacy of cost functions based on studies in which cost functions were validated with only a small part of the possible force conditions are likely not justified.

The energy-related cost function

Two main energy consuming processes in the muscle are the calcium uptake in the sarcoplasmic reticulum (calcium dynamics) and the cross-bridge detachment (contraction dynamics). Hill-type muscle models have descriptive functions for activation and contraction dynamics, which in general do not permit for an accurate assessment of energy consumption. Huxley-type models do have a detailed description of the cross-bridge dynamics, resulting in a fair estimation of the energy

consumption. Ideally, a cost function minimising energy consumption should be based on a Huxley-type muscle model. Unfortunately, such models, as developed by Ma and Zahalak (1991), in general require parameters that are not available for human muscles. For this reason we defined an energy-related cost function that included mechanical muscle parameters in a Hill-type muscle model, which approximates the two main energy-consuming processes in the muscle. One may assume that the approximation is reasonably well under isometric conditions.

Based on the results of Chapter 3 we concluded that the energy-related cost function was promising for one joint position. In Chapter 5 we improved it by including the force-length relationship. A broader validation in which a large spectrum of external moments and joint angles was studied revealed, however, that this new cost function still had some discrepancies with experimental results.

The observed discrepancies raise the question whether indeed energy consumption is optimised but it can also be argued whether our cost function is a valid description of muscle energy consumption. Assuming that energy consumption is nevertheless the quantity that is being optimised *in vivo* it seems reasonable to expect that better results can be achieved by further improving our cost function, for instance by optimising the weight factors for the contribution of activation and contraction dynamics that are included in the equation (Eq. 5.2).

The energy-related cost function is written as a function of muscle force and consists of two parts: the energy consumed for the re-uptake of calcium (E_{ca}) and the energy consumed for the detachment of cross-bridges (E_{cb}) (Eq. 5.2). Whereas E_{cb} is linearly related to muscle force (Huxley, 1957) the exact relationship between E_{ca} and muscle force is unknown. From *in-vitro* studies it is known, however, that E_{ca} is linearly related to stimulation frequency (Figure 6.2b) and that muscle force does not increase directly proportional to the stimulation frequency (Figure 6.2c) (Blinks et al., 1978). This means that at higher forces E_{ca} would increase exponentially (Figure 6.2d). In our cost function we approximated this by a quadratic function.

The weight factors we used were chosen based on rational assumptions on the relationships between activation and contraction dynamics and energy consumption. The chosen weight factors lead to a distribution in which for maximal activation the Ca^{2+} uptake consumes more energy than the cross-bridge detachment. This does not correspond to the experimental findings (close to maximal stimulation) that only about 30% of the total energetic cost is consumed by the Ca^{2+} re-uptake (E_{ca})

(Homsher and Kean, 1978; Wendt and Barclay, 1980; Woledge et al., 1985; De Haan et al., 1986; Lou et al., 1997). Changing the weight factors such that this 2:1 ($E_{cb}: E_{ca}$) ratio would be reached at maximal activation, however, does not lead to realistic model predictions. As E_{ca} is exponentially related to muscle activation this implies that during submaximal activation its contribution is even smaller, resulting in a cost function which for the main part consists of a linear function. Though, a linear optimisation criterion will result in sequential muscle recruitment (Dul et al., 1984; Tsirakos et al., 1997), which is evidently not the case.

The chosen weight factors can not accurately describe all the relationships that are known from physiological experiments, e.g. because the Hill-type muscle model does not describe these physiological conditions in detail. In addition, physiological experiments do not cover all possible conditions and for some situations still guesses have to be made. It has to be noticed that what is known from physiology is based on *in vitro* experiments. Muscle stimulation *in vitro* is always synchronous stimulation whereas *in vivo* muscles are always stimulated a-synchronous. This implies that the relationships found *in vitro* might be different for *in vivo* situations.

Hence, one has to search for the true non-linear relationships between muscle energy consumption and force generation, or to reject the assumption that the human body attempts to optimise the global energy consumption.

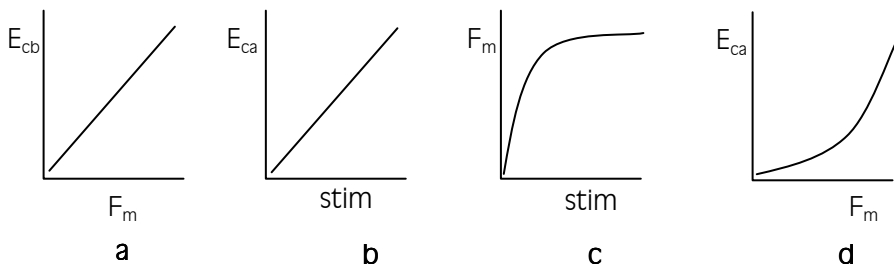


Figure 6.2 E_{cb} (energy consumed by the detachment of cross-bridges) is linearly related to muscle force (F_m) (a). E_{ca} (the energy consumed by the Ca^{2+} re-uptake) is assumed to be non-linearly related to F_m (d) based on the linear relationship between E_{ca} and stimulation frequency ($stim$) (b) and the non-linear relationship between F_m and $stim$ (c). See text for further explanation.

Relationship between EMG and NIRS

As mentioned before, validation of cost functions is usually performed by comparing predicted force patterns to measured EMG. We did not only want to know whether our cost functions did predict realistic force patterns, which can be quantified on the basis of (normalised) EMG, but also wanted to know whether they were indeed related to muscle energy consumption. Therefore, experiments were done in which muscle oxygen consumption was measured with Near InfraRed Spectroscopy (NIRS). As EMG and NIRS apply to different levels of the process of force production, it is plausible that these two techniques show different results.

NIRS records muscle oxygen consumption and hence gives an indication of both activation and contraction dynamics. EMG, on the other hand, records the excitation of the muscle only, which initiates the calcium flow from the Sarcoplasmic Reticulum. The exact relationship between the EMG signal and calcium flow or cross-bridge attachment is unknown. Since activation and force are not linearly related (Figure 6.2c) we expected there would be a non-linear relationship between the EMG and $\dot{V}O_2$ as well. We found, however, that the relationship between EMG and $\dot{V}O_2$ could be described by a linear relationship (Chapter 2) and that joint angle, and therefore muscle length and moment arm, did not appear to have a major effect on this linear relationship as long as the change in muscle length remained limited (Chapter 4).

The finding that EMG and $\dot{V}O_2$ seem to be linearly related could lead to the suggestion that muscle force and $\dot{V}O_2$ are linearly related as well. Based on the assumption that energy consumption is optimised this implies that an energetic cost function should be a linear function of force. As mentioned before, it is known (Dul et al., 1984; Tsirakos et al., 1997) that linear cost functions lead to sequential muscle recruitment and can not sufficiently predict load sharing. From that point of view, again, it can be suggested that it might not be energy consumption that is optimised in real life.

Alternatively, it has to be noticed that a linear relationship between two variables that indicate states at both ends of the process does not necessarily mean that all the processes in between have to be linearly related as well. It might as well be that the observed (apparent) linear relationship is in fact the result of two opposing non-linear relationships. The practical implication of the linear behaviour of EMG and $\dot{V}O_2$ would be that, at least for static conditions, instead of (the very time consuming method) NIRS, EMG can be used as predictor of energy

consumption. It can not be concluded though, that this linear relationship is based on solely linear relationships in between.

Subject differences

The observed inter-individual differences found in Chapter 4 strongly suggested that one of the basic assumptions for using biomechanical models, namely that there exists a general and generally applied way in which the central nervous system controls the musculoskeletal system, is not entirely correct. We found that for a seemingly simple (but extensive) set of force tasks, one of our four subjects showed a clearly different muscle activation pattern: he produced a high activation in m. biceps brachii when an extension-supination moment was required in comparison to the activation level in flexion tasks, whereas others showed a much lower activation level. This finding is not unique: other researchers have reported comparable phenomena (Buchanan et al., 1989). Earlier experiments (Chapters 3 and 4) also showed that m. biceps activity during flexion-supination varied between subjects. Subject differences were also found in the amount of co-contraction for the m. triceps brachii caput laterale (experiment I vs. II in Chapter 4) during flexion.

Differences between subjects were not only seen in the amount of muscle activity during a certain task (external moment) but the patterns of muscle activation between different moment combinations differed between subjects as well (see for instance the measured $\dot{V}O_2$ of m. triceps brachii caput laterale during flexion-supination, Figure 6.3).

The variance found in the experimental data was not caused by variation in body position. Since the position of each subject was continuously measured and used as input to the model, possible differences in posture should also be reflected by the model simulations. Small differences in position were indeed observed, but these differences only led to slight variances in activation patterns which could not explain the large variance found in the experimental data.

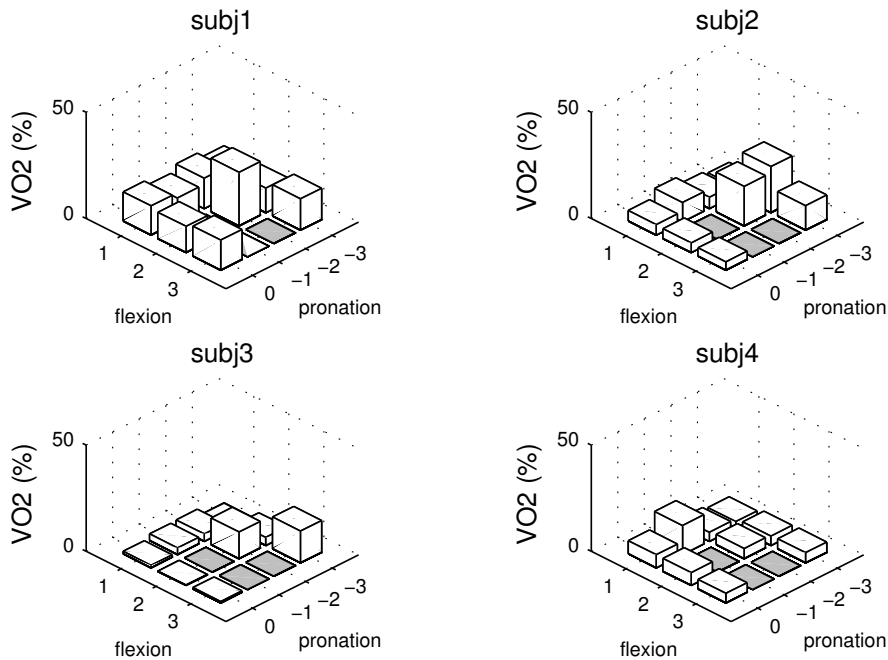


Figure 6.3 Experimentally obtained $\dot{V}O_2$ for *m. triceps caput laterale* during combined flexion-supination tasks for four different subjects. Differences between subjects are not only found in the amount of $\dot{V}O_2$ but also in the pattern over the different conditions. For example, the condition for which the highest $\dot{V}O_2$ is measured differs over the subject.

Can cost functions predict subject variability?

All in all, if force tasks produce muscle activation patterns that are not directly explicable from the general anatomical lay-out and show subject variability that is not explicable from variance in position, two possible alternative hypotheses arise:

1. There might be a general control pattern, but humans are extremely lazy and 'could not be bothered less': if energy costs are not too high they use any muscle combination that produces the end result. These potential muscle combinations converge to a general and repeatable pattern when energy cost goes up.
2. There is a general control pattern, but differences in muscle activation are sensitive to seemingly minor differences in morphology.

Both arguments could explain subject variability. The first hypothesis would be in line with results of Alexander (1997). His minimum energy

model gave reasonable predictions for very fast movements, but poorer predictions for slower movements. He explained this finding by the fact that if energy expense is already low, there would be less advantage in minimising energy even further.

When this results in a different strategy for each subject, resulting in different activation patterns, this could explain the variability between subjects. To ascertain whether minimisation of energy consumption indeed would appear at higher energy levels and would make subject differences disappear, experiments should be done in which force tasks at high force levels are included as well. Results of our repeated EMG measurements (not presented in this thesis), however, indicate that patterns within subjects are rather consistent, invalidating the first hypothesis.

In case the second hypothesis is correct, and differences between subjects are caused by differences in anatomy, these differences will not be predicted by one single model parameter set. Cadaver studies are rather scarce but the available studies do show a wide range in moment arms and physiological area's (An et al., 1984; Murray et al., 1995; Veeger et al., 1997; Ettema et al., 1998; Klein Breteler et al., 1999; Murray et al., 2000), and a large variance in size distributions between muscles. So it seems reasonable to expect that the morphologies of our subjects differ from each other as well as from the morphology of the model. As subjects differ, it can be argued that the individual variance in muscle activation patterns is caused by these differences. As the model is based on one anthropometrical data set such differences will not be reflected by the model. Model simulations with different cadavers (Chapter 3 versus Chapter 5) indicated that morphology of the model indeed influences model outcome. In Chapter 5, we attempted to fit the model onto the experimental data by varying the model's morphology. Morphology adjustments concentrated on moment arms and PCSA's (and therefore also muscle mass). For the model version that used the energy-related cost function, individual optimisation led to a substantially better fit between predictions and experimental results. This was, however, not the case for the version that used the stress cost function.

Individual muscle forces were calculated by solving the moment equations such that the total cost over the muscles was minimised. A change in moment arm indirectly influences the force and activation of the particular muscle, though in a different way for both cost functions. By changing the PCSA (and mass) the force and weighing factors of a muscle directly changes.

Using the energy-related cost function, not only muscles with large moment arms and large PCSA's were preferred but also those with small masses and short fibre lengths. In addition, the activation level was also weighed in the costs. Therefore, it is not surprising that this cost function was more sensitive to differences in morphology than the stress cost function. In conclusion, it appeared that part of the differences between subjects could be explained by differences in morphology, though these differences could not be predicted with the stress cost function and that a cost function containing more specific parameters, such as the energy-related cost function, would be needed. Based on this thesis no final conclusion can be drawn upon one of the two mentioned hypotheses. However, the finding *that* variance exists, might be an important limitation for the use of musculoskeletal models. If one does not get a grip on the reason for these inter-individual differences, modelling results can not be interpreted as representative for the manner in which all individuals perform the task. Conversely, to validate modelling outcomes using information on muscle activation of just one individual will not be sufficiently for the whole population. But on the other hand, a biomechanical model can be a major help in understanding the relationship between variations in morphology and muscle activation.

Future directions

Stability

Findings of co-contraction of m. biceps brachii and m. triceps brachii (Chapters 4 and 5) have been reported before (Hebert et al., 1991; Gribble and Ostry, 1998; Calder and Gabriel, 2007) but could not be explained from an energetic point of view. Moreover, co-contraction would not be predicted by any optimisation criteria minimising any cost at all. A possible explanation for co-contraction could be the need for stability (Gribble et al., 2003; Calder and Gabriel, 2007), the activity of an antagonist can be important for maintaining the integrity of the joint (Gabriel et al., 2006). As Gabriel et al. (2006) pointed out: "it is not clear what the central nervous system will optimise: force production or joint integrity".

In order to study the effect of stability on the predicted muscle patterns it is necessary to extend our DSEM with an extra stability constraint. Despite previous efforts (Van der Helm, 2000) it has not been implemented yet. For the spine it has been shown (Brown and Potvin,

2005) that inclusion of a stability constraint in an optimisation model led to realistic predictions of antagonistic muscle activity.

The differences found in co-contraction in our experiments (Chapter 4) between the subjects might be caused by the fact that some subjects paid more attention to the instruction to keep the bar horizontal than others, introducing more effort for stability. Buchanan and Lloyd (1995) also showed that muscle activity is different during static tasks that require force control compared to tasks that require position control but that these differences manifest differently between different subjects. Biomechanical models in general do not take into account differences in position versus force control. Inverse modelling requires more experimental information on the existence of a need for stability. If the need for stability indeed differs between subjects we would still be confronted with differences between model predictions and experimental results, albeit on a different level.

Other type of cost function

Although the energy-related cost function led to more realistic muscle activation patterns than the stress cost function, there were still conditions for which predictions did not correspond to experimental findings.

It can be hypothesised that energy consumption is optimised though, but only on the level of individual muscles, independent of and not necessarily leading to a minimisation of overall energy consumption. This means that load sharing is chosen such that all participating muscles are minimally activated. This concept could be reproduced by a MINMAX criterion. Although such criteria have been used before (Van der Helm, 1991; Rasmussen et al., 2001) these criteria were always based on muscle stress (minimisation of maximal muscle stress) and never on muscle energy consumption (minimisation of maximal energy consumption, per muscle). Therefore, a logical next step would be to define an energetic MINMAX criterion (based on our energy-related cost function) to investigate whether the above mentioned hypothesis could be genuine.

Experiments

This thesis describes one of the first studies that uses experimentally recorded muscle oxygen consumption for the validation of (metabolic) cost functions. The experiments were highly extensive in the sense that a large set of moment combinations was measured which was also repeated at different elbow angles. Due to the use of NIRS,

measurements were extremely time-consuming and the number of measured muscles and subjects, therefore, was limited. To sufficiently validate the predicted load sharing, experimental data on a larger set of muscles would be appreciated.

Load sharing around the elbow is also influenced by the moments and muscles around adjacent joints. For further understanding of the concepts behind this load sharing and for the validation of cost functions that predict this load sharing, it would be extremely valuable to measure energy consumption of shoulder muscles as well. Regrettably, NIRS measurements of these muscles are hindered by the fact that no occlusion can be applied to this region. Since pro- and supination moments appear to have a large effect on the predicted load sharing it would be very helpful if oxygen consumption of the pronator and supinator muscles could be collected as well. Unfortunately, most of these muscles lay deep, only the m. pronator teres lays superficial. We have experienced, however, that for the force tasks in our experiments it was not possible to perform NIRS measurements on this muscle. Contraction of m. brachioradialis and the additional movements of the skin above the m. pronator teres shifted the optodes placed on the muscle.

If another, possibly intra-muscular, method would come available which enables measurements of muscle energy consumption of shoulder muscles, or even deep muscles, this would open great opportunities for validation. In the future this might be possible with microdialysis technique which is able to provide insight into the metabolic changes in the interstitial space during muscle contraction (Henriksson, 1999; Lott and Sinoway, 2004).

Individualisation of model parameters

Previous studies also showed that the geometry of the model is very critical for the model outcome (Brand et al., 1986; Herzog, 1992). Raikova and Prilutsky (2001) showed that deviations of model parameters (PCSA and moment arm) from their nominal values affected the predicted load sharing. They concluded that different opinions in the literature on cost functions could be potentially explained by differences in used model parameters. Chapter 5 also showed that model predictions are influenced by the used morphological parameters and further indicated that part of the variability between subjects could possibly be explained by such differences. If the latter is indeed the case, scaling of model parameters to individual subjects can possibly lead to better model predictions. In our opinion, segment scaling is not

sufficient. Intra-segmental variation of the proportions between muscles is expected to be the main factor of intra-individual differences.

Therefore, more insight is needed into the actual morphology of the subject, i.e. in vivo determination of muscle moment arm, PCSA and attachment sites. Common MRI measurements can be used to quantitatively measure inner structures of the human body, but the resolution is not high enough to accurately distinguish muscles from each other (Kaptein, 1999). However, development of MRI has led to MRI systems which can measure below 1mm/pixel. Although, to date, such methods are very expensive, in the future such accurate systems might offer the opportunity to scale model parameters and to investigate whether subject differences are indeed caused by differences in morphology.

Conclusions

- The unique method of validating model predictions with NIRS has proven to be a good method for validating energetic cost functions.
- Load-sharing is the result of the dominance of the one muscle to the other and depends on many different factors which can not easily be distinguished.
- Validation of cost functions can only be done with multiple muscle and joint models, including the actual number of degrees of freedom as well as all of the actual adjacent joints.
- Just as important it is to validate these models with extensive sets of experimental data including not only different force levels but especially tasks that cover all of the possible moment combinations around these degrees of freedom as well.
- Despite the existing doubts about the quantity that is optimised, at the moment the energy-related cost function performs better than the stress cost function.
- Inclusion of individual morphological parameters is only effective when the energy-related cost function is used.





References



References

- Alexander R M. (1997) A minimum energy cost hypothesis for human arm trajectories. *Biol Cybern* 76:97-105
- Alfonsi E, Pavesi R, Merlo I M, Gelmetti A, Zambarbieri D, Lago P, Arrigo A, Reggiani C and Moglia A. (1999) Hemoglobin near-infrared spectroscopy and surface EMG study in muscle ischaemia and fatiguing isometric contraction. *J Sports Med Phys Fitness* 39:83-92
- Amis A A, Downson D and Wright V. (1979) Muscle strength and musculo-skeletal geometry of the upper limb. *Engineering Medicine* 8:41-47
- An K N, Takahashi K, Harrigan T P and Chao E Y. (1984) Determination of muscle orientations and moment arms. *J Biomech Eng* 106:280-282
- Balnave C D and Allen D G. (1996) The effect of muscle length on intracellular calcium and force in single fibres from mouse skeletal muscle. *J Physiol* 492 (Pt 3):705-713
- Bechtel R and Caldwell G E. (1994) The influence of task and angle on torque production and muscle activity at the elbow. *J Electromyogr Kinesiol* 4:195
- Bernstein N. (1967) The problem of co-ordination and localization. In: *The co-ordination and regulation of movements*, New York: Pergamon, pp 15-59
- Blinks J R, Rudel R and Taylor S R. (1978) Calcium transients in isolated amphibian skeletal muscle fibres: detection with aequorin. *J Physiol* 277:291-323
- Brand R A, Pedersen D R and Friederich J A. (1986) The sensitivity of muscle force predictions to changes in physiologic cross-sectional area. *J Biomech* 19:589-596
- Brown S H and Potvin J R. (2005) Constraining spine stability levels in an optimization model leads to the prediction of trunk muscle cocontraction and improved spine compression force estimates. *J Biomech* 38:745-754
- Buchanan T S, Almdale D P, Lewis J L and Rymer W Z. (1986) Characteristics of synergic relations during isometric contractions of human elbow muscles. *J Neurophysiol* 56:1225-1241
- Buchanan T S, Rovai G P and Rymer W Z. (1989) Strategies for muscle activation during isometric torque generation at the human elbow. *J Neurophysiol* 62:1201-1212

- Buchanan T S and Lloyd D G. (1995) Muscle activity is different for humans performing static tasks which require force control and position control. *Neurosci Lett* 194:61-64
- Buchanan T S and Shreeve D A. (1996) An evaluation of optimization techniques for the prediction of muscle activation patterns during isometric tasks. *J Biomech Eng* 118:565-574
- Calder K M and Gabriel D A. (2007) Adaptations during familiarization to resistive exercise. *J Electromyogr Kinesiol* 17:328-335
- Caldwell G E and Van Leemputte M. (1991) Elbow torques and EMG patterns of flexor muscles during different isometric tasks. *Electromyogr Clin Neurophysiol* 31:433-445
- Challis J H and Kerwin D G. (1993) An analytical examination of muscle force estimations using optimization techniques. *Proc Inst Mech Eng [H]* 207:139-148
- Challis J H. (1997) Producing physiologically realistic individual muscle force estimations by imposing constraints when using optimization techniques. *Med Eng Phys* 19:253-261
- Colier W N, Ringnald B E, Evers J A and Oeseburg B. (1992) Evaluation of the algorithm used in near infrared spectrophotometry. *Adv Exp Med Biol* 317:305-311
- Colier W N, Meeuwssen I B, Degens H and Oeseburg B. (1995) Determination of oxygen consumption in muscle during exercise using near infrared spectroscopy. *Acta Anaesthesiologica Scandinavica. Supplementum* 107:151-155
- Crowninshield R D and Brand R A. (1981) A physiologically based criterion of muscle force prediction in locomotion. *J Biomech* 14:793
- d'Avella A, Portone A, Fernandez L and Lacquaniti F. (2006) Control of fast-reaching movements by muscle synergy combinations. *J Neurosci* 26:7791-7810
- De Blasi R A, Cope M, Elwell C, Safoue F and Ferrari M. (1993) Noninvasive measurement of human forearm oxygen consumption by near infrared spectroscopy. *Eur J Appl Physiol Occup Physiol* 67:20-25
- De Blasi R A, Alviggi I, Cope M, Elwell C and Ferrari M. (1994) Noninvasive measurement of forearm oxygen consumption during exercise by near infrared spectroscopy. *Advances in Experimental Medicine & Biology* 345:685-692
- De Haan A, De Jong J, Van Doorn J E, Huijting P A, Woittiez R D and Westra H G. (1986) Muscle economy of isometric contractions as a function of stimulation time and relative muscle length. *Pflugers Arch* 407:445-450

- De Luca C J. (1997) The use of electromyography in biomechanics. *Journal of Applied Biomechanics*. 13:115-163
- de Serres S J, Hebert L J, Arsenault A B and Goulet C. (1992) Effect of pronation and supination tasks on elbow flexor muscles. *Journal of Electromyography and Kinesiology* 2:53
- Delp S L and Loan J P. (1995) A graphics-based software system to develop and analyze models of musculoskeletal structures. *Computers in Biology and Medicine* 25:21
- Delp S L, Wixson R L, Komattu A V and Kocmond J H. (1996) How superior placement of the joint center in hip arthroplasty affects the abductor muscles. *Clin Orthop Relat Res*:137-146
- Dul J, Johnson G E, Shiavi R and Townsend M A. (1984a) Muscular synergism--II. A minimum-fatigue criterion for load sharing between synergistic muscles. *Journal of Biomechanics* 17:675-684
- Dul J, Townsend M A, Shiavi R and Johnson G E. (1984b) Muscular synergism--I. On criteria for load sharing between synergistic muscles. *Journal of Biomechanics* 17:663-673
- Duncan A, Meek J H, Clemence M, Elwell C E, Tyszczyk L, Cope M and Delpy D T. (1995) Optical pathlength measurements on adult head, calf and forearm and the head of the newborn infant using phase resolved optical spectroscopy. *Phys Med Biol* 40:295-304
- Ettema G J C, Styles G and Kippers V. (1998) The moment arms of 23 muscle segments of the upper limb with varying elbow and forearm positions: Implications for motor control. *Human Movement Science* 17:201
- Felici F, Sbriccoli P, I. B, Figura F, Ferrari M and V. Q. (2001) Biceps Brachii O₂Hb de-saturation and surface EMG modifications during sustained constant and rhythmic isometric contractions. In: *International Workshop on Non invasive Investigation of Muscle Function*, Marseille, France
- Ferrari M, Wei Q, Carraresi L, De Blasi R A and Zaccanti G. (1992) Time-resolved spectroscopy of the human forearm. *J Photochem Photobiol B* 16:141-153
- Fick R. (1910) *Handbuch der anatomie und mechanik der gelenke: unter berucksichtigung der bewegenden muskeln*. Jena: Fischer
- Gabriel D A, Kamen G and Frost G. (2006) Neural adaptations to resistive exercise: mechanisms and recommendations for training practices. *Sports Med* 36:133-149
- Glitsch U and Baumann W. (1997) The three-dimensional determination of internal loads in the lower extremity. *J Biomech* 30:1123-1131

- Gribble P L and Ostry D J. (1998) Independent coactivation of shoulder and elbow muscles. *Exp Brain Res* 123:355-360
- Gribble P L, Mullin L I, Cothros N and Mattar A. (2003) Role of cocontraction in arm movement accuracy. *J Neurophysiol* 89:2396-2405
- Happee R. (1994) Inverse dynamic optimization including muscular dynamics, a new simulation method applied to goal directed movements. *Journal of Biomechanics* 27:953
- Happee R and Van der Helm F C T. (1994) Inverse dynamic optimization of shoulder muscle activity during fast, goal directed arm movements. *Journal of Biomechanics* 27:779
- Happee R and Van der Helm F C T. (1995) The control of shoulder muscles during goal directed movements, an inverse dynamic analysis. *Journal of Biomechanics* 28:1179
- Hardt D E. (1978) Determining muscle forces in the leg during normal human walking: an application and evaluation of optimization methods. *Journal of Biomechanical Engineering* 100:72–78
- Hatze H and Buys J D. (1977) Energy-optimal controls in the mammalian neuromuscular system. *Biol Cybern* 27:9-20
- Hebert L J, De Serres S J and Arsenault A B. (1991) Cocontraction of the elbow muscles during combined tasks of pronation-flexion and supination-flexion. *Electromyogr Clin Neurophysiol* 31:483-488
- Henriksson J. (1999) Microdialysis of skeletal muscle at rest. *Proc Nutr Soc* 58:919-923
- Herzog W and Leonard T R. (1991) Validation of optimization models that estimate the forces exerted by synergistic muscles. *J Biomech* 24 Suppl 1:31-39
- Herzog W. (1992) Sensitivity of muscle force estimations to changes in muscle input parameters using nonlinear optimization approaches. *J Biomech Eng* 114:267-268
- Hogfors C, Sigholm G and Herberts P. (1987) Biomechanical model of the human shoulder--I. Elements. *Journal of Biomechanics* 20:157
- Hogfors C, Peterson B, Sigholm G and Herberts P. (1991) Biomechanical model of the human shoulder joint--II. The shoulder rhythm. *Journal of Biomechanics* 24:699
- Homsher E and Kean C J. (1978) Skeletal muscle energetics and metabolism. *Annu Rev Physiol* 40:93-131
- Hoozemans M J, Kuijer P P, Kingma I, Van Dieen J H, De Vries W H, Van der Woude L H, Veeger D J, Van der Beek A J and Frings-Dresen M H. (2004) Mechanical loading of the low back and shoulders during pushing and pulling activities. *Ergonomics* 47:1-18

- Huxley A F. (1957) Muscle structure and theories of contraction. *Progresses in biophysics and biophysical chemistry* 7:257-318
- Jamison J C and Caldwell G E. (1993) Muscle synergies and isometric torque production: influence of supination and pronation level on elbow flexion. *J Neurophysiol* 70:947-960
- Jamison J C and Caldwell G E. (1994) Dual degree of freedom tasks: Flexion effect on supination/pronation response. *Journal of Electromyography and Kinesiology* 4:143
- Jinha A, Ait-Haddou R, Binding P and Herzog W. (2006a) Antagonistic activity of one-joint muscles in three-dimensions using non-linear optimisation. *Math Biosci* 202:57-70
- Jinha A, Ait-Haddou R and Herzog W. (2006b) Predictions of co-contraction depend critically on degrees-of-freedom in the musculoskeletal model. *J Biomech* 39:1145-1152
- Kaptein B L. (1999) Towards in vivo parameter estimation for a musculoskeletal model of the human shoulder, Delft: Delft University of Technology
- Kaptein B L and Van der Helm F C T. (2004) Estimating muscle attachment contours by transforming geometrical bone models. *Journal of Biomechanics* 37:263
- Karlsson D, Hogfors C and Peterson B. (1992) Biomechanical modeling of the human shoulder. *Journal of Biomechanics* 25:766
- Kasprisin J E and Grabiner M D. (2000) Joint angle-dependence of elbow flexor activation levels during isometric and isokinetic maximum voluntary contractions. *Clin Biomech (Bristol, Avon)* 15:743-749
- Kaufman K R, An K N, Litchy W J and Chao E Y. (1991a) Physiological prediction of muscle forces--II. Application to isokinetic exercise. *Neuroscience* 40:793-804
- Kaufman K R, An K W, Litchy W J and Chao E Y. (1991b) Physiological prediction of muscle forces--I. Theoretical formulation. *Neuroscience* 40:781-792
- Kistemaker D A, Van Soest A K and Bobbert M F. (2007) Equilibrium point control cannot be refuted by experimental reconstruction of equilibrium point trajectories. *J Neurophysiol*
- Klein Breteler M D, Spoor C W and Van der Helm F C. (1999) Measuring muscle and joint geometry parameters of a shoulder for modeling purposes. *J Biomech* 32:1191-1197

- Klein Breteler M D, Meulenbroek R G and Gielen S C. (2002) An evaluation of the minimum-jerk and minimum torque-change principles at the path, trajectory, and movement-cost levels. *Motor Control* 6:69-83
- Klein Horsman M D, Koopman H F J M, Veeger H E J and Van der Helm F C T. (2006) Musculoskeletal model of the lower extremity: validation of muscle moment arms and maximal isometric muscle force. *Journal of Biomechanics* 39:S52
- Klein Horsman M D, Koopman H F J M, Van der Helm F C T, Prose L P and Veeger H E J. (2007) Morphological muscle and joint parameters for musculoskeletal modelling of the lower extremity. *Clinical Biomechanics* 22:239
- Koopman B, Grootenboer H J and de Jongh H J. (1995) An inverse dynamics model for the analysis, reconstruction and prediction of bipedal walking. *J Biomech* 28:1369-1376
- Kreulen M, Smeulders M J, Veeger H E and Hage J J. (2006) Movement patterns of the upper extremity and trunk before and after corrective surgery of impaired forearm rotation in patients with cerebral palsy. *Dev Med Child Neurol* 48:436-441
- Kuijjer P P, Hoozemans M J, Kingma I, Van Dieen J H, De Vries W H, Veeger D J, Van der Beek A J, Visser B and Frings-Dresen M H. (2003) Effect of a redesigned two-wheeled container for refuse collecting on mechanical loading of low back and shoulders. *Ergonomics* 46:543-560
- Lacquaniti F and Soechting J F. (1986) EMG responses to load perturbations of the upper limb: effect of dynamic coupling between shoulder and elbow motion. *Exp Brain Res* 61:482-496
- Lawrence J H and De Luca C J. (1983) Myoelectric signal versus force relationship in different human muscles. *J Appl Physiol* 54:1653-1659
- Leedham J S and Dowling J J. (1995) Force-length, torque-angle and EMG-joint angle relationships of the human in vivo biceps brachii. *Eur J Appl Physiol* 70:421-426
- Lott M E and Sinoway L I. (2004) What has microdialysis shown us about the metabolic milieu within exercising skeletal muscle? *Exerc Sport Sci Rev* 32:69-74
- Lou F, Curtin N and Woledge R. (1997) The energetic cost of activation of white muscle fibres from the dogfish *Scyliorhinus canicula*. *J Exp Biol* 200:495-501
- Ma S P and Zahalak G I. (1991) A distribution-moment model of energetics in skeletal muscle. *Journal of Biomechanics* 24:21-35

- Magermans D J, Chadwick E K J, Veeger H E J, Rozing P M and van der Helm F C T. (2004) Effectiveness of tendon transfers for massive rotator cuff tears: a simulation study. *Clinical Biomechanics* 19:116
- Magermans D J, Chadwick E K J, Veeger H E J and Van der Helm F C T. (2005) Requirements for upper extremity motions during activities of daily living. *Clinical Biomechanics* 20:591
- Miura H, Araki H, Matoba H and Kitagawa K. (2000) Relationship among oxygenation, myoelectric activity, and lactic acid accumulation in vastus lateralis muscle during exercise with constant work rate. *Int J Sports Med* 21:180-184
- Morris M D and Mitchell T J. (1995) Exploratory designs for computational experiments. *Journal of Statistical Planning and Inference* 43:381
- Murray W M, Delp S L and Buchanan T S. (1995) Variation of muscle moment arms with elbow and forearm position. *Journal of Biomechanics* 28:513
- Murray W M, Buchanan T S and Delp S L. (2000) The isometric functional capacity of muscles that cross the elbow. *J Biomech* 33:943-952
- Pandy M G, Sasaki K and Kim S. (1998) A Three-Dimensional Musculoskeletal Model of the Human Knee Joint. Part 1: Theoretical Construct. *Comput Methods Biomech Biomed Engin* 1:87-108
- Pierrynowski M R. (1995) Analytic representation of muscle line of action and geometry. In: *Three-Dimensional Analysis of Human Movement. Human Kinetics* (Allard, P., Stokes, I.A.F. and Bianchi, J.P., ed), Champaign,IL, p 214–256
- Praagman M, Veeger H E J, Chadwick E K J, Colier W N J M and Van der Helm F C T. (2003) Muscle oxygen consumption, determined by NIRS, in relation to external force and EMG. *Journal of Biomechanics* 36:905-912
- Praagman M, Chadwick E K J, Van der Helm F C T and Veeger H E J. (2006) The relationship between two different mechanical cost functions and muscle oxygen consumption. *Journal of Biomechanics* 39:758-765
- Prilutsky B I. (2000) Coordination of two- and one-joint muscles: functional consequences and implications for motor control. *Motor Control* 4:1-44.
- Pronk G M. (1991) The shoulder girdle. In: *Man-Machine systems*, Delft: Delft University of Technology

- Raikova R. (1996) A model of the flexion-extension motion in the elbow joint some problems concerning muscle forces modelling and computation. *J Biomech* 29:763-772
- Raikova R T and Prilutsky B I. (2001) Sensitivity of predicted muscle forces to parameters of the optimization-based human leg model revealed by analytical and numerical analyses. *Journal of Biomechanics* 34:1243
- Rasmussen J, Damsgaard M and Voigt M. (2001) Muscle recruitment by the min/max criterion -- a comparative numerical study. *Journal of Biomechanics* 34:409
- Sacks J, Welch W J, Mitchell T J and Wynn H P. (1989) Design and analysis of computer experiments. *Statistical Science* 4: 409-435
- Soechting J F and Lacquaniti F. (1988) Quantitative evaluation of the electromyographic responses to multidirectional load perturbations of the human arm. *J Neurophysiol* 59:1296-1313
- Stephenson D G and Wendt I R. (1984) Length dependence of changes in sarcoplasmic calcium concentration and myofibrillar calcium sensitivity in striated muscle fibres. *J Muscle Res Cell Motil* 5:243-272
- Stokes I A and Gardner-Morse M. (2001) Lumbar spinal muscle activation synergies predicted by multi-criteria cost function. *J Biomech* 34:733-740
- Tsirakos D, Baltzopoulos V and Bartlett R. (1997) Inverse optimization: functional and physiological considerations related to the force-sharing problem. *Crit Rev Biomed Eng* 25:371-407
- Van Beekvelt M C, Colier W N, Wevers R A and Van Engelen B G. (2001) Performance of near-infrared spectroscopy in measuring local O₂ consumption and blood flow in skeletal muscle. *J Appl Physiol* 90:511-519
- Van Beekvelt M C, Van Engelen B G, Wevers R A and Colier W N. (2002) In vivo quantitative near-infrared spectroscopy in skeletal muscle during incremental isometric handgrip exercise. *Clin Physiol Funct Imaging* 22:210-217
- Van Bolhuis B M and Gielen C C. (1997) The relative activation of elbow-flexor muscles in isometric flexion and in flexion/extension movements. *J Biomech* 30:803-811
- Van den Bogert A J, Read L and Nigg B M. (1999) An analysis of hip joint loading during walking, running, and skiing. *Med Sci Sports Exerc* 31:131-142

- Van der Helm F C T. (1991) The shoulder mechanism, a dynamic approach. In: *Man Machine Systems Group*, Delft: Delft University of Technology.
- Van der Helm F C T, Veeger H E J, Pronk G M, Van der Woude L H and Rozendal R H. (1992) Geometry parameters for musculoskeletal modelling of the shoulder system. *Journal of Biomechanics* 25:129-144
- Van der Helm F C T. (1994a) Analysis of the kinematic and dynamic behavior of the shoulder mechanism. *Journal of Biomechanics* 27:527-550
- Van der Helm F C T. (1994b) A finite element musculoskeletal model of the shoulder mechanism. *Journal of Biomechanics* 27:551-569
- Van der Helm F C T. (1997a) A standardized protocol for motion recordings of the shoulder. In: *First Conference of the International Shoulder Group* (Veeger, H. E. J. V. d. H., F.C.T.; Rozing, P.M., ed, Delft University of Technology, The Netherlands: Shaker Publishers BV, pp 7-12
- Van der Helm F C T. (1997b) A three-dimensional model of the shoulder and elbow. In: *First Conference of the International Shoulder Group* (Veeger, H. E. J., van der Helm, F. C. T., Rozing, P. M., eds), Delft University of Technology, The Netherlands.: Shaker Publishers BV, pp 65-70
- Van der Helm F C T. (2000) Large-scale musculoskeletal systems: sensorimotor integration and optimization. In: *Neural control of posture and movement* (Winters, J. M., Cragg, P., eds), NY: Springer Verlag, pp 407-424
- Van der Sluijs M C, Collier W N J M, Houston R J F and Oeseburg B. (1998) A new highly sensitive continuous wave near-infrared spectrophotometer with multiple detectors. *SPIE*:63-72
- Van der Woude L H, Veeger H E, Dallmeijer A J, Janssen T W and Rozendaal L A. (2001) Biomechanics and physiology in active manual wheelchair propulsion. *Med Eng Phys* 23:713-733
- Van der Zee P, Cope M, Arridge S R, Essenpreis M, Potter L A, Edwards A D, Wyatt J S, McCormick D C, Roth S C, Reynolds E O and et al. (1992) Experimentally measured optical pathlengths for the adult head, calf and forearm and the head of the newborn infant as a function of inter optode spacing. *Adv Exp Med Biol* 316:143-153
- Van Dieën J H. (1996) Asymmetry of erector spinae muscle activity in twisted postures and consistency of muscle activation patterns across subjects. *Spine* 21:2651-2661

- Van Drongelen S, Van der Woude L H, Janssen T W, Angenot E L, Chadwick E K and Veeger D H. (2005a) Glenohumeral contact forces and muscle forces evaluated in wheelchair-related activities of daily living in able-bodied subjects versus subjects with paraplegia and tetraplegia. *Arch Phys Med Rehabil* 86:1434-1440
- Van Drongelen S, Van der Woude L H, Janssen T W, Angenot E L, Chadwick E K and Veeger D H. (2005b) Mechanical load on the upper extremity during wheelchair activities. *Arch Phys Med Rehabil* 86:1214-1220
- Van Drongelen S, Van der Woude L H, Janssen T W, Angenot E L, Chadwick E K and Veeger H E. (2006) Glenohumeral joint loading in tetraplegia during weight relief lifting: a simulation study. *Clin Biomech (Bristol, Avon)* 21:128-137
- Van Soest A J, Gfohler M and Casius L J. (2005) Consequences of ankle joint fixation on FES cycling power output: a simulation study. *Med Sci Sports Exerc* 37:797-806
- Van Zuylen E J, Gielen C C and Denier van der Gon J J. (1988) Coordination and inhomogeneous activation of human arm muscles during isometric torques. *J Neurophysiol* 60:1523-1548
- Veeger H E J, Van der Helm F C T, Van der Woude L H V, Pronk G M and Rozendal R H. (1991a) Inertia and muscle contraction parameters for musculoskeletal modelling of the shoulder mechanism. *Journal of Biomechanics* 24:615-629
- Veeger H E J, Van der Woude L H V and Rozendal R H. (1991b) Load on the upper extremity in manual wheelchair propulsion. *Journal of Electromyography and Kinesiology* 1:270
- Veeger H E J, Lute E M, Roeleveld K and Van der Woude L H. (1992a) Differences in performance between trained and untrained subjects during a 30-s sprint test in a wheelchair ergometer. *Eur J Appl Physiol Occup Physiol* 64:158-164
- Veeger H E J, Van der Woude L H and Rozendal R H. (1992b) A computerized wheelchair ergometer. Results of a comparison study. *Scand J Rehabil Med* 24:17-23
- Veeger H E J, Yu B, An K N and Rozendal R H. (1997) Parameters for modeling the upper extremity. *J Biomech* 30:647-652
- Veeger H E J, Rozendaal L A and van der Helm F C. (2002a) Load on the shoulder in low intensity wheelchair propulsion. *Clin Biomech (Bristol, Avon)* 17:211-218
- Veeger H E J, Rozendaal L A and Van der Helm F C T. (2002b) Load on the shoulder in low intensity wheelchair propulsion. *Clinical Biomechanics* 17:211

- Veeger H E J, Kreulen M and Smeulders M J C. (2004) Mechanical evaluation of the Pronator Teres rerouting tendon transfer. *The Journal of Hand Surgery: Journal of the British Society for Surgery of the Hand* 29:259
- Veeger H E J and Van der Helm F C T. (2007) Shoulder function: the perfect compromise between mobility and stability. *J Biomech* 40:2119-2129
- Veeger H E J, Van der Helm, F.C.T., Rozendal, R.H. (1993) Orientation of the scapula in a simulated wheelchair push. *Clinical Biomechanics* 8:81-90
- Wendt I R and Barclay J K. (1980) Effects of dantrolene on the energetics of fast- and slow-twitch muscles of the mouse. *Am J Physiol* 238:C56-61
- Woledge R C, Curtin N A and Homsher E. (1985) Energetic aspects of muscle contraction. *Monogr Physiol Soc* 41:1-357
- Woods J J and Bigland-Ritchie B. (1983) Linear and non-linear surface EMG/force relationships in human muscles. An anatomical/functional argument for the existence of both. *Am J Phys Med* 62:287-299
- Yamaguchi G T, Sawa A G U, Moran D W, Fessler M J and Winters J M. (1990) A survey of human musculotendon actuator parameters. In: *Multiple Muscle Systems: Biomechanics and Movement Organisation*. (Winter, J. M., Woo, S.L.Y., ed), Berlin: Springer, pp 717-773
- Yoshitake Y, Ue H, Miyazaki M and Moritani T. (2001) Assessment of lower-back muscle fatigue using electromyography, mechanomyography, and near-infrared spectroscopy. *Eur J Appl Physiol* 84:174-179
- Zahalak G I and Ma S P. (1990) Muscle activation and contraction: constitutive relations based directly on cross-bridge kinetics. *Journal of Biomechanical Engineering* 112:52-62



Summary

Summary

Muscle load sharing, an energy-based approach

Musculoskeletal models are a valuable tool in the study on human movement. When the kinematics and external forces that act on the human body are known, such models can be used to calculate the resultant joint moments for a given posture or motion by simple Newtonian mechanics. It is, however, difficult to determine the contribution of the individual muscles to these moments. In general, there are more muscles crossing a joint than is theoretically necessary in order to perform all possible movements. This is called the indeterminacy problem or the load sharing problem. Inverse dynamic models often make use of cost functions to solve this load sharing problem. The use of cost functions is based on the assumption that the central nervous system controls the musculoskeletal system in an optimal manner, optimising a certain cost or objective. It is, however, difficult to find the right criterion, since it is unknown what quantity is optimised in real life. Therefore, only assumptions can be made.

Most cost functions, that have been proposed, are mechanical cost functions, which are based on muscle force and often weighed by maximal force or a morphological parameter such as physiological cross sectional area (PCSA). Although some of these functions are assumed to be related to physiological costs like energy consumption or fatigue, clear relationships have never been proven. The validation of cost functions is hampered by the fact that muscle force can not easily be measured *in vivo* and is therefore often restricted to a comparison between calculated muscle force and recorded EMG patterns.

Especially for submaximal activities, it has often been assumed that movements are performed by minimising energy consumption. Nevertheless, up till now there are no cost functions defined, based on muscle energy consumption. The aims of this thesis were to define a cost function that represents muscle energy consumption and to validate this cost function with a metabolic parameter.

In a model, the predicted function of a muscle depends on the total number of degrees of freedom included. Not only the number of degrees of freedom, used for a single joint, is of great influence for muscle function. Because of the special role of bi- and poly-articular muscles, it also depends on the distribution of muscle forces around adjacent joints. As a consequence, the effect of cost functions on model predictions should ideally be studied with the help of models that include all degrees of freedom instead of using simple one- or two joint models. Therefore, in the current thesis the Delft Shoulder and Elbow

Model (DSEM) was used, which is a 3D inverse dynamic musculoskeletal model of the upper extremity.

Validation of the cost functions, studied in this thesis, was done with the help of Near InfraRed Spectroscopy (NIRS). NIRS is a non-invasive method which can be used to measure the oxygenation of biological tissue. It has been proven to be a valid method to measure muscle oxygenation. Up till now, however, little is known about the relationship between muscle oxygen consumption ($\dot{V}O_2$), determined with NIRS, and muscle activation, determined with EMG.

When a muscle is stimulated, calcium is released from the sarcoplasmic reticulum (SR), enabling the cross-bridges to attach and consequently to produce force. The two major energy-consuming processes in a muscle are the re-uptake of calcium in the SR (activation dynamics) and the detachment of cross-bridges (contraction dynamics). Since EMG and NIRS apply to different levels of the process of force production, it is plausible that these two techniques show different results. NIRS registers muscle oxygen consumption and hence gives an indication of both the activation and the contraction dynamics process. EMG, on the other hand, registers the excitation of the muscle only, which initiates the calcium flow from the SR and therefore should give an indication of the contraction dynamics only.

The exact relationship between the EMG signal and calcium flow or cross-bridge attachment is unknown. Since activation is not linearly related to force, we expected a non-linear relationship between the EMG and $\dot{V}O_2$. In Chapter 2 we performed experiments to investigate this relationship. Both EMG and $\dot{V}O_2$ of two arm muscles (m. biceps brachii caput breve and m. brachioradialis) were measured during several isometric contractions in which subjects had to perform combinations of elbow flexion and pro/supination moments at force levels up to 70% of their maximum force. The results of these experiments showed that both EMG and $\dot{V}O_2$ were linearly related to the performed external moment and that the relationship between $\dot{V}O_2$ and EMG could be described by a linear equation.

In Chapter 3 an experiment was performed in which the $\dot{V}O_2$ of four elbow muscles (the m. biceps brachii caput breve, the m. biceps brachii caput longum, the m. brachioradialis and the m. triceps brachii caput laterale) was recorded. The subjects had to perform isometric contractions, generating several combinations of elbow flexion/extension and pro/supination moments. The measured $\dot{V}O_2$ of the arm muscles was used in this experiment to validate two different cost functions. The first cost function was the well known stress cost function, in which the sum of squared muscle stress is minimised. Although it has been suggested previously that the stress cost function

is related to energy consumption, validation with a metabolic variable was never done. The second cost function, used in this study, was a newly proposed cost function which is further referred to as the energy-related cost function. This cost function is based on the two main energy-consuming processes of the muscle mentioned before, namely activation dynamics and contraction dynamics. The metabolic cost of a muscle is equal to the summed energy cost over the activated sarcomeres. Therefore, not only the PCSA, representing the cross-bridges that are in parallel, but also muscle fibre length, which is related to the number of sarcomeres in series, should be included in the cost function. For that reason, in Chapter 3 both PCSA and fibre length were incorporated in the new cost function. It was expected that this energy-related cost function would give a better representation of muscle energy consumption than the stress cost function. To find out if this was really the case, both cost functions were implemented into the inverse dynamic version of the Delft Shoulder and Elbow Model. For each of the four measured elbow muscles experimentally obtained $\dot{V}O_2$ values were compared to individual predicted cost values. The analyses focused on two different measures: first the overall fit (correlation and RMSE values) between model predictions and experimental results and secondly the number of the so-called 'false negatives' and 'false positives' (conditions in which the model predicted NO muscle activity where muscle activity was indeed recorded, and vice versa). For the m. triceps brachii caput laterale the stress cost function led to a good correspondence between $\dot{V}O_2$ and cost. For the flexor muscles, however, the predicted metabolic cost was significantly lower than the experimentally obtained $\dot{V}O_2$ values and a large number of 'false negatives' were found. It seemed that, compared to flexion/extension moments, pro/supination moments had a disproportional large effect on the predicted activity of these muscles. Compared to the stress cost function, the energy-related cost function showed a better correspondence between $\dot{V}O_2$ and cost and fewer 'false negatives'. It was therefore concluded that the energy-related cost function appears to be a better measure for muscle energy consumption than the stress cost function and leads to more realistic predictions of load sharing.

Although the measurements, described in Chapter 3, included several combinations of flexion/extension and pro/supination moments, not all possible combinations of joint moments were included. Furthermore, all measurements were performed at one fixed elbow angle (90°) only. Consequently, muscle length was not varied, which means that the force-length characteristics were not taken into account. Therefore, in Chapter 4 new experiments were performed in which elbow angle (and therefore muscle length) was varied for a range of elbow flexion angles

from 55° to 120°. Two different experiments were performed in Chapter 4. In the first experiment, EMG of eight elbow muscles was recorded while the subjects ($n = 6$) performed a full range of all possible (49) combinations of elbow flexion/extension and forearm pro/supination moments, varied over three different force levels. All 49 measurements were repeated at four different elbow angles. The set-up of the second experiment was comparable to the first experiment; except that in this experiment besides EMG measurements $\dot{V}O_2$ measurements with NIRS were performed as well. Due to the fact that NIRS measurements are very time-consuming, the number of moment combinations, muscles and subjects was limited compared to the first experiment.

When the elbow angle changes, not only the lengths of the muscles, which span the elbow joint, change but the moment arms as well. Since the maximal force, that can be produced by a muscle, depends on its actual muscle length and the moment that can be produced depends on the actual moment arm, it seems obvious that elbow angle will influence muscle activity. It is, however, unclear what the effect of this change in elbow angle will be on the muscle load sharing. From a single muscle perspective it could be expected that muscle activity *decreases* at optimum length/optimum moment arm as the muscle can achieve the same force/moment with less activity. Conversely, from a multiple-muscle point of view the opposite can be expected: as the muscle becomes 'cheaper' its contribution might *increase*, since the use of that muscle has become 'cheaper'.

The results of Chapter 4 showed that joint angle, and therefore moment arm and muscle length, influences both the activity level of the muscle as well as the load sharing between muscles. Unfortunately, the principles behind this load sharing were difficult to quantify, since it was impossible to distinguish all the individual aspects that affect muscle activity. Furthermore, the results of Chapter 4 confirmed the conclusion of Chapter 2 that the relationship between EMG and $\dot{V}O_2$ can be described as a linear relationship and that this relationship is not influenced by elbow angle. Another important result of Chapter 4 was that although, in general, subjects showed comparable muscle activation patterns, there were also some striking inter-individual differences. Assuming that the subjects used the same optimisation strategy, these inter-individual differences might be explained by differences in muscle morphology. As biomechanical models are in general based on a single anthropometrical data set, inter-individual differences will not be reflected by these models.

In Chapter 5, it was investigated whether the correspondence between model predictions and recorded muscle oxygen consumption (presented in Chapter 4) could be improved when for each subject an individualised

morphological data set was used. If subjects indeed differ in muscle morphology, it is possible that for any given subject a different combination of for instance PCSA and moment arm values might lead to a better fit between experimental and model data. In Chapter 5, also the interaction between morphology and optimisation criteria was investigated. Again, model simulations were done with the DSEM and the stress cost function was compared to the energy-related cost function. In this experiment a new morphological data set was used in the model. This new set includes data on optimal fibre length, which made it possible to implement force-length characteristics. The energy-related cost function could therefore be reformulated such that the force-length characteristics of the muscles were included. The PCSA and moment arm values of eight upper- and forearm muscles were varied in the model. An approximative optimisation strategy was used to find for each subject the individual parameter set that was expected to correspond best with the experimental data. The fit between the experimental data and the model predictions, done with this optimal morphological parameter set, can be seen as the maximum improvement that can be attained by the inclusion of individual morphology in the model.

The results showed that the load sharing is strongly dependent on cost function, as well as on morphology. The modelling results improved by using the individually optimised morphological data. This could explain part of the inter-individual variability in the experimental results, and also led to a better morphological parameter set for individual subjects than the 'generic' model morphology that was based on one specimen only. Fitting individual morphological data, however, was only effective for the energy-related cost function. Although not all the 'false negatives' disappeared, the energy-related cost function again showed a better fit to experimental results than the stress cost function. The remaining 'false negatives' were predominately found in conditions, including a moment for which the particular muscle had no or even the opposite effect. In these conditions, muscles seem to be activated due to a compensating effect for one of the other muscles or due to their effect on another degree of freedom.

In Chapter 6, the Epilogue, the main findings of the research, described in this thesis, were summarised and discussed. The present thesis shows that the use of Near Infrared Spectroscopy, to measure muscle oxygen consumption is a valuable development in cost function validation. Furthermore, it becomes clear that load sharing, not always leads to the same muscle activation pattern and that it is influenced by different factors. As the exact principles behind load sharing are still unknown, it is difficult to find the right optimisation criterion (cost function). In

addition, the evaluation of a cost function is hampered by the fact that the predicted load sharing is not only influenced by the type of cost function but also by factors such as morphological parameters. It is difficult, if not impossible, to separate the individual effects of morphological parameters on the predicted load sharing. In Chapter 6, it is also stressed that validation of cost functions can only be done with multiple-muscle and -joint models that include the actual number of degrees of freedom as well as all actual adjacent joints.

It is clear that the stress cost function does not predict realistic muscle activation patterns, since using this cost function resulted in a relatively large amount of 'false negatives' and 'false positives'. The energy-related cost function performed better, but also needs improvement. The fact that 'false negatives' and 'false positives' were mainly seen in paradoxical conditions in which the activated muscle contributes to one of the requested moments only and counteracts to the other moment or in which the muscle does not directly contribute to one of the requested moments at all emphasises the significance of including a wide range of force tasks into the experimental set-up, covering all degrees of freedom.

Since the energy-related cost function still shows some discrepancies with experimental data, it can be questioned whether it is indeed energy consumption that is optimised during submaximal movements. Furthermore, it can be argued whether the energy-related cost function, proposed in the present thesis, is a valid description of muscle energy consumption. Further improvement of the cost function can possibly be achieved by optimising the weight factors of the cost function. It should also be studied whether energy consumption is optimised on the level of the individual muscles, independent of and not necessarily leading to a minimisation of overall energy consumption. Based on the observed inter-individual differences in the present thesis, it can also be questioned if the assumption of a general optimisation criterion is valid and that people use different optimisation strategies. The results of Chapter 5 indicated, however, that part of the inter-individual differences could be explained by possible differences in morphology, although this was only effective using the energy-related cost function. Inter-individual differences could, on the other hand, also be caused by different strategies in coping with stability. It is likely, that proper validation of cost functions can not be done without including a task constraint such as stability.



Samenvatting

Samenvatting

Krachtenverdeling tussen spieren, een energetische benadering.

In het onderzoek naar het menselijk bewegen wordt vaak gebruik gemaakt van biomechanische spierskeletmodellen. Als de houding/positie van een persoon en de externe krachten die op het lichaam aangrijpen bekend zijn, kunnen met een dergelijk model de externe momenten, die heersen rond de verschillende gewrichten, relatief eenvoudig berekend worden. Moeilijker wordt het wanneer de bijdrage van de individuele spieren aan het betreffende externe moment berekend moeten worden. Er zijn namelijk altijd meerdere spieren die het betreffende moment zouden kunnen leveren. Dit wordt het onbepaaldheidsprobleem genoemd. Om dit onbepaaldheidsprobleem op te lossen, maken modellen veelal gebruik van zogenaamde kostfuncties. Hierbij wordt aangenomen dat het centrale zenuwstelsel het spierskelet-systeem optimaal aanstuurt, waarbij een bepaalde grootte (kost) geoptimaliseerd (geminimaliseerd) wordt. Tot op heden is het moeilijk gebleken de juiste kostfunctie te bepalen omdat onbekend is welke grootte tijdens bewegingen geoptimaliseerd wordt. Er kunnen daarom slechts aannames gedaan worden.

De meest gebruikte kostfuncties zijn gebaseerd op spierkracht, waarbij vaak geoptimaliseerd wordt voor maximale spierkracht of voor de fysiologische dwarsdoorsnede van de spier. Het valideren van deze kostfuncties is moeilijk omdat het niet mogelijk is spierkracht in vivo te meten. Daarom blijft validatie meestal beperkt tot het vergelijken van de berekende spierkracht met gemeten spieractiviteit door middel van electromyografie (EMG).

Met name voor submaximale activiteiten wordt vaak aangenomen dat niet de spierkracht, maar het energieverbruik van de spieren geoptimaliseerd wordt. Desondanks bestaan er nog geen kostfuncties die gebaseerd zijn op energieconsumptie. Het doel van dit proefschrift was om een energetische kostfunctie te ontwikkelen en deze vervolgens te valideren aan de hand van een metabole parameter.

Het door een spierskeletmodel voorspelde effect van een spier is afhankelijk van het aantal vrijheidsgraden van het model. Daarbij is niet alleen het aantal vrijheidsgraden van een bepaald gewricht van belang, maar ook het aantal meegenomen aangrenzende gewrichten, aangezien bi- en poly-articulare spieren over meerdere gewrichten lopen en dus op meerdere gewrichten een effect hebben. Dit betekent dat het effect van kostfuncties idealiter niet bestudeerd zou moeten worden met eenvoudige één- of twee-gewrichtsmodellen maar met behulp van een model dat alle vrijheidsgraden bevat. In dit proefschrift is daarom een 3-

dimensionaal spierskeletmodel van de bovenste extremiteit gebruikt, te weten het Delft Schouder en Elleboog Model (DSEM).

De kostfuncties, die in dit proefschrift zijn bestudeerd, zijn gevalideerd met behulp van Near InfraRed Spectroscopy (NIRS), of wel Nabij-InfraRood Spectroscopie. NIRS is een niet-invasieve methode waarmee de hoeveelheid zuurstof die aanwezig is in een bepaald weefsel (de oxygenatie), bepaald kan worden. Eerder onderzoek heeft aangetoond dat NIRS een valide methode is om de oxygenatie van een spier te bepalen. Er is echter nog weinig bekend over de relatie tussen de met NIRS gemeten zuurstofconsumptie van de spier ($\dot{V}O_2$) en EMG (spieractiviteit).

Als een spier wordt gestimuleerd, komt er calcium vrij uit het sarcoplasmatisch reticulum. Dit zorgt ervoor dat er dwarsverbindingen (cross-bridges) kunnen ontstaan tussen de twee verschillende contractiele eiwitten waaruit de spier bestaat. Hierdoor kan de spier samentrekken en op die manier kracht leveren. De twee processen in de spier die de meeste energie kosten tijdens krachtleverantie zijn 1) het terugpompen van het calcium in het sarcoplasmatische reticulum (activatie-dynamica) en 2) het ontkoppelen van de cross-bridges (contractie-dynamica). Aangezien EMG en NIRS aangrijpen op een verschillend niveau in het krachtsleverantieproces, is het goed mogelijk dat deze twee technieken verschillende resultaten geven. NIRS registreert de zuurstofconsumptie van de spier en geeft daarmee een indicatie van zowel de activatie- als de contractie-dynamica. EMG, daarentegen, registreert alleen de excitatie (prikkeling) van de spier, die leidt tot het vrijkomen van calcium en zou dus alleen een indicatie van de contractie-dynamica moeten geven. De exacte relatie tussen het EMG-signaal en het vrijgekomen calcium of het ontkoppelen van de cross-bridges is echter onbekend. Aangezien activatie en kracht niet lineair aan elkaar gerelateerd zijn, verwachtten we dat EMG en $\dot{V}O_2$ ook niet lineair aan elkaar gerelateerd zouden zijn. Om dit na te gaan hebben we in hoofdstuk 2 experimenten uitgevoerd waarbij we van twee armspieren (de m. biceps brachii caput breve en de m. brachioradialis) zowel EMG als $\dot{V}O_2$ gemeten hebben tijdens isometrische contracties. Proefpersonen moesten verschillende combinaties van elleboogflexie- en pro/supinatie-momenten leveren op krachtniveaus, variërend van 10 tot 70% van hun maximale kracht. De resultaten van deze experimenten toonden aan dat er voor zowel EMG als $\dot{V}O_2$ een lineaire relatie bestaat met het externe moment en dat ook de relatie tussen EMG en $\dot{V}O_2$ met een lineaire relatie beschreven kan worden.

In hoofdstuk 3 werden opnieuw experimenten met NIRS en EMG uitgevoerd, ditmaal bij vier armspieren (de m. biceps brachii caput breve, de m. biceps brachii caput longum, de m. brachioradialis en de m.

triceps brachii caput laterale). Proefpersonen moesten isometrische contracties uitvoeren waarbij ze verschillende combinaties van flexie/extensie- en pro/supinatie-momenten moesten leveren. De met behulp van NIRS gemeten $\dot{V}O_2$ werd vervolgens gebruikt om twee verschillende kostfuncties te valideren. De eerste kostfunctie was de "stress kostfunctie". Hierbij wordt spierspanning (= (kracht/fysiologische dwarsdoorsnede)²) geminimaliseerd. Dit is één van de meest gebruikte kostfuncties. Ondanks dat eerder aangenomen is dat deze kostfunctie een goede maat zou zijn voor energieverbruik is deze kostfunctie nog nooit eerder gevalideerd met een metabole parameter. De tweede kostfunctie is een in dit proefschrift voor het eerst beschreven kostfunctie, die vanaf nu de energiegerelateerde kostfunctie genoemd zal worden. Deze kostfunctie is gebaseerd op de twee eerder genoemde meest energierovende processen in de spier: het terugpompen van calcium en de ont koppeling van cross-bridges. De totale metabole kost van een spier wordt bepaald door de som van de kosten van alle geactiveerde sarcomeren (een sarcomeer is de kleinste functionele eenheid van een spier). Daarom moet niet alleen de fysiologische dwarsdoorsnede van de spier, die een maat is voor het aantal parallelle sarcomeren, meegenomen worden, maar ook de vezellengte, die een maat is voor het aantal sarcomeren in serie. In de ontwikkelde energiegerelateerde kostfunctie zijn beide variabelen meegenomen. De verwachting was dat de energiegerelateerde kostfunctie een betere weergave is van het energieverbruik van de spier dan de stress kostfunctie. Beide kostfuncties zijn daartoe geïmplementeerd in de in vers dynamische versie van het Delft Schouder en Elleboog Model.

Voor elk van de vier gemeten elleboogspieren werden de experimenteel bepaalde $\dot{V}O_2$ -waardes vergeleken met de door het model bepaalde kostwaardes. De analyse richtte zich op twee verschillende waardes: de algehele overeenkomst (correlatie en RMSE) tussen de modelvoorspellingen en de experimentele resultaten en het aantal 'vals negatieven' en 'vals positieven' (condities waarvoor het model *geen* spieractiviteit voorspelde terwijl er wel activiteit gemeten was en vice versa). Met de stress kostfunctie werd voor de m. triceps brachii caput laterale een goede overeenkomst tussen $\dot{V}O_2$ en kost gevonden. Voor de elleboogflexoren was de voorspelde kostwaarde significant lager dan de gemeten $\dot{V}O_2$ -waarde en werd een groot aantal 'vals negatieven' gevonden. Het leek er op dat de pro/supinatie-momenten, in vergelijking tot de flexie/extensie-momenten, een disproportioneel groot effect hadden op de voorspelde activiteit van deze spieren. De energiegerelateerde kostfunctie vertoonde een betere overeenkomst tussen voorspelde en gemeten waardes en liet ook veel minder 'vals negatieven' zien. Op grond van deze resultaten werd daarom

geconcludeerd dat de energiegerelateerde kostfunctie een betere maat is voor energieconsumptie van de spier dan de stress kostfunctie en tot realistischere voorspellingen van krachtsverdeling (load sharing) tussen spieren leidt.

Ondanks dat in de hierboven beschreven experimenten verschillende combinaties van flexie/extensie- en pro/supinatie-momenten zijn gemeten, werden niet alle mogelijke combinaties gemeten en werd elke meting slechts bij één ellebooghoek (90°) uitgevoerd. Dit laatste betekent dat spierlengte niet werd gevarieerd en dat kracht-lengte-karakteristieken van de spier niet in de kostfunctie geïmplementeerd konden worden. In hoofdstuk 4 zijn daarom nieuwe metingen uitgevoerd waarbij de ellebooghoek (en dus spierlengte) wel gevarieerd werd (van 55° tot 120° elleboogflexie). Er zijn twee verschillende experimenten uitgevoerd. In het eerste experiment werd bij zes proefpersonen van acht elleboogspieren EMG gemeten tijdens 49 combinaties van richting en grootte van het opgelegde moment van elleboog flexie/extensie en pro/supinatie. Alle 49 metingen werden vervolgens herhaald voor vier verschillende ellebooghoeken. De opzet van het tweede experiment was gelijk aan die van het eerste experiment, maar nu werd naast EMG ook $\dot{V}O_2$ gemeten met NIRS. Aangezien NIRS-metingen erg tijdrovend zijn, werden tijdens dit experiment een kleiner aantal condities (variërend tussen 16 en 36), spieren (3) en proefpersonen (4) gemeten. Door de flexiehoek van de elleboog te variëren werd in dit experiment niet alleen de spierlengte maar ook de momentsarm gevarieerd. Aangezien de maximale kracht, die een spier kan produceren, afhangt van de actuele vezellengte en het moment dat de spier kan leveren afhangt van de actuele momentsarm, ligt het voor de hand dat de ellebooghoek invloed heeft op de spieractiviteit. Het is echter onduidelijk wat het precieze effect van een dergelijke verandering in ellebooghoek is op de krachtsverdeling tussen de spieren. Bekeken vanuit één enkele spier kan verwacht worden dat de spieractiviteit *afneemt* bij de optimum lengte (of momentsarm) aangezien de spier dan dezelfde kracht (of moment) kan produceren met minder activiteit. Vanuit meerdere spieren bekeken, kan echter ook verwacht worden dat het tegenovergestelde gebeurt: de activiteit van de spier neemt toe doordat de spier 'goedkoper' wordt. Dit zou betekenen dat tegelijkertijd de activiteit van (één van) de synergisten (spieren met eenzelfde effect rond een bepaald gewricht) af zou moeten nemen.

De resultaten, beschreven in hoofdstuk 4, laten zien dat gewrichtshoek, en dus momentsarm en spierlengte, zowel het activiteitsniveau van de spier als de krachtsverdeling tussen de spieren beïnvloedt. De wetmatigheden achter deze krachtsverdeling waren moeilijk te

achterhalen omdat het onmogelijk was om alle individuele aspecten die invloed hebben op de spieractiviteit van elkaar te scheiden. De resultaten bevestigden verder de conclusie uit hoofdstuk 2 dat de relatie tussen EMG en $\dot{V}O_2$ een lineaire relatie is. Deze relatie werd niet beïnvloed door ellebooghoek. Een andere belangrijke bevinding was dat, ondanks dat proefpersonen over het algemeen vergelijkbare patronen van spieractiviteit lieten zien, er ook enkele opvallende interindividuele verschillen gevonden werden. Als er vanuit gegaan wordt dat personen dezelfde optimalisatiestrategie gebruiken, is een mogelijke verklaring voor de gevonden interindividuele verschillen dat de proefpersonen verschillen in spiermorfologie. Aangezien biomechanische modellen normaal gesproken gebruik maken van één antropometrische data-set, kunnen dergelijke verschillen niet voorspeld worden.

In hoofdstuk 5 is daarom onderzocht of de overeenkomst tussen modelvoorspellingen en de gemeten zuurstofconsumptie (zoals gepresenteerd in hoofdstuk 4) verbeterd kon worden door voor iedere proefpersoon geïndividualiseerde morfologische data te gebruiken. Als proefpersonen inderdaad verschillen in spiermorfologie, is het mogelijk dat voor iedere proefpersoon een andere combinatie van bijvoorbeeld fysiologische dwarsdoorsnede en momentsarmen tot een betere overeenkomst tussen modelvoorspellingen en experimentele data leidt. Tevens werd de interactie tussen morfologie en kostfunctie onderzocht. Ook in dit hoofdstuk werd het DSEM gebruikt voor de modelsimulaties en werden opnieuw de stress kostfunctie en de energiegerelateerde kostfunctie met elkaar vergeleken. In dit experiment werd in het model een andere (nieuwere) morfologische data-set gebruikt dan in hoofdstuk 3. Deze nieuwe data-set bevat ook gegevens van optimale vezellengte wat het mogelijk maakte ook kracht-lengte-karakteristieken te implementeren. De energiegerelateerde kostfunctie kon hierdoor zodanig worden herschreven dat de kracht-lengte-relatie van de spier meegenomen werd.

In het model werden vervolgens van acht armspieren de fysiologische dwarsdoorsnedes en momentsarmwaardes gevarieerd. Er werd gebruik gemaakt van een indirecte strategie om voor iedere proefpersoon een bij benadering optimale individuele parameterset te vinden. Modelsimulaties die gedaan worden met deze individuele parameterset, zouden in theorie het best overeen moeten komen met de gemeten data. De overeenkomst tussen de experimentele data en de modelvoorspellingen, die gedaan zijn met de optimale morfologische data set, kan daarom gezien worden als de maximale verbetering die bereikt kan worden door het gebruik van individuele morfologiegegevens. De resultaten lieten zien dat de krachtsverdeling tussen spieren niet alleen sterk afhangt van de gekozen kostfunctie maar ook

van de gekozen morfologie. De modelresultaten verbeterden inderdaad door de morfologische parameters zo te kiezen dat er een zo goed mogelijke fit ontstond tussen de experimentele data en de modeluitkomsten. Een deel van de gevonden interindividuele variatie in de experimentele data kon hierdoor worden verklaard.

Het fitten van de individuele morfologiegegevens bleek overigens alleen effectief voor de energiegerelateerde kostfunctie. Ondanks dat nog niet alle 'vals negatieven' verdwenen door het gebruik van de individuele morfologiegegevens, liet de energiegerelateerde kostfunctie opnieuw een veel betere overeenkomst met de experimentele data zien dan de stress kostfunctie. De overgebleven 'vals negatieven' werden met name gevonden in condities die een moment betroffen waarvoor de betreffende spier geen effect of zelfs het tegenovergestelde effect had. Het lijkt er op dat deze spieren in deze condities geactiveerd worden omdat ze of een ongewenst effect van één van de andere spieren moeten compenseren dan wel vanwege het effect dat ze op één van de andere vrijheidsgraden hebben.

In hoofdstuk 6, de epiloog, zijn de belangrijkste bevindingen van dit proefschrift samengevat en bediscussieerd. Dit proefschrift laat zien dat het gebruik van NIRS om de zuurstof consumptie in de spier te bepalen, een waardevolle methode is voor het valideren van kostfuncties. Het is ook duidelijk geworden dat optimale krachtsverdeling tussen spieren niet altijd leidt tot een en hetzelfde activiteitspatroon tussen spieren en dat deze door verschillende factoren wordt beïnvloed. Aangezien de exacte principes achter de krachtsverdeling tussen de spieren nog steeds onbekend zijn, blijft het lastig om de juiste kostfunctie voor menselijke bewegingen te vinden. Daarbij komt dat validatie van de kostfunctie bemoeilijkt wordt door het feit dat de voorspelde krachtenverdeling niet alleen bepaald wordt door de gekozen kostfunctie, maar ook door andere factoren, zoals de gebruikte morfologische parameters. Het is moeilijk, misschien zelfs onmogelijk, om de individuele effecten van de verschillende morfologische parameters op de voorspelde krachtenverdeling van elkaar te scheiden. Bovendien kan validatie van kostfuncties eigenlijk alleen maar gedaan worden met behulp van meervoudige spier- en gewrichtsmodellen, die zowel het werkelijke aantal vrijheidsgraden als alle relevante aangrenzende gewrichten meenemen.

Het is duidelijk dat de stress kostfunctie geen realistische patronen van spieractiviteit voorspelt, omdat tijdens de experimenten een relatief groot aantal 'vals negatieven' en 'vals positieven' gevonden is. De energiegerelateerde kostfunctie doet het beter dan de stress kostfunctie, maar heeft toch ook nog enige verbetering nodig. Bij de energiegerelateerde kostfunctie werden 'vals negatieven' met name

gevonden worden in paradoxale condities, waarin de geactiveerde spier slechts aan één van de gevraagde momenten of zelfs helemaal niet direct aan het gevraagde moment bijdraagt. Dit benadrukt het belang van het meten van veel verschillende condities, die alle vrijheidsgraden beslaan.

Aangezien er nog enige discrepanties gevonden zijn tussen de energiegerelateerde kostfunctie en de experimentele data kan afgevraagd worden of het wel energieverbruik is dat tijdens bewegingen geoptimaliseerd wordt. Daarnaast kan ook betwist worden of de in dit proefschrift gepresenteerde kostfunctie wel een valide beschrijving is van het energieverbruik van de spier. Verdere verbetering kan mogelijk bereikt worden door de weegfactoren van de kostfunctie te optimaliseren. Daarnaast zou ook onderzocht moeten worden of energieverbruik wellicht geoptimaliseerd wordt op het niveau van de individuele spier in plaats van op het niveau van de totale energieconsumptie. Uitgaande van de gevonden interindividuele verschillen kan ook gesuggereerd worden dat er helemaal geen algemeen optimalisatie-principe bestaat en dat verschillende personen verschillende optimalisatiestrategieën gebruiken. De resultaten van hoofdstuk 5 geven echter aan dat een deel van de interindividuele verschillen verklaard zou kunnen worden door mogelijke verschillen in spiermorfologie, ondanks dat dit alleen effectief was voor de energiegerelateerde kostfunctie. Interindividuele verschillen zouden tevens verklaard kunnen worden door een verschil in aanpak bij het omgaan met stabiliteit. Mogelijk is een goede validatie van kostfuncties daarom niet mogelijk zonder stabiliteit als randvoorwaarde (constraint) mee te nemen.



Finally...

Dankwoord

Het is er dan toch van gekomen, mijn proefschrift is af! Dit zou niet gelukt zijn als er ook hierbij niet sprake was geweest van 'load sharing'. Er zijn de afgelopen jaren vele mensen geweest die direct of indirect een bijdrage hebben geleverd aan het tot stand komen van dit proefschrift. Een aantal van hen wil ik hier specifiek bedanken.

Allereerst wil ik mijn promotor Frans van der Helm en copromotor DirkJan Veeger bedanken. Frans, je was niet meteen vanaf het begin mijn promotor, maar ik was erg blij toen besloten werd dat jij (ondanks dat je verbonden was aan de TU Delft) mijn promotor zou worden. Jouw grote kennis van zaken is van zeer grote waarde geweest en ik bewonder jouw onaflatende enthousiasme. Voor jou is onderzoek altijd leuk, of het nou tegen zit of niet, ook als er niets uit lijkt te komen (al was dat voor mij wel eens frustrerend). Als ik weer eens vast liep zorgden onze overleggen in Delft er bijna altijd voor dat ik weer vol goede moed aan de slag ging (al betekende dat ook regelmatig: weer talloze nieuwe simulaties). DirkJan, ik heb het erg getroffen met jou als begeleider. Ik heb erg veel van je geleerd, jij bent erg goed in dingen terug brengen tot de essentie en het in de gaten houden van de rode lijn, dat was in dit project onmisbaar. Ook bewonder ik het gemak waarmee jij Engelse zinnen formuleert. Naast je inhoudelijke bijdrage heb ik ook op het persoonlijke vlak veel steun van je ondervonden. Met name, in de perioden dat ik, wegens mijn persoonlijke omstandigheden, noodgedwongen minder tijd aan mijn promotiewerk kon besteden of het zelfs helemaal stil kwam te liggen. Jij hebt altijd het vertrouwen gehad (of in ieder geval mij het gevoel gegeven dat je dat had) dat het ondanks alle vertragingen toch af zou komen. Daar ben ik je heel erg dankbaar voor! De laatste jaren was het afronden van mijn promotie iets wat ik 'erbij deed' en wat dus ergens in mijn vrije tijd moest gebeuren. Frans en DirkJan, dank voor alle uren die ook jullie in die laatste jaren, ondanks jullie volle agenda's, toch steeds weer voor mij vrij gemaakt hebben. Ondanks dat ik ontzettend blij ben dat het nu afgerond is, zal ik onze gezellige overlegmomenten en leuke discussies stiekem best een beetje missen.

Ed, toen jij naar Delft kwam vond ik dat vooral heel gezellig, maar later werd je ook betrokken bij mijn begeleiding en dat bleek zeer waardevol. Met name jouw hulp en bemoeienissen met het model waren van onschatbare waarde. Luc van de Woude, wil ik bedanken voor zijn inhoudelijke bijdrage in de tijd dat ik nog geen promotor had.

De afdeling fysiologie, van de medische faculteit van de universiteit van Nijmegen ben ik zeer dankbaar dat ik gebruik kon maken van hun NIRS apparatuur en ook een deel van mijn eerste experimenten daar uit mocht voeren. Willy Colier, jij, als NIRS expert, hebt mij wegwijs gemaakt in die techniek en ik ben je zeer dankbaar voor alle ondersteuning die je me daarbij hebt gegeven. De afdeling mens-machine-systemen van de TU Delft wil ik bedanken voor hun gastvrijheid. Het was erg fijn dat ik de laatste jaren van mijn AIO periode op de woensdagen, de dag dat Frans en Dirkjan daar ook beiden waren, ook daar over een werkplek kon beschikken. Dat maakte het gezamenlijk overleggen een stuk eenvoudiger. De faculteit bewegingswetenschappen dank ik voor hun gastvrijheid gedurende de jaren dat ik er niet meer werkzaam was maar nog wel met mijn promotie bezig was.

Bij mijn metingen waren altijd vele handen nodig en ik had ze dan ook niet uit kunnen voeren zonder de hulp van de vele studenten die mij daarbij geassisteerd hebben of data voor me hebben verzameld. Allen bedankt. Veel dank gaat ook uit naar de proefpersonen (veelal collega's) die uren (soms zelfs dagen) voor mij op een stoel zaten en eindeloos allerlei (saaie) statische contracties uit moesten voeren. Voor de technische snufjes en hulpstukken die gemaakt moesten worden voor mijn opstelling kon ik altijd rekenen op de hulp van Jos van den Berg, Hans de Koning en Micha Paalman. Bedankt daarvoor!

Mijn collega's van de faculteit Bewegingswetenschappen wil ik bedanken voor de ontzettend leuke tijd die ik daar als AIO gehad heb. De lunchgroep, het AIO-clubje en mijn lijngenoten van A4, zorgden ervoor dat ik me altijd erg thuis gevoeld heb op de faculteit. Een aantal van hen wil ik graag wat uitgebreider bedanken. Als eerste natuurlijk Kirsten. Kirsten, wij begonnen op dezelfde dag als AIO en kwamen samen bij Han op de kamer. Jij werd al snel mijn maatje op de VU. Ook was het de basis voor een lange vriendschap die hopelijk nog heel lang zal blijven bestaan. Jij was en bent er altijd voor me. Ook in de tijd dat jij ver weg in Boulder zat en tijdens de jaren dat ik bij BT werkte. Heel veel dank daarvoor! Ik ben heel blij dat jij straks als paranimf naast me wil staan en ook heel erg bedankt voor al het laatste correctiewerk en voor het leesbaar maken van de Nederlandse samenvatting. Han jij werd halverwege je promotietraject met Kirsten en mij en onze klaarblijkelijke slappe thee opgescheept. Ik denk met veel plezier terug aan die periode. Dank voor al je gezelligheid en aandacht, ook in de jaren dat we geen kamergenoten meer waren. Mirjam, bedankt voor de tijd die je altijd hebt om naar mijn verhalen te luisteren en je betrokkenheid, ook in de tijd dat ik van de VU weg was. Stefan, Sonja, Petra en Maaïke, ook jullie wil ik bedanken voor de gezellige tijd samen.

Dennis, samen met Ed zorgde jij er voor dat het ook in Delft altijd erg gezellig was. In de periode dat jij daar AIO was en ik daar wekelijks kwam hadden we zeer intensief contact. We deelden begeleiders, model-frustraties, matlabprogramma's, maar ook goede gesprekken en gezellige congressen. Dank voor al je hulp en vriendschap in die tijd. Mariëlle, ik vind het erg leuk dat ook jij mijn paranimf wilt zijn. Tijdens onze eerste onderzoeksstage (ook al met het schoudermodel) kreeg ik de smaak van het onderzoek te pakken en onze samenwerking was super. Beiden begonnen we na onze studie aan een promotietraject binnen de Schoudergroep, jij in Leiden en ik in Amsterdam. Dat zorgde weer voor veel gezelligheid en lol tijdens gezamenlijke bijeenkomsten en congressen. Ook onze gesprekken tijdens onze etentjes in de jaren daarna zijn altijd erg waardevol voor me geweest.

Mijn collega's van bewegingstechnologie wil ik bedanken voor de ontzettend leuke jaren die ik daar, na mijn AIO tijd heb gehad. Op het moment dat ik bij jullie begon had ik het met dat promotie onderzoek wel gehad en het was heerlijk om heel ander werk te doen en veel minder solistisch bezig te zijn. Monique, Hester en Jorine, jullie wil ik in het bijzonder bedanken voor jullie betrokkenheid en steun bij de afronding van mijn promotiewerk. Mijn huidige collega's van EXPres en Bart Visser in het bijzonder, wil ik bedanken voor hun geduld. Doordat er nog een onafgemaakt proefschrift op mijn schouders rustte kon ik er bij mijn start bij EXPres niet meteen volledig voor gaan. Bedankt voor jullie begrip.

Rachel wil ik bedanken voor het mooie ontwerp van de kaft en de opmaak van dit proefschrift en Han, Mirjam, Sonja, Marco en M&M, voor het laatste correctiewerk.

Vrienden en familie, dat het combineren van de afronding van een promotie onderzoek met een baan en gezin me vaak zwaar viel, zal jullie niet zijn ontgaan. Dat betekende ook vaak dat ik minder tijd voor jullie had, ook al dacht ik keer op keer dat het nog maar van korte duur zou zijn. Ik ben jullie ontzettend dankbaar voor al jullie steun en welkome afleiding. Jaap en Gerdien, bedankt voor de geweldige basis die jullie me hebben gegeven, jullie onvoorwaardelijke steun en vertrouwen. Jaap het was altijd al leuk om samen ook inhoudelijk over mijn werk te praten, maar jouw daadwerkelijke inhoudelijke bijdrage maakte het wel heel bijzonder. Gerdien, dank voor al je goede adviezen en je praktische hulp door op Tieme te passen zodat ik tijd had om dit proefschrift af te maken. Bert en Anneke, ook jullie wil ik bedanken voor het creëren van promotietijd door alle extra dagen dat jullie op Tieme hebben gepast.

Lieve Bart, Jij hebt me op zoveel manieren geholpen! Naast alle mogelijke praktische hulp: o.a. bij mijn meetopstellingen en als proefpersoon, maar zeker ook door het draaiende houden van ons gezin in de jaren dat het er allemaal naast moest gebeuren, ben ik jou toch nog het allermeest dankbaar voor je mentale steun. Ik weet dat het ook heel wat van jou gevraagd heeft en ik ben je oneindig dankbaar voor je eindeloze geduld en vertrouwen! Zonder jou was het me niet gelukt. Ik kijk ontzettend uit naar het leven zonder promotiewerk waarin ik mijn vrije tijd gewoon met jou en Tieme kan door brengen.

List of publications

Articles in international journals:

- Praagman M, Stokdijk M, Veeger H E and Visser B. (2000) Predicting mechanical load of the glenohumeral joint, using net joint moments. *Clin Biomech* 15:315-321
- Praagman M, Veeger H E J, Chadwick E K J, Colier W N J M and Van der Helm F C T. (2003) Muscle oxygen consumption, determined by NIRS, in relation to external force and EMG. *Journal of Biomechanics* 36:905-912
- Praagman M, Chadwick E K J, Van der Helm F C T and Veeger H E J. (2006) The relationship between two different mechanical cost functions and muscle oxygen consumption. *Journal of Biomechanics* 39:758-765

Abstracts:

- Praagman M, Veeger H E J and Colier W N J M. (2000) A method for biomechanical modeling of energy consumption. *Clinical Biomechanics* 15 (S1). *Proceedings of the 2nd conference of the International Shoulder Group*, p.53-54. Calgary.
- Praagman M, Veeger H E J, Van der Helm F C T and Chadwick E K J. (2002) Mechanical cost functions and muscle oxygen consumption. In: *Proceedings of the 4th meeting of the International Shoulder Group* (Editor B. Kirsch), Cleveland
- Praagman M, Veeger H E J, Chadwick E K J and Van der Helm F C T. (2003) The Relationship between mechanical cost functions and muscle oxygen consumption. In: *Proceedings of the 19th congress of the International Society of Biomechanics*. (Editors P Milbourn, B Wilson and T Yanai). Dunedin

Musculoskeletal models are a valuable tool in the study on human movement. When the kinematics and external forces that act on the human body are known, such models can be used to calculate the resultant joint moments for a given posture or motion by simple Newtonian mechanics. It is, however, difficult to determine the contribution of the individual muscles to these moments. In general, there are more muscles crossing a joint than is theoretically necessary in order to perform all possible movements. This is called the indeterminacy problem or the load sharing problem. Inverse dynamic models often make use of cost functions to solve this load sharing problem. The use of a cost function is based on the assumption that the central nervous system controls the musculoskeletal system in an optimal manner, optimising a certain cost. It is however difficult to find the right criterion, since it is unknown which quantity is optimised in real life. Therefore, only assumptions can be made. It has often been assumed that movements are performed by minimising energy consumption. Nevertheless, most cost functions are mechanical cost functions and up till now, no cost functions have been defined, which are based on the calculation of muscle energy consumption. The aims of this thesis were to define a cost function that represents muscle energy consumption and to validate this cost function with a metabolic parameter.